PERFORMANCE OF LOG SHEAR WALLS AND LAG SCREW CONNECTIONS SUBJECTED TO MONOTONIC AND REVERSE-CYCLIC LOADING

By

DREW ABRAM GRAHAM

A thesis submitted in partial fulfillment of
the requirements for the degree of

MASTER OF SCIENCE IN CIVIL ENGINEERING

WASHINGTON STATE UNIVERSITY
Department of Civil and Environmental Engineering

MAY 2007

To the Faculty of Washington State University:

The members of the Committee appointed to examine the thesis of DREW ABRAM GRAHAM find it satisfactory and recommend that it be accepted.

_____
Co-Chair

_____
Co-Chair

_____

_____

ACKNOWLEDGMENTS

With the utmost gratitude I would like to thank the following for all that they did for me while I worked on this research:

- *God:* for his love and provision in my life.
- *Parents:* Ross and Pam Graham for instilling in me to "Never give up" and for always being there at the drop of a hat to listen, provide advice, and most importantly pray for my life everyday.
- *Brothers & Sisters:* Justin, Elizabeth, Hillary, Tammy, Forrest and J.P. for their laughter, consistent interest and continual support as not only my siblings but my best friends.
- *Committee members:* Dr. Donald Bender, Dr. David Carradine, Dr. J. Daniel Dolan and Dr. Tom Gorman for keeping me on the right path and providing their invaluable knowledge to aid in my research.
- *WMEL:* Bob Duncan and Scott Lewis for their persistent help in my testing process. I'd still be in the lab trying to figure out how to control the actuator if it wasn't for their assistance.
- *Extra hands:* Jon, Fred, Tyler, Jason and everyone else who threw their backs out helping me stack log after log after log after log……..
- *Edgewood Log Structures:* for log donations.
- *Jeff Sharpe:* for providing his knowledge on log structures.
- *USDA*: for funding this research.

PERFORMANCE OF LOG SHEAR WALLS AND LAG SCREW CONNECTIONS SUBJECTED TO MONOTONIC AND REVERSE-CYCLIC LOADING

Abstract

Drew Abram Graham, M.S.
Washington State University
May 2007

Co-Chairs: David M. Carradine & Donald A. Bender

Lateral loads in low-rise buildings due to wind and earthquakes are primarily resisted by shear walls and horizontal diaphragms. Shear walls in wood-frame construction consist primarily of framing members, sheathing, and sheathing-to-framing connectors, and are designed to resist shear force per unit length of the wall as required by calculated loads. Log home construction techniques differ from traditional wood-frame construction in that walls are formed by stacking horizontal layers of logs, known as courses, where log cross-section, grade, and construction details vary among manufacturers.

Methods and test data are needed to assist designers of log structures with accurately determining the behavior of log shear walls subjected to lateral loads. To address these needs, monotonic and reverse-cyclic log connection tests as well as monotonic and reverse-cyclic log shear wall tests at various aspect ratios were conducted using lag screws as a mechanical fastener. By providing designers and code officials with data on the performance of log shear walls, building regulatory barriers can be removed and markets can be opened to log structures in active seismic and high wind regions around the world.

Analyses were conducted in order to assess the shear strength, stiffness, equivalent energy elastic plastic (EEEP) parameters and hysteretic behavior of the tested connections and log shear wall specimens. Testing also provided a basis for making recommendations to building designers regarding methods for estimating seismic design coefficients used to determine earthquake loads on buildings, which are lacking in current building codes.

TABLE OF CONTENTS

LIST OF FIGURES

LIST OF TABLES

CHAPTER 1

Introduction

In order to better understand the performance of log shear walls utilized as lateral force resisting systems (LFRS) within buildings subjected to seismic and wind loading, research was conducted at the Washington State University Wood Materials and Engineering Laboratory (WMEL) in Pullman, Washington, U.S.A. A growing market for log homes in active seismic and high wind regions has prompted this study in order to assist with the development of cyclic parameters and strength of structures with log shear walls. The current state of log shear wall design requires the designer to use a design approach that is without any underlying performance based considerations other than the success of past designs. The need for a performance-based design methodology has served as impetus for this research in order to provide designers with a body of experimental data on the strength, stiffness, ductility and overall hysteretic behavior of log shear walls constructed using lag screws as the primary connection between log courses.

This study investigates the monotonic and cyclic response of connections in log shear walls using lag screws as mechanical fasteners, as well as the monotonic and cyclic response of full-scale log shear walls at various aspect ratios. Objectives necessary for validating the beginnings to a process that provide log wall designers with a more performance-based design process will be discussed. A literature review will highlight current design needs for log walls used as lateral force resisting systems (LFRS) and previously obtained experimental results.

The objectives of this study were achieved by conducting a series of monotonic and reverse-cyclic log connection tests as well monotonic and reverse-cyclic full-scale log shear wall tests. Experimental data obtained from these tests were used to develop energy based parameters, strength properties, and the hysteretic behavior of the log connections and log shear wall test specimens. Based on the experimental data and general test observations, recommendations were made to increase the safety and efficiency of log shear wall design. It was also recommended that the log shear wall data obtained from the current study be incorporated into the methodology for reliably quantifying building system performance and response parameters for use in seismic design once the Applied Technology Council's (ATC) ATC-63 Project is complete (ATC, 2007). The failure modes of the log shear walls in this study are discussed, and were unique compared to that of light-frame shear walls because of the fact that the systems are constructed vastly different structural elements.

CHAPTER 2

Monotonic and Reverse-Cyclic Loading of Lag Screw Connections for Log Shear Wall Construction

ABSTRACT

The log building industry favors simple to install mechanical connections between log layers, also referred to as log courses, to facilitate fast and efficient construction. In active seismic regions, lag screws are commonly used: however, research is lacking on how these connections between log courses perform in monotonic and reverse-cyclic loading scenarios. For the current study, 406 mm long logs were used to fabricate connection test specimens in a double-shear configuration, so as to mimic a typical lag screw layout used in typical log shear wall construction. The intent of this study was to develop baseline data on these connections in order to relate log connection performance to full-scale log shear wall performance. A preliminary study of four commonly used lag screws of different sizes was conducted to assess the monotonic performance within log connections. Predictions of design capacities were calculated using the National Design Specification for Wood Construction (NDS) which is based on derived equations from the European Yield Model (EYM). Predicted NDS design capacities were compared to experimental data. Monotonic test results revealed that a specific lag screw 254 mm long and 12.7 mm in diameter, chosen for further study, exhibited lower 5% offset yield capacities than those predicted by the EYM. Reverse-cyclic tests revealed failures due to low-cycle fatigue of the lag screws, leading to prevalent cyclic stiffness degradation as displacements were increased.

INTRODUCTION

The log building industry in North America favors easily installed mechanical connections between log layers, also referred to as log courses, to facilitate construction flexibility and rapid on-site assembly. In active seismic and high wind regions, lag screws are commonly used for these connections: however, research is lacking on how these connections between log courses perform when subjected to monotonic and reverse-cyclic loading.

Minimal research has been conducted on lag screw connections, in log wall construction but related studies have proved to be helpful for comparisons with the current study. Popovski et al. (2002) presented results from monotonic and quasi-static cyclic tests of connections used in heavy timber construction. Fasteners used in their study were steel bolts and glulam rivets. Test results indicated superior seismic performance of the glulam rivet connections when compared to the steel bolt connections at similar design level loads (Popovski et al., 2002). One specific area of research on deck ledgers, bolts, and lag screws was conducted by Carradine et al. (2007). Carradine et al. tested three connection details in order to determine required spacing for 12.7mm diameter lag screws and bolts used to connect deck ledgers to house band joists. Scott et al. (2005) investigated foundation anchorage connections and base shear capacities for log buildings. A more in-depth study on connections by Anderson (2001), determined the significance of the group action factor at the 5% offset yield capacity of single-shear bolted wood connections loaded parallel to grain. Anderson's (2001) results indicate the importance of adequate bolt spacing to control the brittle connection behavior that directly affected the group action factor at capacity. Dolan and Madsen (1992) conducted

a study that related monotonic and cyclic nail connection test results with that of a larger study of nailed timber shear walls. Monotonic and cyclic lateral connection behaviors were developed in their study and the connection characteristics were found to translate into similar behavior within nailed timber shear walls (Dolan and Madsen, 1992). Dolan (1989) also proposed a test method for determining dynamic properties of connections assembled with mechanical fasteners and parameter definitions provided in his proposal were used in the current study and are presented in the *Definitions of Calculated Parameters* section of this paper.

Johansen (1949) developed the European Yield Model (EYM) for dowel type fasteners in wood connections, which was intended for members with solid cross-sections. The model predicts the yield strength of a connection taking into consideration the bending yield strength of the dowel, the bearing strength of the member material, and the geometry of the members and dowel that make up the connection. The EYM is the underlying theory used today in wood design to predict lateral design values for dowel type connections and was adopted by the National Design Specification for Wood Construction (NDS) in 1991. In prior years connection design was empirical. The EYM can be applied to the monotonic log connections herein but results were not always accurate and are discussed in this paper in the *Monotonic Connection Test Results* section.

For the current study 406 mm long logs were used to fabricate connection test specimens in a double-shear configuration, so as to mimic a typical lag screw layout used in typical log shear wall construction. The intent of this study was to develop baseline data for log shear wall connections so as to relate log connection performance to full-

scale log shear wall performance as was similarly done by Dolan and Madsen (1992) for nailed connections and nailed timber shear walls. It was also intended to provide a body of experimental data for monotonic lag screw connection capacities and cyclic response parameters by means of reverse-cyclic tests to be used for subsequent modeling of log shear walls. Literature exists on this topic for bolted wood connections but not for lag screw wood connections. Improving the understanding of log shear wall connections will subsequently aid in improving the understanding of log shear walls and their behavior when subjected to lateral loading.

The objectives of this research were as follows:

1) Assess the monotonic performance of four log connections that were fabricated with different sized lag screws commonly used in the log building industry.
2) Characterize the monotonic response of the best performing connection from Objective 1 while mimicking in-service conditions.
3) Characterize the hysteretic behavior of the log connection mentioned in Objective 2 when subjected to reverse-cyclic loading.

METHODS AND MATERIALS

Materials

Many log species are used in the log construction industry. Engelmann Spruce, Lodgepole Pine and Grand Fir logs were obtained from Edgewood Log Homes of Athol, ID USA. Logs were harvested in North Idaho and were of log grade LHC #1. All logs were 254 mm in diameter and machined with a Swedish Cope profile to an average stack

height (measured from the apex of the Swedish Cope to the apex of the top of the log) of 228 mm.

A preliminary study was conducted to evaluate the monotonic performance of four common sizes of zinc plated lag screws that are commonly used in the log building industry. Based on the results of the preliminary study and the availability of the log dimensions mentioned previously, lag screws selected for further study were 254 mm long and 12.7 mm in diameter, and consisted of full-body diameter on the unthreaded portion of the screw as shown in NDS Table L2 (AF&PA, 2005). All lag screws were manufactured from A307, Grade 2, low carbon steel. Materials used in the preliminary lag screw study will be discussed in the *Results and Discussion* section.

Connection Fabrication

Monotonic and cyclic connection tests were conducted using the same connection fabrication method and configuration. Connections were fabricated with three logs machined to 406 mm lengths each and attached together in a double shear configuration. The middle log served as the point of load application and was offset by 152 mm to allow for sufficient displacement between logs during testing. In a log shear wall, lag screws are alternated and offset at prescribed distances to avoid interfering with lag screws in the log course below. Lag screws were offset by 76 mm for these connection tests (Figure 2.1). Countersink holes, clear holes, and lead holes were all drilled to meet NDS (AF&PA, 2005) provisions for installation of lag screws. All lag screws were installed using an air impact wrench with double washers underneath the hex head of each screw. Each lag screw was tightened just to the point where the washers made contact with the

log and no wood crushing was observed. The intent was to mimic in-service conditions of shrinkage and stress relaxation which would thereby minimize any potential effects of friction between log layers.

Monotonic Test Methods

Monotonic log connection tests were conducted according to ASTM D5652-95 Standard Test Methods for Bolted Connections in Wood and Wood-Base Products (ASTM, 2001). This standard suggests a displacement rate of 1.0 mm/min to meet the target time to failure of 5 to 20 minutes. The suggested load rate for the log connection tests was determined to be too slow to meet the upper time limit. Through repeated preliminary tests, a displacement rate of 6.35 mm/min was selected to meet the time to failure constraints. Specimens were loaded monotonically until failure of the logs due splitting was achieved, or until the middle member, which served as the point of load application, exceeded the displacement limit of 152 mm and made contact with the test frame. During each of the tests, data were recorded using LabView Version 8 data acquisition system and were then used to derive load-displacement curves and other performance parameters for the connections.

Tests were performed using an electro-mechanical test frame with 134 kN capacity. Linear variable differential transducers (LVDTs) were mounted onto each side of the middle log to record the relative displacement between the outer logs and the middle log. A photo of the test setup is shown in Figure 2.2. Shims were placed underneath the outer log members to minimize eccentric loading. Load was applied

using a self-aligning compression fixture and a 150 kN load cell was installed in line between the compression fixture and the test frame crosshead.

Cyclic Test Methods

Cyclic log connection tests were conducted according to the CUREE (Krawinkler et. al., 2001) displacement controlled quasi-static cyclic loading protocol. The CUREE protocol was carried out to 68 cycles with 18 of the cycles being primary cycles. Cyclic loads were applied at 0.5 Hz using a double acting hydraulic actuator with a 49 kN capacity. A 45 kN load cell was securely installed in line between the actuator and the test specimens to record the loads. A data collection rate of 15 Hz was used to record load and displacement data throughout all testing.

Log connection specimens were mounted to the base of a rigid test frame. Steel plates were placed on top of the outer two logs and secured down to the base of the test frame with four segments of 12.7 mm diameter threaded rod manufactured from Grade B7 steel alloy mix as shown in Figure 2.3. This figure also illustrates the use of steel plates and threaded rod on the middle log, which allowed the actuator to apply load by pushing and pulling on the center log. String potentiometers were mounted on the two outer edges of the middle log and attached to the two outer logs to record the relative displacements between the members.

Moisture Content and Specific Gravity Measurements

Moisture content (MC) and specific gravity (SG) samples were taken from the approximate center of each of the tested log specimens and were 102 mm in length and

width and 25.4 mm in thickness. Test methods outlined in ASTM D4442-92 (ASTM, 2003) were used for MC. Each specimen's "wet" weight was measured and then placed in a forced-convection oven at a temperature of 103°C for 48 hours. The oven-dry weight was then measured and used for calculating MC using ASTM D4442-92 (ASTM, 2003) equation (1). ASTM D2395-02 (ASTM, 2006) Method A test methods were used to determine SG. Specimen dimensions were measured with a micrometer and were input into equation (2) of ASTM D2395-02 (ASTM, 2006) to determine SG.

Lag Screw Bending Yield Strength Tests

Lag screw bending yield moment tests were conducted on a total of 20 of the lag screws used for log connection testing to determine the properties such as 5 % diameter offset yield strength and bending yield strength for the lag screws. No current standard exists for determination of lag screw bending yield strength; therefore, tests conformed to ASTM F1575-03 (ASTM, 2003) and were conducted using an electro-mechanical test frame. The lag screws were centered across a 147.3 mm span and loaded at their midspan at a rate of 6.35 mm/min. Load and deflection data were recorded at a rate of 2 Hz. The bending yield strength was determined by dividing the calculated midspan moment by the lag screws effective plastic section modulus.

RESULTS AND DISCUSSION

The mean value of MC for log segments used in connection tests was 15% with a coefficient of variation (COV) = 9%. The mean value of SG was 0.44 with a COV of

9%. The mean and COV for lag screw bending yield strength were 588 MPa and 4%, respectively.

Definitions of Calculated Parameters

When analyzing data from a reverse-cyclic connection test there are parameters, proposed by Dolan (1989), that are quantified based on the development of *backbone curves* and *equivalent energy elastic plastic* curves (EEEP), as well as parameters determined on a cycle-by-cycle basis known as *hysteretic parameters.* Both sets of parameters are calculated differently, but each yields valuable information about the connection in terms of quantifying the strength and response to reverse-cyclic loading of the connections. Definitions of all calculated parameters herein were consistent with those given by Dolan (1989). Those parameters were ductility (D), hysteretic energy, strain energy, equivalent viscous damping ratio (ζ), cyclic stiffness, elastic stiffness, equivalent energy elastic plastic (EEEP), peak load (F_{peak}), and 5% diameter offset yield.

Backbone curves for reverse-cyclic tests were constructed by connecting the peak loads of each hysteresis loop using straight line segments. These curves were developed in order to compare monotonic tests with reversed cyclic tests because the backbone curve has been shown to be representative of the load versus deflection curve for monotonic tests.

Once the previously discussed backbone curves were developed, EEEP curves were constructed. EEEP curves represent a perfectly elastic-plastic response and are constructed so that the area underneath it is equal to the area underneath the back bone curve up to the point of failure. A perfect elastic-plastic response describes a material

that can deform and resist increasing loads, without experiencing permanent deformations, until it reaches its yield point. After the yield point is exceeded that material undergoes permanent deformations as the displacements are increased without an increase in load. Although wood connections do not respond to load in this way, the EEEP curve and parameters obtained from it allow comparisons to be drawn between connections of different materials by observing the equivalent yield points and energy dissipated for idealized perfectly elastic-plastic responses. A methodology for constructing the EEEP curves in the current study can also be found in Dolan (1989). Figure 2.4 illustrates an EEEP curve and backbone curve superimposed on a typical load versus deflection hysteresis curve developed from the experimental data collected herein.

All parameters were calculated with the intent that they could be used in conjunction with future research to compare with additional log connections that utilize mechanical fasteners to help build a body of experimental data for mechanical fasteners used in log construction. It was also intended for the data from these tests to be used to compare to full-scale log shear wall tests to understand how the performance of the log connections can be extrapolated to predict their performance in log shear walls. Furthermore, cyclic response parameters of these log connections would be useful for subsequent modeling of full-scale log shear walls.

Monotonic Connection Test Results

A variety of lag screw sizes are used in the log building industry for connecting log courses. The intent of the preliminary study was to determine which of four different sized lag screws performed best in terms of properties that are most important to seismic

loading such as energy dissipation and ductility leading up to failure. The lag screws screened had the length and diameter dimensions of 203 x 12.7mm, 203 x 19.1mm, 305 x 12.7mm and 305 x 19.1mm. There were a total of four different connection configurations tested at five repetitions per configuration. The connection test specimens were drilled to meet NDS (AF&PA, 2005) countersink, clear hole, and lead hole dimensions which changed slightly to accommodate the different sized lag screws in each test.

The National Design Specification for Wood Construction (NDS) (AF&PA, 2005) utilizes the European Yield Model (EYM) theory to predict lateral connection capacities for dowel type fasteners. Inputs into this yield model include dowel bearing strength of the wood and bending yield strength of the dowel. The NDS (AF&PA, 2005) design values predicted by these yield models are for the 5% diameter offset yield with included adjustment factors. NDS (AF&PA, 2005) design values were calculated for all monotonic connection tests on a per lag screw basis and compared to the experimental test data obtained from the current study.

Results from preliminary monotonic tests conducted on connections fabricated with four commonly used lag screws in the log building industry can be found in Table 2.1. Bending yield strength of all the lag screws was fixed at a value of 310MPa as suggested in the NDS (AF&PA, 2005) for D≥ 3/8" and recommended root diameters from NDS Table L2 (AF&PA, 2005) were used for NDS (AF&PA, 2005) design value calculations. Abrupt failures in connections with 19.1 mm diameter lag screws sometimes occurred making these diameters unfavorable for seismic loading and further study. It is worth noting that these brittle, splitting failures may have been affected by the

short log lengths used to fabricate the test specimens. Subsequently, 19.1 mm diameter lag screws may cause log splitting to occur in high aspect ratio walls (narrow piers) where short log lengths exist. Connections fabricated with lag screws 305 mm long most often experienced abrupt, brittle failures as well. The energy dissipation provided by the 203 mm x 12.7 mm lag screws was the lowest of the 4 lag screws tested but was considered to have performed the best because of their consistent ductile failures.

In this paper, the overstrength of a connection was defined as the ratio of the adjusted peak load from experimental data to the NDS (AF&PA, 2005) design value. It is worth noting that the 203 mm x 12.7 mm lag screws exhibited the second highest overstrength factor of 8. Based on the availability of 254 mm diameter logs used for this research, it was decided to use 12.7 mm diameter lag screws having a length of 254 mm. This was the same diameter as the lag screws that performed most favorably in the preliminary monotonic connection tests, yet with a slightly different length to accommodate the log diameters used in the subsequent phase of testing.

Results from ten monotonic connection tests fabricated with the lag screw chosen for further study (254 mm long x12.7 mm in diameter) can be found in Table 2.2 and are developed based on a per lag screw basis. The average peak load was found to be less than all of those in the preliminary study because connections were fabricated to mimic in-service conditions where stress relaxation and shrinkage would have occurred. Subsequently, the average overstrength of 254 mm long x 12.7 mm diameter lag screw connections was lower than most of the connections in the preliminary study and was calculated to be approximately 5. Actual bending yield strength of 588 MPa from

bending yield strength tests was used for lag screws in the EYM to predict NDS (AF&PA, 2005) design values.

Failure Modes

Ten monotonic tests and fifteen reversed cyclic tests were conducted on log shear wall connections fabricated with 254 mm long and 12.7 mm diameter lag screws chosen for further study. Failure modes for monotonic connection tests were due to pull through of the washers and lag screw heads. Figure 2.5 shows a cross-section of a typical connection test specimen following a monotonic test. Significant lag screw yielding was apparent with one plastic hinge being formed per shear plane. Lag screw thread withdrawal was minimal and only occurred after large displacements were observed in the connections. Withdrawal resistance was attributed to the penetration depth of 12D, which was much more than the required 8D as specified in NDS (AF&PA, 2005) in order to develop full connection capacity of lag screw connections.

The failure mode for all cyclic connection tests was low-cycle fatigue of the lag screws as a result of repetitive bending. Fatigue fractures occurred in the threaded portion of all lag screws within approximately 25.4 mm of the transition between the threaded and unthreaded portions.

Cyclic Equivalent Elastic Plastic Parameters

As mentioned previously, a typical load versus deflection hysteresis curve is shown in Figure 2.4. A summary of cyclic equivalent elastic-plastic parameters calculated can be found in Table 2.3. It should be noted that one cyclic test specimen

was destroyed due to a power outage during testing and the data was censored from the data set. The mean peak load (F_{peak}) and failure load ($F_{failure}$) attained for cyclic tests were 25.1kN and 20.1kN, respectively. Elastic stiffness (k_e) exhibited the largest variance between EEEP parameters with a coefficient of variation (COV) of 34% which reinforces the idea that wood, as a material, is highly variable and its ability to resist displacements in fabricated connections is hard to estimate during initial loading phases. Reverse-cyclic test results indicate that a high degree of ductility (D) was provided by these connections when compared to results obtained by Popovski et al.(2002) and Anderson (2001). The mean ductility ratio ($D = \Delta_{failure}/ \Delta_{EEEP\ yield}$) was found to be 9 compared to values of approximately 2 for connections using 12.7 mm diameter bolts in the study conducted by Popovski et al. (2002). Ductility was calculated slightly differently by Popovski et al. (2002) by way of a yield deformation equal to the deformation at the intercept of the initial stiffness line and a tangent line with stiffness equal to 1/6 of the initial stiffness. The current study used $\Delta_{EEEP\ yield}$ in the definition of ductility, but using the yield displacement in the ductility definition used by Popovski et al. would have increased ductility values in this study. Therefore it is valid to say that these log connections exhibited high degrees of ductility compared to the bolted and riveted connections, used in heavy timber construction, tested by Popovski et al. (2002).

Hysteretic Parameters

All reverse-cyclic connections exhibited pinching hysteresis behavior which indicated wood crushing by the lag screws working larger and larger holes in the logs as loads were reversed. The pinching behavior refers to the shape of a hysteresis curve

caused by the physical occurrence in the connection. Pinching occurs in these connections because as the direction of loading is reversed, load decreases due to the fact that the lag screw shank must move across the diameter of the hole that has been worked into the log before it finds resistance once it bears against the outer edge of the opening. This pinched behavior is consistent with the behavior observed by Popovski et al. (2002) for connections in heavy timber construction. Table 2.4 describes the average changing hysteretic parameters for all tests at every other primary cycle over a total of a total of 18 primary cycles.

Several distinct trends for calculated hysteretic parameters were observed. Cyclic stiffness degradation was prevalent in these connections as displacement levels were increased. A drastic drop in cyclic stiffness occurred within the first few primary cycles of each test, and the average percentage lost from the beginning primary cycle to failure was approximately 90%. This degrade in cyclic stiffness was consistent with the dominant failure mode of lag screw low cycle fatigue in the cyclic connection tests. Equivalent viscous damping (ζ) values decreased 34% between the 2^{nd} and 4^{th} primary cycles and remained fairly constant with slight variation until the end of most tests. For the most part, calculated strain energy per cycle was higher than the hysteretic energy on average which is typical for a pinched system response. Following failure due to lag screw fatigue, connections were still held in place by the test fixtures therefore, hysteretic and strain energy were attributed to friction developed between the logs after the lag screws had fatigued making hysteretic and strain energy illegitimate after fatigue.

SUMMARY AND CONCLUSIONS

Monotonic and reverse-cyclic tests were performed on a typical log shear wall connection fabricated with lag screws. In the preliminary study of connections fabricated with four different size lag screws test results indicated that the 203 mm long x 12.7 mm diameter fasteners performed the best because of the consistent ductile failures observed. EYM estimates of connection yield strength were calculated based on the dowel bearing strength of the surrounding wood, bending yield strength of the lag screws, and geometry of the lag screws and members. Connections fabricated with 254 mm long x 12.7 mm diameter lag screws typically provided an average overstrength of 5.

Monotonic test results of connections fabricated with 254 mm long and 12.7 mm diameter lag screws, indicated that these connections were able to effectively resist increasing loads well after the yield point of the connection was reached. A designer could use the values found in Table 2.2 and predict the spacing required of the lag screws in a log shear wall in order to resist design loads. This could be accomplished by dividing the connection capacity by 2 (for the number of fasteners in the connection) to attain the fastener capacity and then divide the design load for the log shear wall by the fastener capacity to determine how many fasteners are needed per course. The amount of fasteners needed per course could then be evenly distributed along the length of the wall at an evenly distributed spacing determined by the wall length.

Penetration depth of lag screws proved to be sufficient considering the minimal evidence of lag withdrawal observed, even after large amounts of deflection were induced between adjacent log members. Pulling through of the lag screw heads and washers, combined with significant wood crushing and lag screw bending (one plastic

hinge per shear plane) were dominant failure mechanisms. It is recommended that lag screws have an unthreaded shank length that extends through the log interface to avoid exposing the weakest portion of the lag screw (threaded portion) to high levels of shear in the shear plane.

Reverse-cyclic test results indicate that a high degree of ductility (D) was provided by these connections. Ductility (D) values for these connections were found to be high at a mean value of 9 when compared to the ductility (D) values calculated by Anderson (2001) and Popovski et al. (2002). This indicates that these log connections have a large amount of strength remaining after initial yielding occurs.

Low cycle fatigue of the lag screws caused cyclic stiffness degradation of the log connections and was considered the most negative attribute of these connections. Other mechanical fasteners should be tested in order to mitigate the low cycle fatigue issue found to degrade cyclic stiffness. In a seismic event, the lag screws within a shear wall need to be able to yield and dissipate energy without failing due to fatigue.

LITERATURE CITED

American Forest and Paper Association, Inc (AF&PA) 2005. *National Design Specification for Wood Construction ASD/LRFD*. Washington, DC: AF&PA.

Anderson, Guy. (2001). "Experimental Investigation of Group Action Factor for Bolted Wood Connections." Virginia Tech; Master's Thesis.

ASTM Standards. 2003. F1575-03 Standard Test Method for Determining Bending Yield Moment of Nails. West Conshohocken , PA: ASTM.

ASTM Standards. 2006. D 2395-02 Standard Test Methods for Specific Gravity of Wood and Wood-Based Materials. West Conshohocken, PA: ASTM.

ASTM Standards. 2003. D 4442-92 Standard Test Methods for Direct Moisture Content Measurement of Wood and Wood-Base Materials. West Conshohocken, PA: ASTM.

ASTM Standards. 2001. D 5652-95 Standard Test Methods for Bolted Connections in Wood and Wood-Based Products. West Conshohocken, PA: ASTM.

Carradine, D.M., D.A. Bender, F.E. Woeste, and J.R. Loferski. (2007). Development of Design Capacities for Residential Deck Ledger Connections. *Forest Products Journal* 57(3) (In Press).

Dolan, J.D. and Madsen, B., (1992). "Monotonic and Cyclic Nail Connection Tests.", *Canadian Journal of Civil Engineering. 19(1):97-104.*

Dolan, J. D., (1994). "Proposed Test Method for Dynamic Properties of Connections Assembled with Mechanical Fasteners." *ASTM Journal of Testing and Evaluation*. 22(6):542-547.

Johansen, K.W. (1949). "Theory of timber connections." *International Association for Bridge and Structural Engineering (IABSE) Pub.* 9:249-262.

Krawinkler, Helmut, Parisi, Francisco, Ibarra, Luis, Ayoub, Ashraf, and Medina Ricardo, (2001). "Development of a Testing Protocol for Wood Frame Structures (CUREE Publication No. W-02)", CUREE, Richmond, CA.

Popovski, M., Prion, Helmut G.L., Karacabeyli, E., (2002). "Seismic performance of connections in heavy timber construction." *Canadian Journal of Civil Engineering*. 29(3):389-399.

Scott, Randy J., Leichti, Robert J., and Miller, Thomas M., (2005). "An experimental investigation of foundation anchorage details and base shear capacity for log buildings.", *Forest Products Journal*. 55(4):38-45.

NOTATION

The following symbols are used in this paper:

Δ = reference deformation for CUREE protocol (mm or m)

$\Delta_{EEEP\ yield}$ = deflection corresponding to equivalent energy elastic plastic yield (mm or m)

$\Delta_{failure}$ = deflection at failure (mm or m)

Δ_m = monotonic deformation capacity (mm or m)

Δ_{max} = maximum deflection (mm or m)

Δ_{min} = minimum deflection (mm or m)

$\Delta_{5\%\ yield}$ = deflection corresponding to 5% offset yield (mm or m)

ζ = equivalent viscous damping ratio

C_d = NDS load duration factor

COV = coefficient of variation

D = ductility ratio (m/m)

EEEP = equivalent energy elastic plastic (N-m or kN-m)

$F_{EEEP\ yield}$ = load corresponding to equivalent energy elastic plastic yield (N or kN)

$F_{failure}$ = load corresponding to failure (N or kN)

$F_{5\%\ yield}$ = load corresponding to 5% offset yield (N or kN)

k_e = elastic stiffness (N/m or kN/m)

R = seismic response modification factor

R_d = NDS reduction term

SC = Swedish cope

SG = specific gravity

LIST OF FIGURES

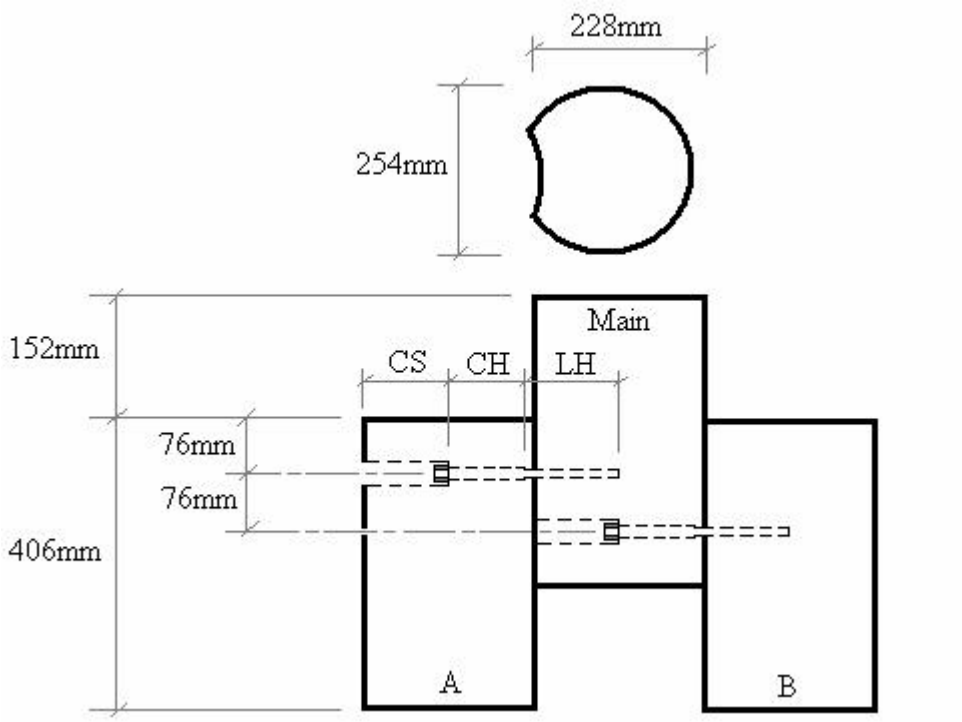

Figure 2.1 Log connection configuration. CS – countersink depth; CH - clear hole depth; LH – lead hole depth.

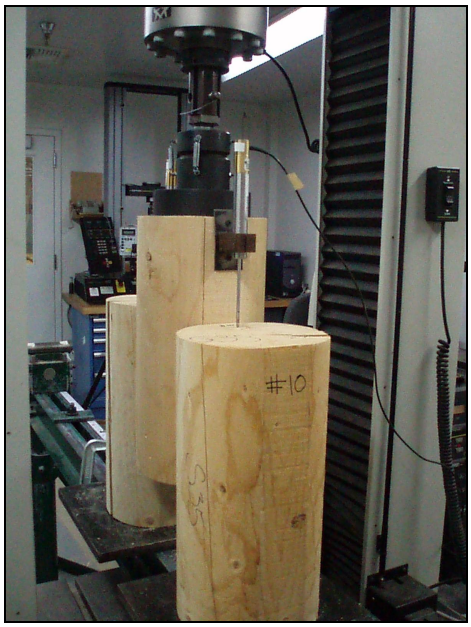

Figure 2.2 Monotonic connection test setup showing LVDT attachment to middle log.

Figure 2.3 Cyclic connection test setup illustrating steel plate fixtures used as hold downs on the outer logs and load application for the middle log.

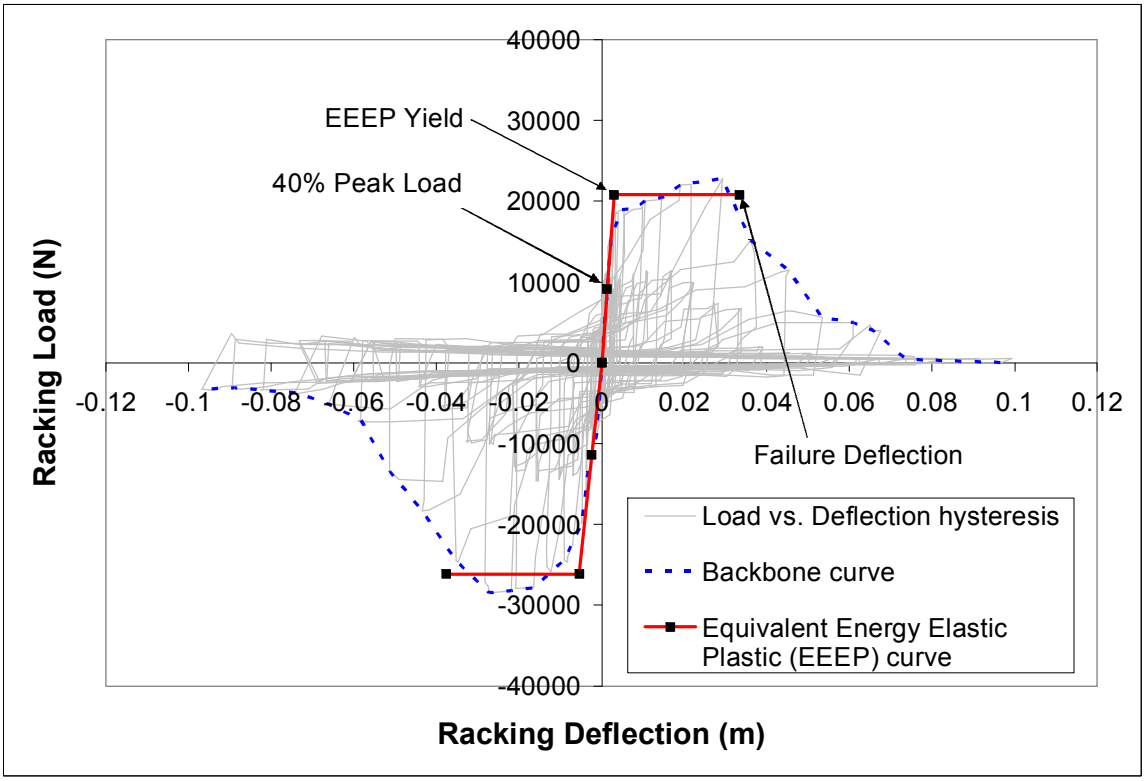

Figure 2.4 EEEP curve and Backbone curve superimposed on a typical load versus deflection hysteresis.

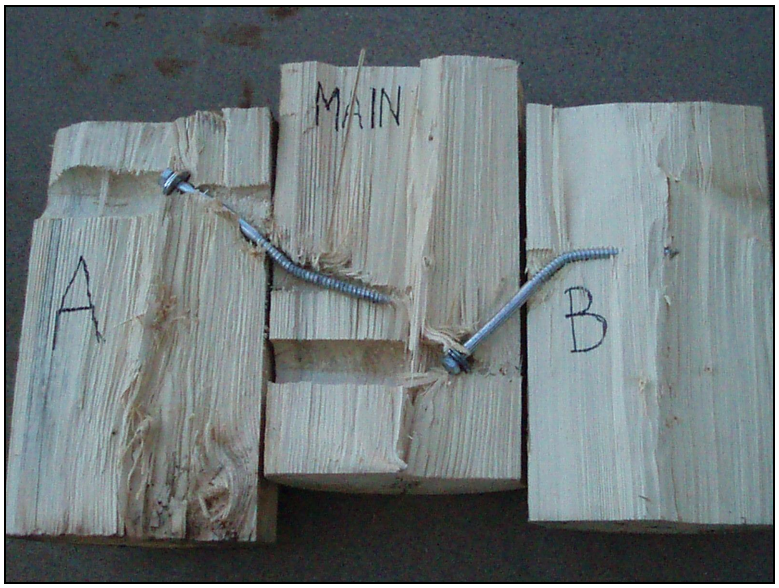

Figure 2.5 Cross-section of connection utilizing 254x12.7 mm lag screws following a monotonic connection test.

LIST OF TABLES

Table 2.1 Monotonic connection test results for preliminary lag screw screening.

Lag size (mm)	Test	Energy (N-m)	[a]F_{peak} adj. (N)	[b]F_{peak} adj./NDS
203x12.7 (Lxdiam.)	FF-MC1	3,424	14,248	9
	FF-MC2	3,168	13,901	8
	FF-MC3	2,960	11,978	7
	FF-MC4	3,615	14,888	9
	FF-MC5	3,280	13,271	8
	MEAN	*3,289*	*13,657*	*8*
	COV	*0.08*	*0.08*	*0.08*
203x19.1 (Lxdiam.)	FF-MC6	6,066	25,619	6
	FF-MC7	5,027	18,641	5
	FF-MC8	5,235	21,185	5
	FF-MC9	2,030	15,527	4
	FF-MC10	5,928	21,477	5
	MEAN	*4,857*	*20,490*	*5*
	COV	*0.34*	*0.18*	*0.18*
305x12.7 (Lxdiam.)	FF-MC11	3,942	18,252	11
	FF-MC12	4,576	22,797	14
	FF-MC13	4,326	22,658	14
	FF-MC14	4,060	20,045	12
	FF-MC15	2,711	22,088	13
	MEAN	*3,923*	*21,168*	*13*
	COV	*0.18*	*0.09*	*0.09*
305x19.1 (Lxdiam.)	FF-MC16	2,603	22,825	6
	FF-MC17	6,218	25,814	6
	FF-MC18	2,020	19,447	5
	FF-MC19	3,376	24,563	6
	FF-MC20	4,267	25,174	6
	MEAN	*3,697*	*23,564*	*6*
	COV	*0.44*	*0.11*	*0.11*

[a] Adjusted peak load = Peak load on a per lag screw basis divided by NDS load duration factor (C_d = 1.6)
[b] Ratio of Adjusted peak load and NDS yield model prediction for design value.

Table 2.2 Monotonic connection test results for connections utilizing 254 x 12.7 mm lag screws**.**

Lag size (mm)	Test	Energy (N-m)	[a]F_{peak} adj. (N)	[b]F_{peak} adj./NDS
254x12.7 (Lxdiam.)	SC-MC1	4,264	11,816	5
	SC-MC2	*3,150	10,008	4
	SC-MC3	4,041	10,565	4
	SC-MC4	*3,351	10,148	4
	SC-MC5	*3,182	11,677	5
	SC-MC6	4,475	12,233	5
	SC-MC7	4,033	10,704	5
	SC-MC8	*4,040	12,094	5
	SC-MC9	3,936	10,287	4
	SC-MC10	4,431	11,955	5
	MEAN	*3,890*	*11,148*	*5*
	COV	*0.13*	*0.08*	*0.08*

[a] (Adjusted peak load) Peak load on a per lag screw basis divided by NDS load duration factor (C_d = 1.6)
[b] Ratio of Adjusted peak load and NDS yield model prediction for design value. (Design value = 2,349N)
*Tests reached an 80% post peak load and energy dissipation was calculated up to 80% post peak load.

Table 2.3 Average cyclic EEEP connection parameters calculated.

Value	F_{peak} (N)	Δ @ F_{peak} (m)	$F_{failure}$ (N)	$\Delta_{failure}$ (m)	$F_{EEEP\ yield}$ (N)	$\Delta_{EEEP\ yield}$ (m)	k_e (N/m)	EEEP (N-m)	D
Mean	25,000	0.0271	20,000	0.0364	22,000	0.0044	5,722,000	762	9
COV	0.14	0.25	0.14	0.13	0.13	0.26	0.34	0.20	0.19

Table 2.4 Average calculated hysteretic parameters for cyclic log connection tests.

Primary Cycle #	Δ_{max} (m)	Δ_{min} (m)	F @ Δ_{max} (N)	F @ Δ_{min} (N)	Strain Energy (N-m)	Hysteretic Energy (N-m)	ζ	Cyclic Stiffness (N/m)
2	0.0012	-0.0010	10,000	-7,000	9	9	0.151	8,104,000
4	0.0039	-0.0037	15,000	-15,000	58	37	0.100	4,088,000
6	0.0096	-0.0094	18,000	-21,000	182	134	0.117	2,046,000
8	0.0211	-0.0213	18,000	-25,000	458	308	0.107	1,022,000
10	0.0362	-0.0360	16,000	-23,000	704	385	0.091	540,000
12	0.0520	-0.0508	7,000	-14,000	533	314	0.102	204,000
14	0.0669	-0.0660	2,000	-7,000	308	170	0.100	71,000
16	0.0826	-0.0810	2,000	-4,000	218	127	0.109	33,000
18	0.0984	-0.0966	1,000	-4,000	250	132	0.109	27,000

CHAPTER 3

Performance of Log Shear Walls Subjected to Monotonic and Reverse-Cyclic Loading

ABSTRACT

Lateral loads in buildings due to wind and earthquake loads are primarily resisted by shear walls and horizontal diaphragms. Log buildings differ from light-frame wood buildings in that walls are formed by stacking horizontal layers of logs, where log cross-section, grade, and construction details vary from one manufacturer to the other. Seismic performance and load behaviors are reasonably well understood for light-frame wood construction; however, this is not true for log construction. For this reason, research is needed to develop this knowledge base for log wall construction to meet modern building code provisions. In this study, monotonic and reverse-cyclic tests were conducted on 1:1, 2:1 and 4:1 aspect ratio log shear walls. Tested walls typically provided higher resistance than conventional light-frame shear walls and showed similar hysteretic behavior to that of ordinary concrete and masonry shear walls because of pinching that occurred. Walls exhibited the ability to withstand large displacements without reduction in load yet seemed unstable in the out-of-plane direction for the configurations tested.

INTRODUCTION

Lateral loads on low-rise buildings due to wind and earthquake events are primarily resisted by horizontal diaphragms and shear walls. Recommended design, or resistance, values for light-frame wood shear walls are published in the Engineered Wood

Construction Guidelines (APA, 2000) and the International Building Code or IBC (ICC, 2006). The IBC also provides means of calculating seismic loads on low-rise buildings using an *equivalent lateral force* method based on the provisions of ASCE 7-05 (ASCE/SEI 7-05, 2005). This method requires knowledge of the wall system ductility and strength beyond the initial wall yield point. Seismic performance and load behaviors are reasonably well understood for light-frame wood construction; however, this is not true for log construction. Experimental studies of shear walls help engineers to understand and improve the behavior of shear walls under dynamic loading, and to improve seismic design approaches and codes (van de Lint, 2004). For this reason research is needed to develop this knowledge base in order for log wall construction to become more codified.

Log buildings differ from light-frame wood buildings in that walls are formed by stacking horizontal layers of logs where log cross-section, grade, and construction details vary from one manufacturer to another. Log shear wall construction can be broadly classified into two categories - spike connections, and through-bolt connections. The spiked connection construction consists of bolting the base log to the foundation utilizing anchor bolts protruding from the foundation slab or wall. Subsequent courses are then secured with either spikes or lag screws, typically spaced approximately 610 mm on center. The through-bolt connection construction consists of galvanized threaded rods passing through logs with pre-drilled oversized holes and secured to the foundation at predefined spacings. The base log is bolted to the foundation, and then the subsequent courses are stacked and secured in place at fixed intervals by bolting them together through the continuous threaded rods extended from the foundation. Corners are typically

constructed using a saddle notch, and are secured with a similar system of threaded rods located near the ends of the logs. Additionally, log structures can be classified as being hand crafted, where the log courses are scribed and cut to get a precise fit between individual courses, or as milled log construction, where the interfaces between log courses have been machined and provide flat, uninterrupted surfaces where courses are stacked.

Two approaches can be used to develop design values for log shear walls. A *prescriptive* approach involves laboratory testing of common constructions and publishing adjusted design values for walls constructed according to the prescriptive construction techniques. This method has advantages in that it is simple to implement; however, it may not apply to constructions different from those tested. Another approach is to develop an *engineering mechanics-based* design methodology. Utilizing this method one can use models of fastener behavior, friction between logs and crushing of the wood to predict the performance of a wall assembly. For example, Scott et al. (2005) developed a finite element model of a log wall based on data obtained from preliminary testing of walls done by Shrestha et al. (in press). Of course, some level of testing would still be required to validate the engineering models.

Research is also needed to understand the yielding behavior of log wall assemblies so that seismic loads on the building can be determined using the *equivalent lateral force* method. Experimental testing is needed to determine what effects fasteners used specifically in the construction of log shear walls have on the ductility and energy dissipation of these walls, in addition to their contribution to the strength and stiffness of the walls. The ICC draft Standard on Log Construction (ICC IS-LOG, 2005) states that,

"Log walls shall be designed to resist wind and seismic loads, gravity loads and uplift loads in accordance with applicable load standards." The IBC (ICC, 2006) seismic design procedures do not specifically accommodate log construction as an option when selecting a basic seismic-force-resisting system. Therefore, designers are forced to use the "other systems" category for the basic seismic-force-resisting system, which potentially results in overly conservative design values. Based on cyclic shear wall testing results, recommendations could be made for estimating seismic performance factors using the methodology developed from the Applied Technology Council ATC-63 Project (ATC, 2007). These factors then could be used for use with IBC (ICC, 2006) seismic design procedures, which would allow designers to more efficiently design code conforming log structures in regions of moderate to high seismic activity.

The study reported herein evaluated the performance of full-scale log shear walls, where the logs were connected with lag screws, 12.7 mm in diameter and 254 mm long, and subjected to a displacement controlled CUREE quasi-static cyclic loading protocol (Krawinkler et. al., 2001). Walls were tested in-plane only and conservatively omitted intersecting walls (pilasters) at their ends and gravity loads that would be applied along the length of the top of the wall. Three different aspect ratios (height: length) were studied - 1:1(2.44 m x 2.44 m), 2:1(2.44 m x 1.22 m) and 4:1(2.44 m x 0.61 m). The objectives of the study were as follows:

1) quantify the seismic response parameters for the selected log wall construction for use as a lateral force-resisting system (LFRS)
    i. energy dissipation
    ii. cyclic stiffness, and it's degradation

iii. peak load

iv. displacement capacity at peak load and failure

v. yield load and corresponding displacement

vi. ductility

vii. equivalent energy elastic-plastic parameters

2) identify where, between aspect ratios, these walls transition between behaving as a shear wall to behaving as a cantilever beam.

3) develop design recommendations for log shear walls to improve the accuracy, safety, and consistency of the design process.

LITERATURE REVIEW

According to the National Association of Home Builders (NAHB) there are currently 400-500 manufacturers of log homes in the United States and more than 500,000 log homes in the United States, which accounts for about 7% of the custom homebuilding market (NAHB, 2007). Log construction is also an industry which makes use of dead and damaged trees thereby creating a market for this underutilized material. Keegan et al. (2000) noted that in Montana, one of the most popular states for log home manufacturers and producers, nearly 80% of the material used for log construction was procured from standing dead trees, mostly those killed by insects and wildfires. As of 2001, Idaho and Montana were among the top ten states for log home production in the United States (NAHB, 2007). Log home sales figures have more than doubled to $1.7 billion since 1995 (NAHB, 2007).

Hahney (2000) presented an overview of how log buildings resist lateral loads. Specifically in regards to seismic loads, he emphasized the importance of all logs in the building being adequately secured to the foundation so that uplift is prevented. Once uplift is eliminated, then friction and interlocking joinery work to the buildings' advantage (Hahney, 2000). This advantage explained by Hahney is friction developed between log courses as they slide across one another allowing the interlocking joinery at the ends to supply resistance to this sliding and the global lateral deflection.

Scott et al. (2005) studied anchorage details and the base shear capacity for log buildings. Friction, static and quasi-static cyclic tests were performed on sill logs mounted to a foundation. Conclusions included that sill logs served as a source of energy dissipation and that connection details had capacities against lateral loading greater than required for the UBC Seismic Zone 4.

Yeh et al. (2006) studied the effect that openings had on the racking strength of structural log walls. Yeh performed monotonic racking tests on 6 types of walls 2.1 m high and 2.4 m in length, which is an aspect ratio of approximately 1:1. Five wall types were constructed using 102x152 mm D-logs and one wall type was constructed using 152 x 152 mm D-logs. D-logs have been machined square on three faces leaving the fourth face as the natural curvature of the log. Lag screws 200 mm in length and 9.5 mm in diameter were used as the mechanical fastener in between log courses. Penetration depth of the screws into the log below was 71.1 mm which does not meet the NDS (AF&PA, 2005) requirement of 8D = 76 mm, to achieve full penetration capacity. Yeh reported that walls without openings constructed with 152 x 152 mm D-logs supplied a maximum horizontal shear strength of 11.4 kN/m. This shear strength was found to be

approximately twice that of the walls constructed with 102 x 152 mm D-logs. The major failures in the walls were found in the lower courses where lag screws went into withdrawal and the wall acted as a deformed cantilever beam (Yeh, 2006). It was also observed that vertical openings between log courses occurred on the end of the wall where load was applied. Yeh reported that that the improvement in the racking performance of a D-log wall might be achieved through the size, number, and penetration depth of lag screws.

Salenikovich (2000) conducted a study on the performance of light-frame shear walls. The objective was to obtain performance characteristics of shear walls with various aspect ratios and overturning restraint via experimental testing and analytical modeling. Walls at 1:1 aspect ratios (2.4 m x 2.4 m) with intermediate anchorage were connected to a rigid base with 15.9 mm diameter anchor bolts made of A307 steel which spaced at 610 mm o.c. Oriented Strand Board (OSB) shear panels were fastened to 51 x 102 mm Spruce-Pine-Fir (SPF) studs spaced at 406 mm using 8d brite common nails. The nailing pattern was 152 mm around the wall perimeter and 305 mm along interior studs. Results from monotonic and cyclic shear wall tests indicate peak shear strengths of 4.9 kN/m and 5.1 kN/m, respectively.

Currently there are no documented or published experimental studies on the hysteretic properties or equivalent energy elastic plastic properties of log shear walls subjected to reverse-cyclic loading such as hysteretic energy, strain energy, equivalent viscous damping and ductility. Clearly more experimental data are needed to be able to effectively understand and design these structures for the wide range of construction techniques that are employed throughout the log building industry. Numerous studies

have been conducted on wood-frame shear walls and have led to a good understanding of those systems. This study is intended to provide a foundation on which to conduct further studies on the performance of log shear walls to gain similar understanding of them as compared to wood-framed shear walls.

METHODS AND MATERIALS

Materials

Many types of log species are used in the log construction industry but are typically softwood species. Engelmann Spruce, Lodgepole Pine and Grand Fir logs were obtained from Edgewood Log Homes of Athol, ID USA. Logs were harvested in North Idaho and were of log grade LHC #1. All logs were 254 mm in diameter and machined with a Swedish Cope profile to a stack height (measured from the apex of the Swedish Cope to the apex of the top of the log) of 229 mm. Zinc plated hex lag screws were 254 mm long and 12.7 mm in diameter and consisted of full body diameter on the unthreaded portion of the screw as shown in NDS Table L2 (AF&PA, 2005). All lag screws were manufactured from A307, Grade 2, low carbon steel. Anchor bolts installed in the sill log were 15.9 mm in diameter.

Wall Construction

Three different wall aspect ratios of 1:1, 2:1 and 4:1 were utilized as test specimens. The wall with a 1:1 aspect ratio had dimensions of 2.4 m:2.4 m (height: length) while 2:1 and 4:1 aspect ratio walls were 2.4 m:1.2 m and 2.4 m:0.6 m respectively. Each wall consisted of 10 full courses and one sill log.

In typical log wall construction, the bottom log, referred to as the sill log, is either bolted to the subfloor or directly onto the foundation by means of an embedded anchor bolt in the foundation. A typical sill log is half or three-fourths of a log profile. For the current study, the sill log was a half log and was mounted with anchor bolts to a rigid floor beam to mimic a direct contact with the foundation (Figure 3.1). Countersink holes 25.4 mm deep and 50.8 mm in diameter were drilled as well as a through hole oversized by 3.2 mm to facilitate placement of the anchor bolts. Lag screws were spaced at 610 mm o.c. down the length of each successive log course above the sill log except for the 4:1 aspect ratio walls, where lags were spaced at 203 mm o.c. As each log course was placed on top of the next the lag screw spacing pattern remained constant but was offset by 152 mm for the 1:1 and 2:1 aspect ratio walls while the 4:1 aspect ratio walls were offset by 76.2 mm to avoid having fasteners drilled directly down into a fastener in the course below. End distances alternated every other log course up the height of the wall because of the previously mentioned offset. The minimum end distance is of the most concern. Therefore, the two alternating minimum end distances for each end of the walls was 305 mm and 152 mm, 305 mm and 152 mm, and 152 mm for 1:1, 2:1, and 4:1 aspect ratio walls, respectively. All end distances in the current study were greater than all minimum end distance requirements found in the NDS (AF&PA, 2005).

Typically in log wall construction lag screws and anchor bolts are tightened down to the point of significant wood crushing underneath the washer heads. This induces vertical compression forces in the wall and tension forces within the mechanical fasteners. While in service, the logs will experience shrinkage and stress relaxation. These phenomena will reduce the vertical compression forces between log layers and can

result in gaps underneath the head of the bolt which reduces the contribution of friction towards wall shear capacity. For this study, walls were fabricated by tightening the lags and anchor bolts just to the point where the washers made contact with the log with no wood crushing, thereby conservatively minimizing resistance due to friction between log layers.

Test Methods

Log shear wall tests were conducted according to Standard Test Methods for Cyclic (Reversed) Load Test for Shear Resistance of Walls for Buildings (ASTM E2126-05) (ASTM, 2006). Standard Test methods for Static Load Test for Shear Resistance of Framed Walls for Buildings (ASTM E564-06) (ASTM, 2006) was used as a guideline for determining a load rate for monotonic tests. Monotonic wall tests were used to develop a reference deformation for the cyclic tests which will be discussed later. Therefore, loads were not applied and released at stepped increments as outlined in ASTM E 564-06. Six different data acquisition channels were monitored during every test as follows:

a) Lateral displacement of top log (global)

b) North full wall uplift (attached to floor and end of Log 10, closest to actuator)

c) South full wall uplift (attached to floor and end of Log 10 away from actuator)

d) Bottom slip

e) Log #3 lateral displacement (global)

f) Log #6 lateral displacement (global)

Figure 3.2 gives a schematic drawing of how these channels were monitored and attached. The first monotonic test was conducted on a 2:1 aspect ratio wall and

conducted at a load rate of 2.5 mm/min. This load rate was decided on based on tests that were conducted by Forintek Canada Corp. (Popovski, 2002) on walls consisting of 1:1 aspect ratios (2.44 m x 2.44 m) with a load rate of 7.6 mm/min. The load rate was determined to be too slow as it exceeded the upper time limit of 20 minutes set forth in ASTM E564-06 (ASTM, 2006). All other monotonic tests were conducted at a load rate of 12.7 mm/min in order to meet this upper time limit.

Reverse-cyclic tests were conducted in conformance with ASTM E2126-05 (ASTM, 2006). The Consortium of Universities for Research in Earthquake Engineering (CUREE) (Krawinkler et. al., 2001) displacement controlled quasi-static cyclic loading protocol was carried out on all walls at a frequency of 0.25 Hz with upper and lower displacement limits of 112 mm and -112 mm respectively. For this study a total of 19 primary cycles were carried, out which nearly exceeded stroke limit (±127 mm) of the hydraulic actuator.

Considering that monotonic wall tests never reached $0.8F_{peak}$ at a useable deformation for the CUREE protocol, a rationale was developed to define the reference deformation Δ as an input into the CUREE protocol. Acceptance Criteria for Prefabricated Wood Shear Panels (AC130) (ICC-ES, 2004) defines the inelastic response drift (δ_x) as the lesser of the inelastic drift limit or allowable drift (Δa) defined in the 2006 IBC (ICC, 2006) via ASCE 7-05 (ASCE/SEI 7-05, 2005) or the mean displacement at the *strength limit state* (Δ_{SLS}) of the tested wall assemblies. The allowable drift in ASCE 7-05 (ASCE/SEI 7-05, 2005) was determined to be the controlling δ_x based on the lateral deflections obtained from the first monotonic test. The deflection amplification factor (C_d) and the seismic response modification factor (R) for log walls must also be known in

order to utilize AC130. Without test data and non-linear analysis, an R-factor is difficult to accurately estimate. Nevertheless, an educated R-factor estimation of 3, using monotonic test observations and test data, was decided upon in order to proceed with the current study. For the tested walls, Δ was determined to be Δ_a based on provisions in the IBC and was divided by the designated R-factor of 3 to result in a final CUREE reference deformation of 16mm.

Shear walls in any structure are held down to some extent at their ends by floor and/or roof diaphragms, and dead weight from above by walls, roofs and floors. The degree to which those walls are held down in order to develop a realistic hold down method for these log shear wall tests was unclear. The case of fully holding the walls down and completely restricting uplift generates unrealistic friction between log courses and would result in non-conservatively high strength values from test data. On the other hand, allowing the walls to freely uplift at their ends without hold downs would result in low friction between log courses. This would yield conservative strength values because of the fact that walls are held down to some degree, thereby producing some friction between log courses as discussed previously. It was decided that the log walls would not be held down to any degree in order to obtain conservative experimental test results and intersecting pilaster walls at the shear wall ends were omitted for the same reason.

A steel load beam used to apply the reverse-cyclic loads was attached to the top log of each wall, and was allowed to slide between lateral roller restraints in order to ensure unidirectional loading along the length of the wall. Lag screws 203 mm long and 12.7 mm in diameter were adequately to fasten the load beam to the top log making the

load beam rigid to effectively transfer the load into the wall. Figure 3.3 illustrates the overall test setup.

Moisture Content and Specific Gravity Measurements

Moisture content (MC) and specific gravity (SG) samples were taken from the approximate center of each of the tested log specimens and were 102 mm in length and width and 25.4 mm in thickness. Test methods outlined in ASTM D4442-92 (ASTM, 2003) were used for MC. Each specimen's "wet" weight was measured and then placed in a forced-convection oven at a temperature of 103°C for 48 hours. The oven-dry weight was then measured and used for calculating MC using ASTM D4442-92 (ASTM, 2003) equation (1). ASTM D2395-02 (ASTM, 2006) Method A test methods were used to determine SG. Specimen dimensions were measured with a micrometer and were input into equation (2) of ASTM D2395-02 (ASTM, 2006) to determine SG.

Lag Screw Bending Yield Strength Tests

Lag screw bending yield moment tests (20) were conducted on the lag screws used for log wall testing in order to develop the fastener properties such as 5 % diameter offset yield strength and bending yield strength for the lag screws. No current standard exists for determination of lag screw bending yield strength, therefore, tests conformed to ASTM F1575-03 (ASTM, 2003) and were conducted using an electro-mechanical test frame. The lag screws were centered across a 147.3 mm span and loaded at their midspan at a rate of 6.35 mm/min. Load versus deflection data were recorded at a rate of

2 Hz. The bending yield strength was determined by dividing the calculated midspan moment by the lag screws effective plastic section modulus.

RESULTS AND DISCUSSION

The following section will describe the results of testing as well as some brief discussion of the results. Conclusions drawn from this section will be presented after this section as well as practical design recommendations.

The mean value of MC and SG for every wall test was measured to be 17% and 0.43, respectively. A total of twenty lag screw bending tests showed that the mean, standard deviation and COV for bending yield strength was 588 MPa, 24 Mpa and 4% respectively for the lag screws that were used as mechanical fasteners in all of the wall tests.

Definitions of Calculated Parameters

When analyzing data from a reverse-cyclic shear wall test there are parameters proposed by Dolan (1989) that are quantified based on the development of backbone curves and *equivalent energy elastic plastic* curves (EEEP), as well as parameters determined on a cycle-by-cycle basis known as *hysteretic parameters.* Both sets of parameters are calculated differently, but each yields valuable information about the wall to quantify the lateral resistance and response to reverse-cyclic loading. Parameters calculated were ductility (D), hysteretic energy, strain energy, equivalent viscous damping ratio (ζ), cyclic stiffness, elastic stiffness, equivalent energy elastic plastic (EEEP), peak load (F_{peak}), and 5% diameter offset yield. Definitions of all calculated

parameters herein were consistent with those given by Dolan (1989) although one deviation from Dolan's definitions occurred and is discussed next.

Typically, the point at which the hysteretic peaks drop below 80% of the peak load ($0.8F_{peak}$) is defined as the failure load ($F_{failure}$), and the corresponding displacement for that load is defined as the displacement failure ($\Delta_{failure}$). It is important to note that for the current study walls rarely reached $F_{failure}$ or $\Delta_{failure}$ based on the given definitions by Dolan (1989) for these parameters. Therefore, deviation from Dolan's (1989) definition occurred by defining failure on a drift limit basis as the allowable story drift in the 2006 IBC (ICC, 2006) via ASCE 7-05 (ASCE/SEI 7-05, 2005) using a category "I" occupancy for the "All other structures" designation resulting in $\Delta_{failure} = \Delta_a = 0.02h_{sx}$, where h_{sx} = story height, (i.e. height of the walls tested in this study). Failure displacement, $\Delta_{failure}$, remained constant at 48.8mm for all of the log walls. The log shear walls herein had much more reserve drift capacity but, further rationale for this failure definition was also because of the fact that the in-plane drift of a log shear wall also affects the out-of-plane drift of an intersecting wall which has a much lower drift capacity. Figure 3.4 illustrates an EEEP curve and backbone curve superimposed on a typical Load versus deflection hysteresis for a 1:1 aspect ratio wall.

All parameters were calculated with the intent that they could be used in future numerical analysis to determine the Seismic Performance Factors, based on the recommended methodology developed from the ATC-63 Project (ATC, 2007), for use in the improvement of seismic design methods and codes for log shear walls.

Failure Modes

One monotonic test and three reverse-cyclic tests were conducted for each wall aspect ratio. All walls typically exhibited failure modes caused by wood crushing under the washers of the sill log anchor bolts and wood crushing under lag screw washers in Logs 1-4. Although, for the 1:1 aspect ratio walls, lag screw withdrawal from the sill log occurred as the primary failure mode. The combined effect of these failures produced an average uplift on the north and south wall ends of 99 mm for 1:1 walls. The 2:1 and 4:1 walls uplifted 48% and 75% less, respectively, at their north and south ends than the 1:1 walls. There were no visible indications of any bending or shear plastic deformations of the lag screws in any of the walls. Large vertical openings between log courses from Logs 1 through 4 at the wall ends occurred comparable to a zipper being unzipped while the upper Log courses 5 through 10 showed almost no sign of vertical opening between courses. Logs 5 through 10 exhibited rigid body rotation as the walls deflected laterally and lifted up. For the 1:1 aspect ratio walls, the lag screw withdrawal that occurred in the sill log from Log 1 above was most likely due to inadequate penetration of the lag screw of only 102 mm when all other lag screws penetrated 152mm into the log below. Slip of the sill log was minimal as it accounted for 1 to 3% of the total lateral deflection measured at the top of the wall. The lower percentage occurred in the higher aspect ratio walls. The failure mode that the walls exhibited caused nearly a no-slip condition between log courses.

When installing the lag screws into the walls, it was nearly impossible to keep each log perfectly plumb with the log below. The nature of the cope along the bottom of each log and different log imperfections caused the logs to settle where the surfaces

mated best together and was unavoidable during fabrication. These logs that were slightly out of plumb caused slight instabilities during cyclic tests which led to significant movement out-of-plane at times but this did not appear to affect the shear strength or behavior of the specimens. Once logs were stacked higher than 1.5 m, out-of-plane instability became a concern which necessitated bracing during construction.

Monotonic Horizontal Shear Strength

Results from monotonic tests indicate that the peak horizontal shear strength (V_{peak}) for a 1:1 aspect ratio was 11.7 kN/m at a deflection of 154 mm and agreed closely at 3% greater than the value found by Yeh (2006) of 11.4 kN/m at 150 mm for 152x152 mm D-logs that were tested in conformance with ASTM E564 (ASTM, 2006). Although test methods were not identical to those used by Yeh (2006), it is still valid to make this comparison for peak horizontal shear strength, being that both tests were monotonic. Considering that the walls in this study were more conservatively constructed for field conditions and not held down, it is speculated that the higher depth of lag screw penetration of 152 mm compared to 71.1 mm in work done by Yeh (2006) attributed to the wall in the current study having higher horizontal shear strength. This indicates the importance of adequate lag screw penetration. The 2:1 and 4:1 walls had peak horizontal shear strengths of 5.6 kN/m at a corresponding displacement of 178 mm, and 4.6 kN/m at 236 mm, respectively. It is also necessary to calculate the horizontal shear strength at the defined $\Delta_{failure} = 48.8$ mm ($V_{failure}$) . At $\Delta_{failure}$ the 1:1 aspect ratio walls had a horizontal shear strength of 7.6 kN/m and a decrease of 56% and 71% occurred in strength as aspect

ratio increased from 2:1 to 4:1. Values for monotonic horizontal shear strength and seismic design shear strength can be found in Table 3.1.

Cyclic Horizontal Shear Strength

Values for cyclic horizontal shear strength and seismic design shear strength can also be found in Table 3.1. Cyclic test results compared well with monotonic test results in regards to peak horizontal shear strength for 1:1 and 2:1 aspect ratio specimens. The 1:1 aspect ratio walls had 12.1 kN/m of strength at a deflection of 90 mm, while 5.3 kN/m at 90 mm was resisted by the 2:1 aspect ratio walls, which was 3% higher and 6% lower, respectively, than results obtained from monotonic tests. Walls at the highest aspect ratio of 4:1 resisted 15% less load per unit length of the wall than was resisted in monotonic tests at a deflection of 110 mm.

The cyclic test results for horizontal shear strength at $\Delta_{failure}$ obtained for 1:1, 2:1 and 4:1 aspect ratios were, respectively, 23%, 12% and 21% higher than the values obtained from monotonic tests. However, recall that these strength values are dependent on the definition of failure displacement and, in fact, the walls have significant more load resistance than these values.

Monotonic Equivalent Elastic Plastic Parameters

All test results concerning the equivalent elastic plastic parameters decreased as aspect ratio increased with the exception of the corresponding deflection at the EEEP yield. The $\Delta_{EEEP\ yield}$ increased by 72% as aspect ratio increased. This is reasonable since if the elastic stiffness decreases as aspect ratio increases, the EEEP yield deflection must

increase as well. For the 1:1 aspect ratio an EEEP yield load ($F_{EEEP\ yield}$) of 16.8 kN was calculated at a corresponding EEEP yield displacement ($\Delta_{EEEP\ yield}$) of 25 mm resulting in elastic stiffness (k_e) of 671 kN/m. In his study of timber shear walls Dolan (1989) mentions that a wall with twice the length and mass of another wall will have approximately twice the stiffness. For these log walls that was not the case for elastic stiffness, as it increased by approximately 400% to 500% when wall length doubled. This indicates different stiffness characteristics between conventional timber shear walls and log shear walls. Figure 3.5 shows typical backbone curves for each wall aspect ratio, illustrating the increase in elastic stiffness as wall length is doubled. The decrease in $F_{EEEP\ yield}$ with respect to the 1:1 aspect ratio was 77% and 92% for 2:1 and 4:1 aspect ratios respectively. Ductility (D) ranged between 1.95 and 1.13 with the higher ductility occurring for the 1:1 aspect ratio specimens. According to the definition used, these walls exhibited a low degree of ductility, but this can be attributed in part to the way failure was defined in this study. If a wall failed at $0.8F_{peak}$ it would have a higher degree of ductility considering the point at which it failed would be a post peak load instead of pre-peak load as is this case for the defined failure point.

Cyclic Equivalent Elastic Plastic Parameters

A general trend of increasing EEEP parameters was observed when comparing the following cyclic test results to monotonic test results, once again assumedly due to the quicker load rate. It should be noted that cyclic test results are based on the average of the three tests for each aspect ratio. Ductility values increased from the lowest to highest aspect ratio and ranged between 2.33 and 1.38. $F_{EEEP\ yield}$ was calculated to be

20.1 kN/m at $\Delta_{EEEP\ yield}$ = 21 mm, 4.2 kN/m at 22 mm and 1.4 kN/m at 35 mm for 1:1, 2:1 and 4:1 aspect ratio walls respectively. The same decreasing trend observed for $F_{EEEP\ yield}$ between aspect ratios was observed for EEEP with 1:1 aspect ratios having a value of 0.76 kN-m which is 26% higher than calculated from a monotonic test.

Hysteretic Parameters

A typical cyclic Load versus deflection hysteresis for a 1:1 aspect ratio wall was previously observed in Figure 3.4. It should be noted that cyclic wall specimens for a 1:1 aspect ratio sometimes failed on the last primary cycle of a positive or negative stroke of the actuator. All walls exhibited pinching behavior similar to that of concrete shear walls. The pinching behavior in concrete shear walls is due to the fact that when cracks open up, load decreases. Although a direct comparison cannot be made between log and concrete shear walls, the vertical openings between log courses is a similar phenomena to that of cracks opening in concrete shear walls. Table 3.2 describes the changing hysteretic parameters on a cycle by cycle basis for the 1:1 aspect ratio specimens. These parameters were calculated for every other primary cycle for the tests conducted.

Equivalent viscous damping (ζ) values started at 10.4% at the first primary cycle and decreased to 5% by the last primary cycle for a 1:1 aspect ratio wall. This was a 52% decrease, with the majority of the decrease occurring between the first and third primary cycle at 35%. The other two aspect ratios exhibited the majority of decrease between the first and third primary cycle at a 40% and 47% for the 2:1 and 4:1 aspect ratio, respectively. As aspect ratio increased, equivalent viscous damping values for the first primary cycle increased but, equivalent viscous damping for the last primary cycle

decreased as seen in Figure 3.6 which is also plotted to reflect the change in strain energy with respect to lateral deflection. Typical light-frame shear walls have been shown to exhibit equivalent viscous damping values of approximately 50% which is much higher than the values found for the log shear walls herein.

Cyclic stiffness degradation was prevalent with an average of 88% decrease between the first and last primary cycle for all aspect ratios. An average plot for each aspect ratio of Cyclic Stiffness versus Lateral Deflection is shown in Figure 3.7. An engineer would like to design for an increase in cyclic stiffness for reverse-cyclic loads but this degradation can be useful when designing for a damage point. For the most part, calculated strain energy per cycle was higher than the hysteretic energy on average which is typical for a pinched system. It should be noted that actual strain energy was most likely lower than the values calculated. This is because the typical methods used to calculate strain energy are based on simplified linear approximations. An example of a typical relationship trend between hysteretic and strain energy for 1:1 aspect ratio walls can be found in Table 3.2.

SUMMARY AND CONCLUSIONS

Reverse-cyclic tests on 1:1, 2:1 and 4:1 aspect ratio log shear walls fastened with lag screws typically exhibited higher peak horizontal shear strength values than most light-frame shear walls. Specifically, the 1:1 aspect ratio walls exhibited 138% higher peak horizontal shear strength values than the light-frame walls tested by Salenikovich (2000). This was true for monotonic and cyclic tests. The 1:1 aspect ratio walls also

showed comparable peak horizontal shear strength values obtained from monotonic log wall tests to those obtained by Yeh et al. (2006).

Failure modes of cyclic wall test specimens were accredited to uplift and excessive story drift, mainly due to crushing under the heads of the washers and no indications of any lag screw yielding were observed.

Cyclic response parameters were experimentally determined, which yielded a better understanding of the behavior of log shear walls subjected to cyclic type loading similar to earthquakes. Walls exhibited pinched Load versus deflection hysteresis curves similar to that of masonry and ordinary concrete shear walls where cracks form and cause a more drastic reduction in load than is observed in walls that do not experience a high amount of pinching as cycles are reversed. The comparison was drawn that the vertical openings that form at the ends of the log walls cause a similar hysteretic pinching that occurs with crack-formation in ordinary concrete shear walls.

Based on comparisons made between systems that exhibit similar hysteretic behavior to that of the log shear walls herein, qualitative estimates of some seismic performance factors were made. ASCE 7-05 (ASCE/SEI 7-05, 2005), Table 12.2-1 lists these factors for different structural systems. It is estimated that log shear walls in the current study have an R-factor ranging between 1 and 3, and an overstrength factor between 2 and 3, as is for the previously mentioned masonry and ordinary concrete shear walls. It could be justified that higher R-factors could be applied to the walls tested herein because the walls were allowed to exhibit a rocking behavior thereby putting less energy into a log structure. Of course, R-factors (as in ASCE 7-05 Table 12.2-1) are based largely on judgment and qualitative comparisons of the known response

capabilities of LFRS in widespread use. These R-factors are somewhat arbitrarily assigned (ATC, 2007). Therefore, cyclic response parameters calculated from the experimental data herein should be incorporated into the methodology for reliably quantifying building system performance and response parameters for use in seismic design recommended in the upcoming ATC-63 Project report (ATC, 2007). This will allow for a more accurate estimation and uniform comparison of these parameters to those of other LFRS.

Considering that no hold-down devices were used, it was difficult to decipher where between aspect ratios the walls transitioned between acting as a shear wall and acting as a vertical cantilever beam. Although, a distinct similar behavior between the 1:1 and 2:1 aspect ratio walls was observed that was not exhibited by the 4:1 aspect ratio walls. All of the walls experienced rigid body rotation from Log 5 through Log 10 because of the fact that they were able to form hinge points at the ends of the walls above log 4. This is not a common response seen in any other shear walls other than these log wall tests. In essence the walls from all of the aspect ratios acted as vertical cantilever beams above Log 4 or Log 5.

Unlike light-frame wood shear walls, a major concern arose from the current study because of the out-of-plane behavior that these walls exhibit. Slight eccentricities in log wall construction introduced out-of-plane instabilities even when subjected to in-plane loads. Further concern for the out-of-plane behavior and strength of log walls is introduced when the walls may be loaded out-of-plane because they act as stacked roller bearings in the out-of-plane direction.

Specific recommendations for log shear wall design and future research derived from this study include the following:

- When half profile sill logs are used, anchor bolts that are embedded in the foundation should pass up through the sill log and connect into Log 1. This is because of the failure seen in the 1:1 aspect ratio walls where lag screws penetrating into the sill log from Log 1 withdrew. This was due to a lack of sill log thickness which did not allow for adequate lag screw penetration.
- Restrain uplift at wall ends.
- Increase the diameter of countersink holes and use larger diameter washers to prevent the heads of the lags and washers from pulling through the log. This will allow the threads of the lag screw to be engaged more, taking advantage of the withdrawal capacity gained at the penetration depth of 12D.
- The strength and energy dissipation of 4:1 aspect ratio walls and higher should be neglected when in line with lower aspect ratio walls. This is clearly observed in Figure 3.5.
- Recommend against the design of multi-story log walls unless intermediate brace points, such as floor diaphragms, exist. This is because log walls are susceptible to out-of-plane buckling due to P-delta effects which are intensified by increasing gravity loads and wall heights.
- Conduct further research to assess the out-of-plane behavior and strength of log shear walls in order to develop design methodology that addresses

this unique characteristic of log shear walls. Also, further research should be conducted on log shear walls that utilize different techniques for fastening log courses as well as walls with fully restrained end conditions.

- Any wall without an intersecting wall at its end should be braced out-of-plane during construction once logs have been stacked higher than 1.5 m.
- In the lower half of log courses, avoid installing logs with checks that extend parallel to the log grain with check openings that face in the out-of-plane direction of the wall (if hold downs are not installed). This will avoid further opening the checks thereby increasing uplift and decreasing horizontal shear strength capacity.
- The results herein should now be used to conduct non-linear analysis of log building systems following the provisions and methodology in the ATC-63 Project (ATC, 2007) to determine seismic performance factors such as the seismic response modification factor (R), deflection amplification factor (C_d), and the overstrength factor (Ω_0). Development of these seismic performance factors will aid in incorporating log structures into the IBC seismic design procedures.

REFERENCES

American Forest and Paper Association, Inc (AF&PA) 2005. *National Design Specification for Wood Construction ASD/LRFD*. Washington, DC: AF&PA.

American Plywood Association (APA). 2000. Design/Construction Guide, APA – The Engineered Wood Association, Tacoma, Washington.

Applied Technology Council (ATC) (2007). "ATC-63 Project: Quantification of Building System Performance and Response Parameters." http://www.atcouncil.org/atc63.shtml. (75% draft due end of February, 2007).

ASCE/SEI 7-05. 2005. Minimum Design Loads for Buildings and Other Structures. American Society of Civil Engineers. Reston, VA.

ASTM Standards. 2003. D 4442-92 Standard Test Methods for Direct Moisture Content Measurement of Wood and Wood-Base Materials. West Conshohocken, PA: ASTM.

ASTM Standards. 2006. D 2395-02 Standard Test Methods for Specific Gravity of Wood and Wood-Based Materials. West Conshohocken, PA: ASTM.

ASTM Standards. 2006. E 2126-05 Standard Test Methods for Cyclic (Reversed) Load Test for Shear Resistance of Walls for Buildings. West Conshohocken, PA: ASTM.

ASTM Standards. 2006. E 564-06 Standard Practice for Static Load Test for Shear Resistance of Framed Walls for Buildings. West Conshohocken, PA: ASTM.

ASTM Standards. 2003. F1575-03 Standard Test Method for Determining Bending Yield Moment of Nails. West Conshohocken , PA: ASTM.

Dolan, J. D., (1994). "Proposed Test Method for Dynamic Properties of Connections Assembled with Mechanical Fasteners." *ASTM Journal of Testing and Evaluation*. 22(6):542-547.

Dolan, J.D. (1989). "The Dynamic Response of Timber Shear Walls." University of British Columbia, Vancouver, British, Columbia. Ph. D. dissertation.

Hahney, Tom. (2000). "How Log Buildings Resist Lateral Loads." *Log Building News*; Number 32.

International Code Council Evaluation Service, Inc. (ICC-ES). 2004. *Acceptance Criteria for Prefabricated Wood Shear Panels (AC 130)*. Whittier, CA, U.S.A. International Code Council Evaluation Service, Inc.

International Code Council, Inc. (ICC). 2006. *International Building Code 2006*. Falls Church, VA: International Code Council, Inc.

International Code Council, Inc. (ICC IS-LOG). 2005. *ICC Standard on Log Construction* (*ICC/ANSI 400-2005)*. Country Club Hills, IL, U.S.A. International Code Council, Inc. (Rough Draft)

Keegan, C.E., A. Chase, S. Shook, and D.D. Van Hooser. 2000. "Montana's log home industry." *Montana Business Quarterly* 38(4):2-9.

Krawinkler, Helmut, Parisi, Francisco, Ibarra, Luis, Ayoub, Ashraf, and Medina Ricardo, (2001). "Development of a Testing Protocol for Wood Frame Structures (CUREE Publication No. W-02)", CUREE, Richmond, CA.

National Association of Home Builders (NAHB). 2003. National Association of Home Builders Web Site: http://www.nahb.org/generic.aspx?genericContentID=10227.

Popovski, Marjan, (2002). "Testing of Lateral Resistance of Handcrafted Log Walls Phase I and II." Forintek Canada Corp. Project No. 3512/3512A. Prepared for International Log Builders Association (ILBA).

Salenikovich, Alexander (2000). "The Racking Performance of Light-Frame Shear Walls". Virginia Tech; PhD Dissertation.

Scott, Randy J., Leichti, Robert J., and Miller, Thomas M., (2005). "An experimental investigation of foundation anchorage details and base shear capacity for log buildings.", *Forest Products Journal*. 55(4):38-45.

Scott, Randy J., Leichti, Robert J., and Miller, Thomas M., (2005). "Finite-element modeling of log wall lateral force resistance.", *Forest Products Journal*. 55(9): 48-54.

Shrestha, Deepak, Carradine, David M., and Gorman, Thomas M., (2006). "Effects of Construction Configuration on the Shear Resistance of Log Shear Walls Subjected to Reversed Cycling Loading", *Prepared for publication in the Forest Products Journal*.

van de Lint, John W. (2004). "Evolution of Wood Shear Wall Testing, Modeling, and Reliability Analysis: Bibliography." *Practice Periodical on Structural Design and Construction.* 9(1):44-53.

Yeh, Min-chyuan, Chiang, Chi-lung, and Lin, De-tsai, (2006). "Effect of openings on the racking strength of structural log walls", *Forest Products Journal*. 56(11/12): 137-141.

NOTATION

The following symbols are used in this paper:

δ_x = inelastic response drift (m or mm)

Δ = reference deformation (m or mm)

Δ_a = allowable drift (m or mm)

$\Delta_{EEEP\ yield}$ = deflection corresponding to equivalent energy elastic plastic yield (m or mm)

$\Delta_{failure}$ = failure deflection (m or mm)

Δ_m = monotonic deformation capacity (m or mm)

Δ_{max} = maximum deflection (m or mm)

Δ_{min} = minimum deflection (m or mm)

Δ_{SLS} = deflection at strength limit state (m or mm)

ζ = equivalent viscous damping ratio

C_d = deflection amplification factor

COV = coefficient of variation

CW = cyclic wall test

D = ductility ratio

EEEP = equivalent energy elastic plastic (N-m or kN-m)

F = load (N or kN)

$F_{EEEP\ yield}$ = load corresponding to equivalent energy elastic plastic yield (N or kN)

$F_{failure}$ = load corresponding to failure (N or kN)

h_{sx} = story height (m or mm)

k_e = elastic stiffness (N/m or kN/m)

MC = moisture content (%)

MW = monotonic wall test

R = seismic response modification factor

SC = Swedish cope

SG = specific gravity

$V_{failure}$ = horizontal shear strength per unit length of wall at failure load (N/m or kN/m)

$V_{failure\ design}$ = design unit shear strength at failure (kN/m)

V_{peak} = horizontal shear strength per unit length of wall at peak load (N/m or kN/m)

$V_{peak\ design}$ = design unit shear strength at peak load (kN/m)

LIST OF FIGURES

Figure 3.1 Sill log attachment to rigid floor beam.

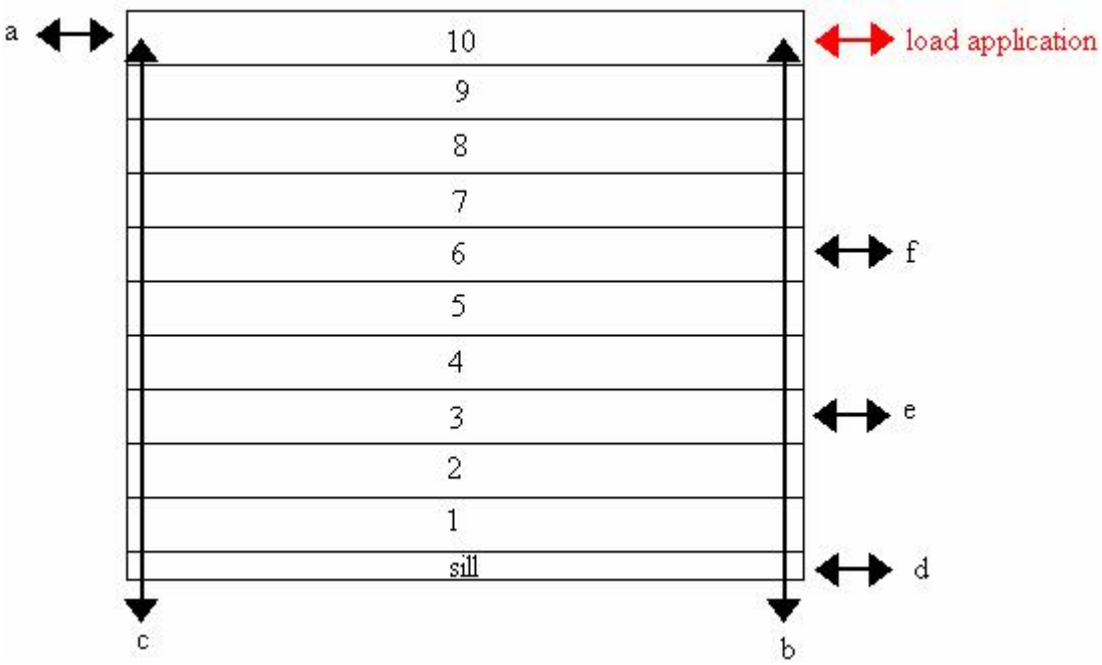

Figure 3.2 Schematic of data acquisition channels monitored and log references for cyclic and monotonic wall tests.

Figure 3.3 Overall test setup (Note: Wall shown has 1:1 aspect ratio).

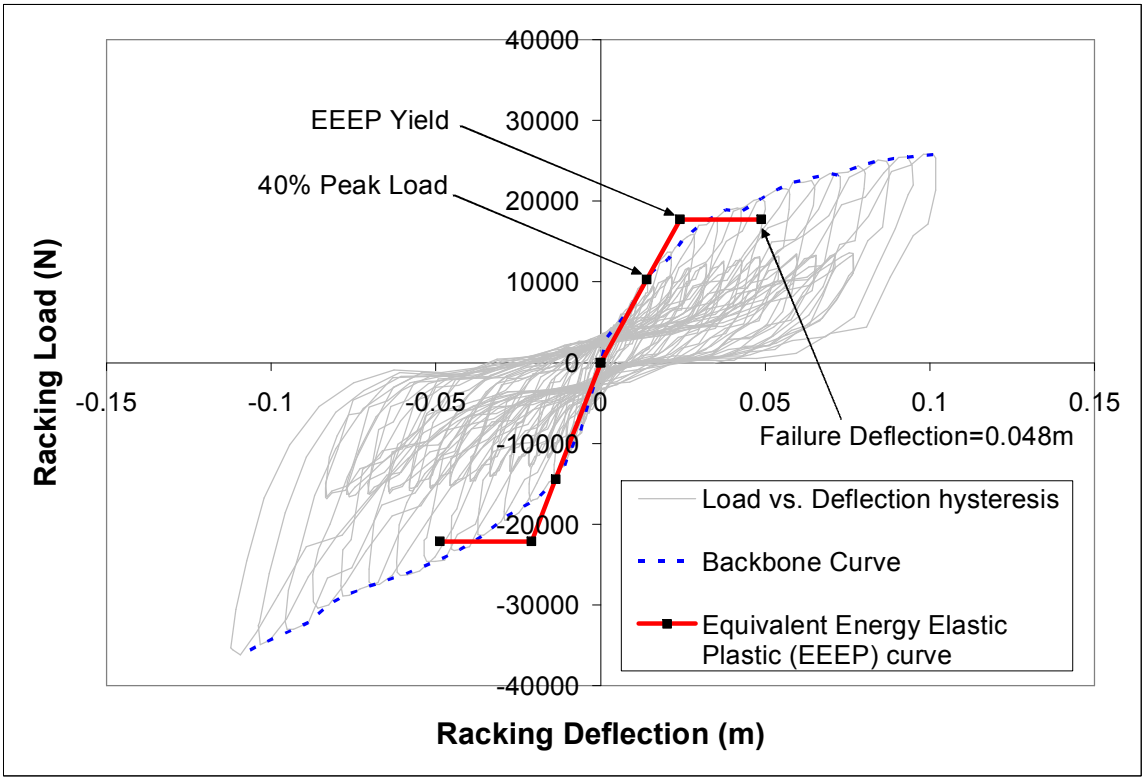

Figure 3.4 EEEP curve and Backbone curve superimposed on a typical Load versus deflection hysteresis for a 1:1 aspect ratio wall.

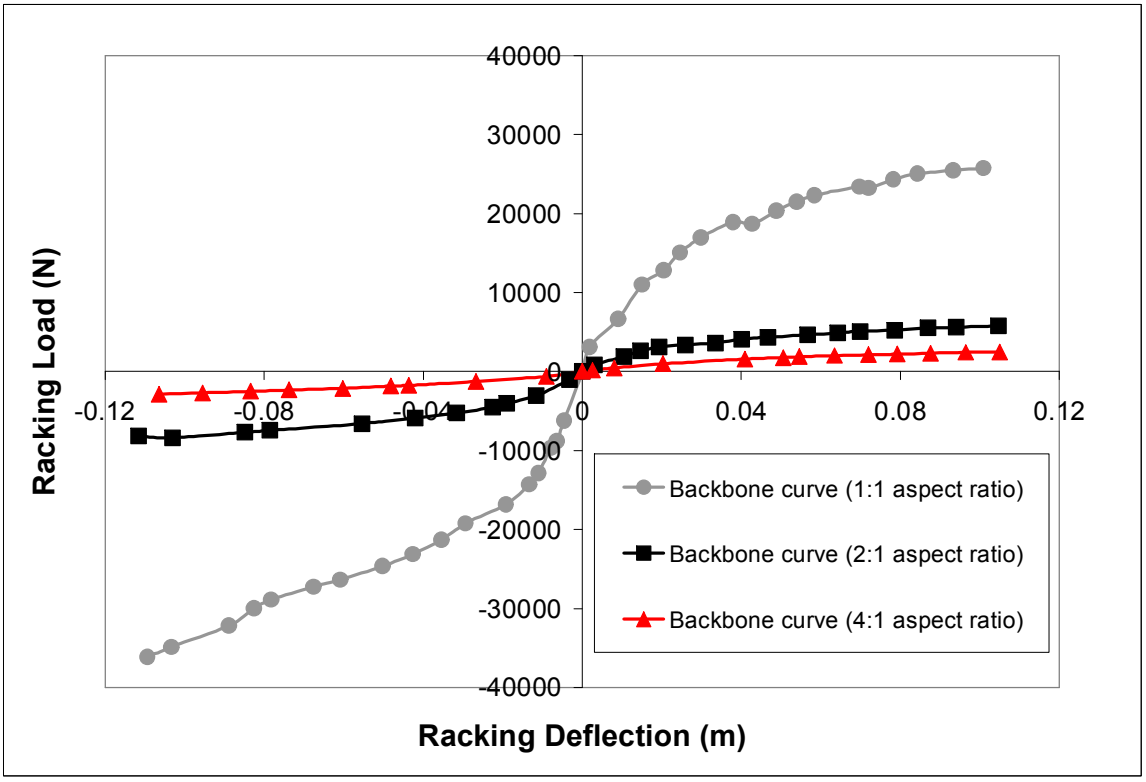

Figure 3.5 Typical Backbone curves for each wall aspect ratio.

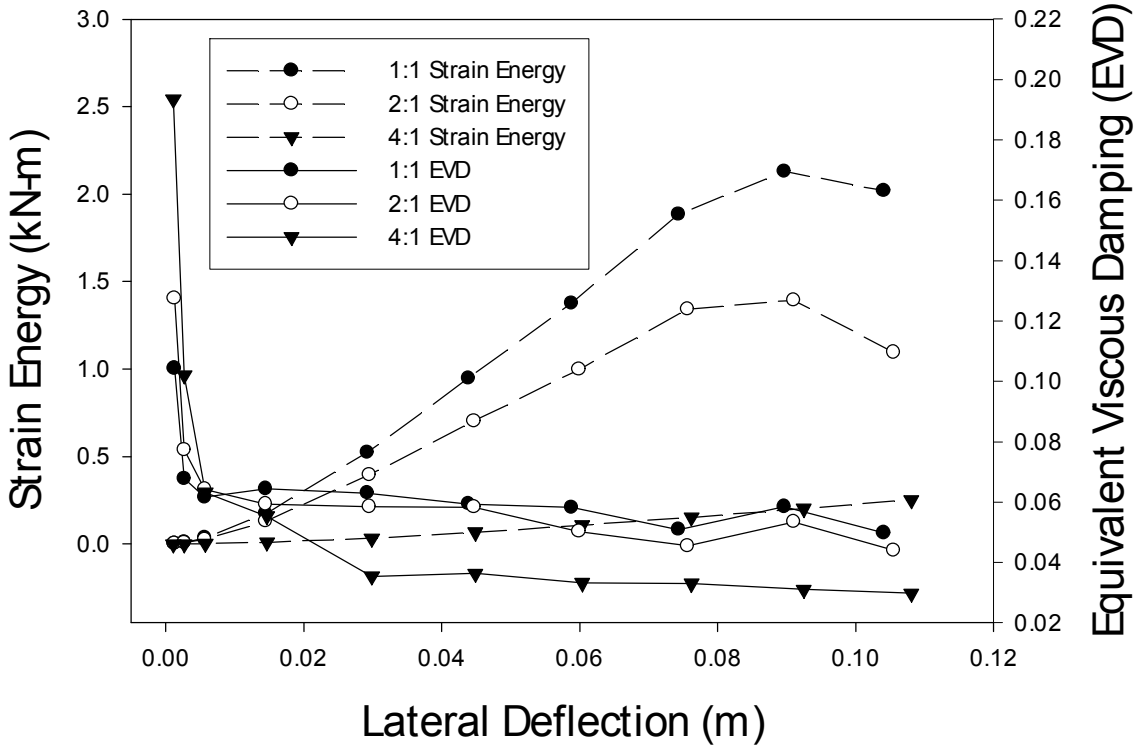

Figure 3.6 Average Equivalent Viscous Damping and Strain Energy vs. Lateral Deflection for each wall aspect ratio.

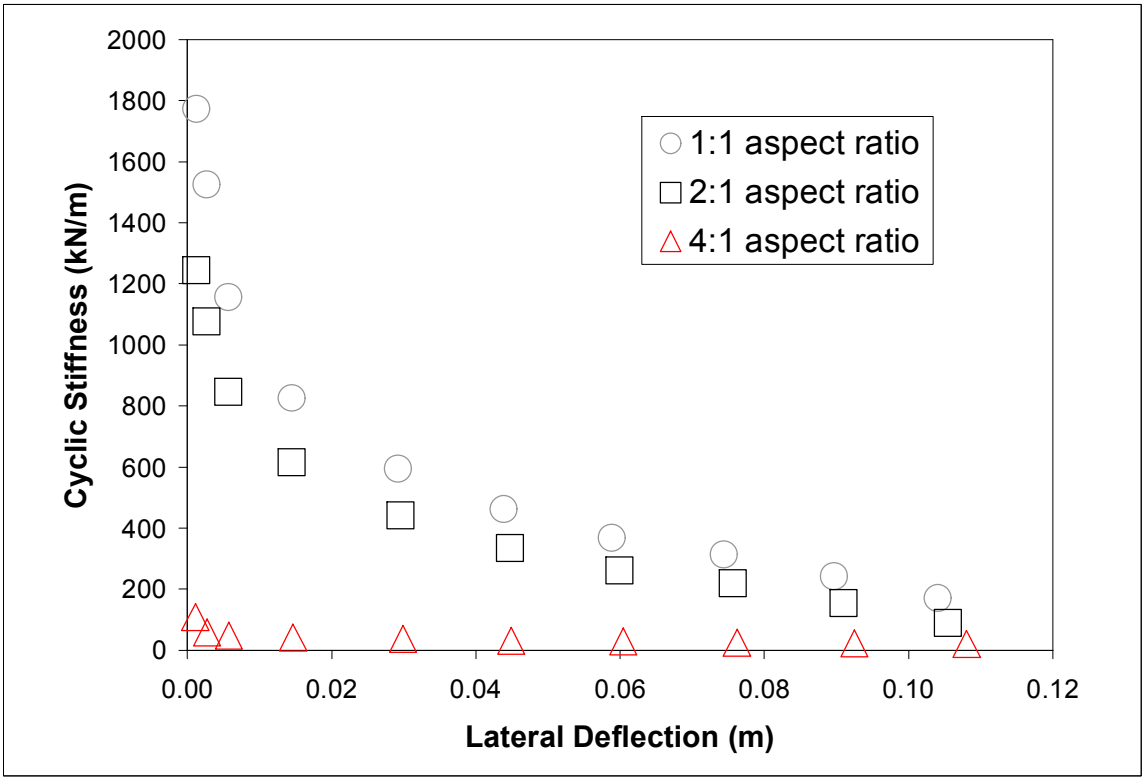

Figure 3.7 Average Cyclic Stiffness vs. Lateral Deflection plot for each wall aspect ratio indicating prevalent cyclic stiffness degradation.

LIST OF TABLES

Table 3.1 Average horizontal shear strengths and seismic design shear strengths per unit wall length at peak and failure load.

Test type	Aspect ratio	V_{peak} (kN/m)	[a]$V_{failure}$ (kN/m)	[b]$V_{peak\ design}$ (kN/m)	[c]$V_{failure\ design}$ (kN/m)
Monotonic	1:1	11.7	7.6	4.2	2.7
	2:1	5.6	3.3	2.0	1.2
	4:1	4.6	2.2	1.6	0.8
Cyclic	1:1	12.1	9.4	4.3	3.3
	2:1	5.3	3.7	1.9	1.3
	4:1	4.0	2.7	1.4	1.0

[a] Shear strength corresponding to the defined failure deflection of 48.8mm.
[b] Peak shear strength divided by a seismic safety factor of 2.8.
[c] Shear strength corresponding to the defined failure deflection divided by a seismic safety factor of 2.8.

Table 3.2 Average calculated hysteretic parameters for 1:1 aspect ratio walls.

Primary Cycle #	Δ_{max} (m)	Δ_{min} (m)	F @ Δ_{max} (N)	F @ Δ_{min} (N)	Strain Energy (N-m)	Hysteretic Energy (N-m)	ζ	Cyclic Stiffness (N/m)
1	0.001	-0.001	1948	-1770	2	1	0.104	1773451
3	0.003	-0.002	3749	-3772	9	4	0.068	1525957
5	0.006	-0.005	5938	-6675	34	13	0.062	1156952
7	0.015	-0.014	11357	-12571	173	70	0.064	826046
9	0.029	-0.030	16647	-18611	523	206	0.063	595046
11	0.044	-0.047	19189	-22584	946	352	0.059	462180
13	0.059	-0.064	22504	-22541	1376	503	0.058	368544
15	0.074	-0.081	24144	-24463	1883	605	0.051	313441
17	0.090	-0.099	19889	-25422	2129	718	0.058	242566
19	0.104	-0.116	19631	-17523	2019	633	0.050	170407

CHAPTER 4

Summary and Conclusions

The International Building Code does not address design procedures for log shear walls as it does for light frame shear walls, yet there is a growing market for log construction. With this growing market engineers will see more and more requests for structural designs of log structures and therefore need to understand their behavior and to provide safe and efficient designs. The preceding research on log shear walls as LFRS and lag screw connections provides baseline experimental data which help to better understand the seismic response of log shear walls. The experimental data collected herein should be used to develop seismic performance factors for log buildings based on the provisions in the ATC-63 Project (ATC, 2007). Furthermore, cyclic response data obtained from log connection tests should be used for subsequent modeling of full-scale log shear walls. No single log wall construction technique is agreed upon between log wall designers and log builders therefore, future monotonic and reverse-cyclic tests should be conducted and will help quantify the horizontal shear strength of different log wall constructions making it more clear for designers to size walls, space mechanical fasteners and design anchorage to resist design level loads. For log shear walls to move toward a performance based design methodology further research should be carried out on log shear walls that utilize various construction techniques.

Detailed experimental test results for log connection tests from Chapter 2 of this study can be found in Appendix “A” and detailed results of test data for log wall tests from Chapter 3 can be found in Appendix “B”.

APPENDIX A – LOG CONNECTION TEST RESULTS

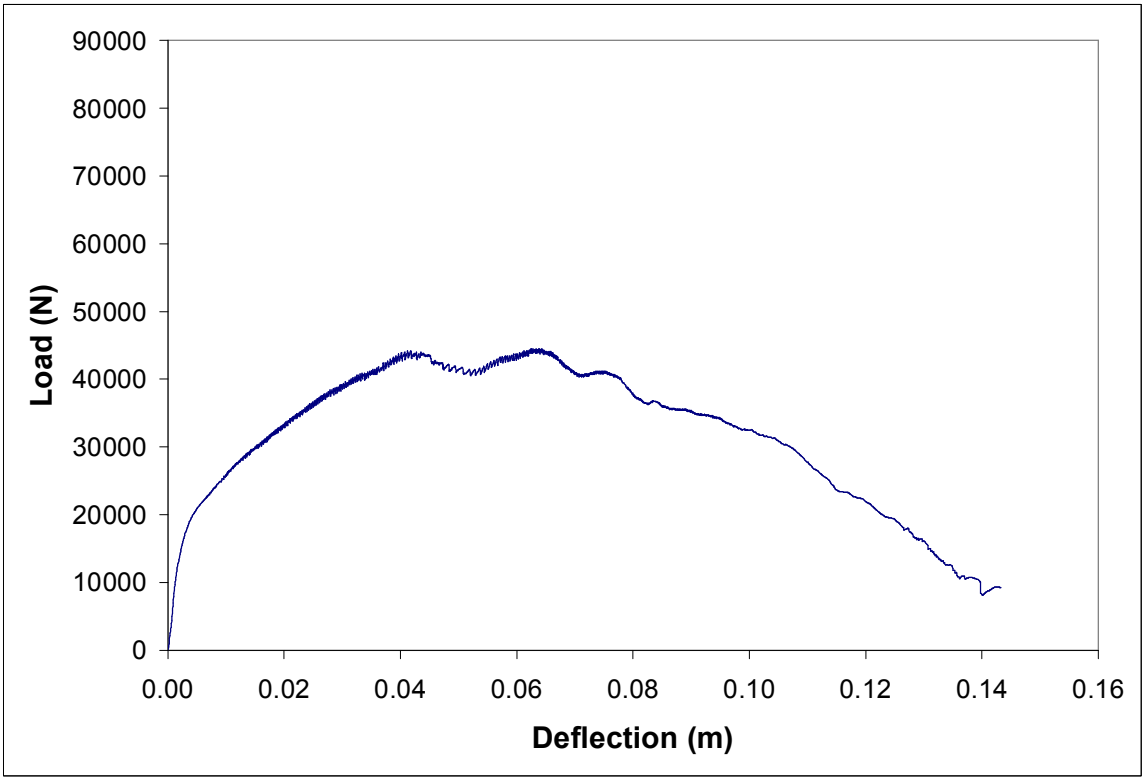

Figure 1A Typical Load versus deflection for 203 mm x 12.7 mm lag screw connections.

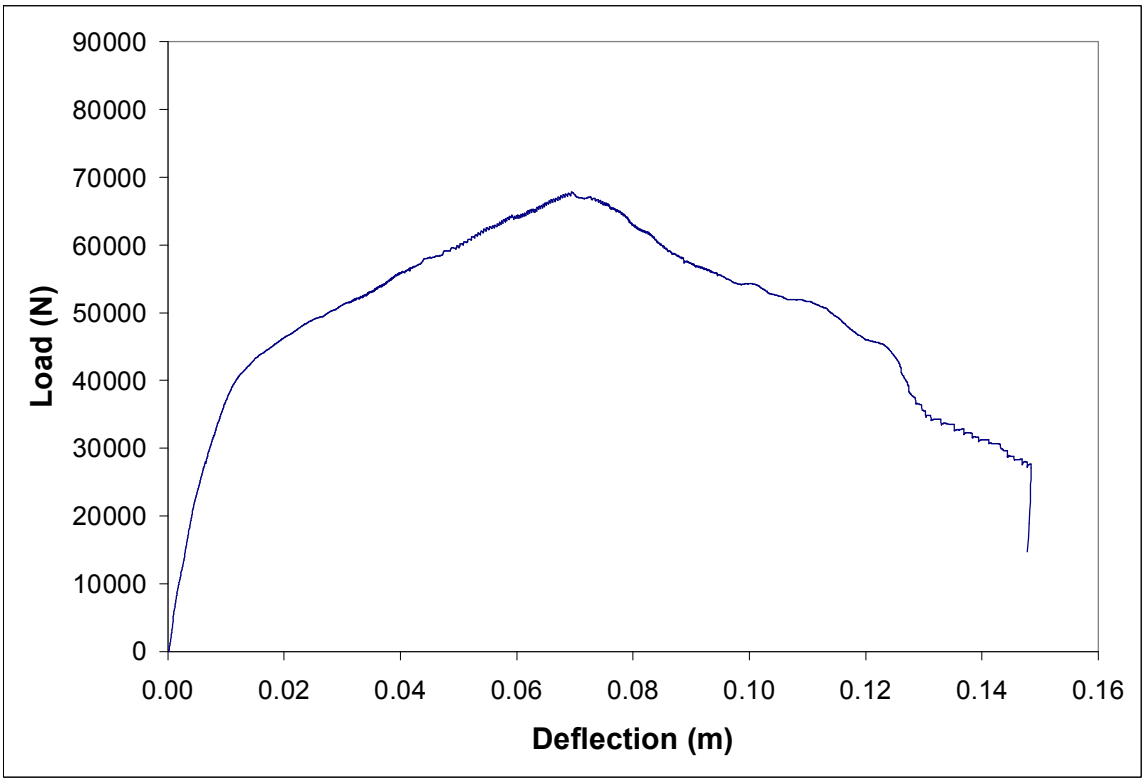

Figure 2A Typical Load versus deflection for 203 mm x 19.1 mm lag screw connections.

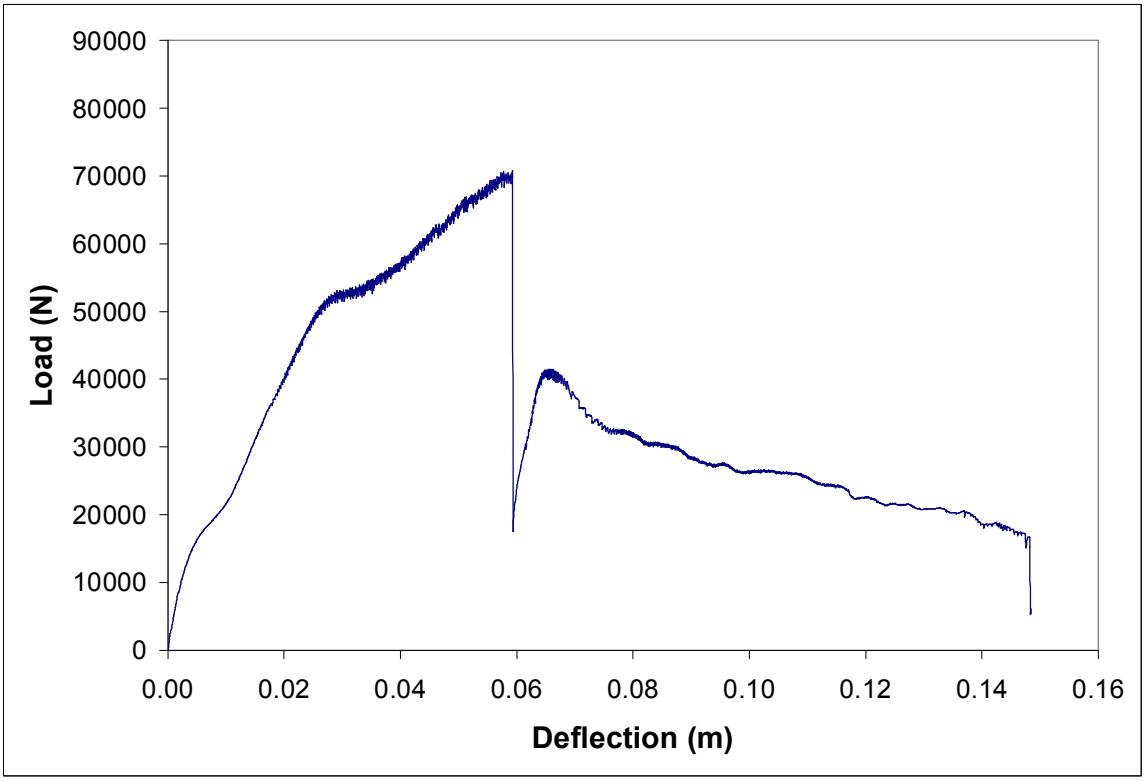

Figure 3A Typical Load versus deflection for 304 mm x 12.7 mm lag screw connections.

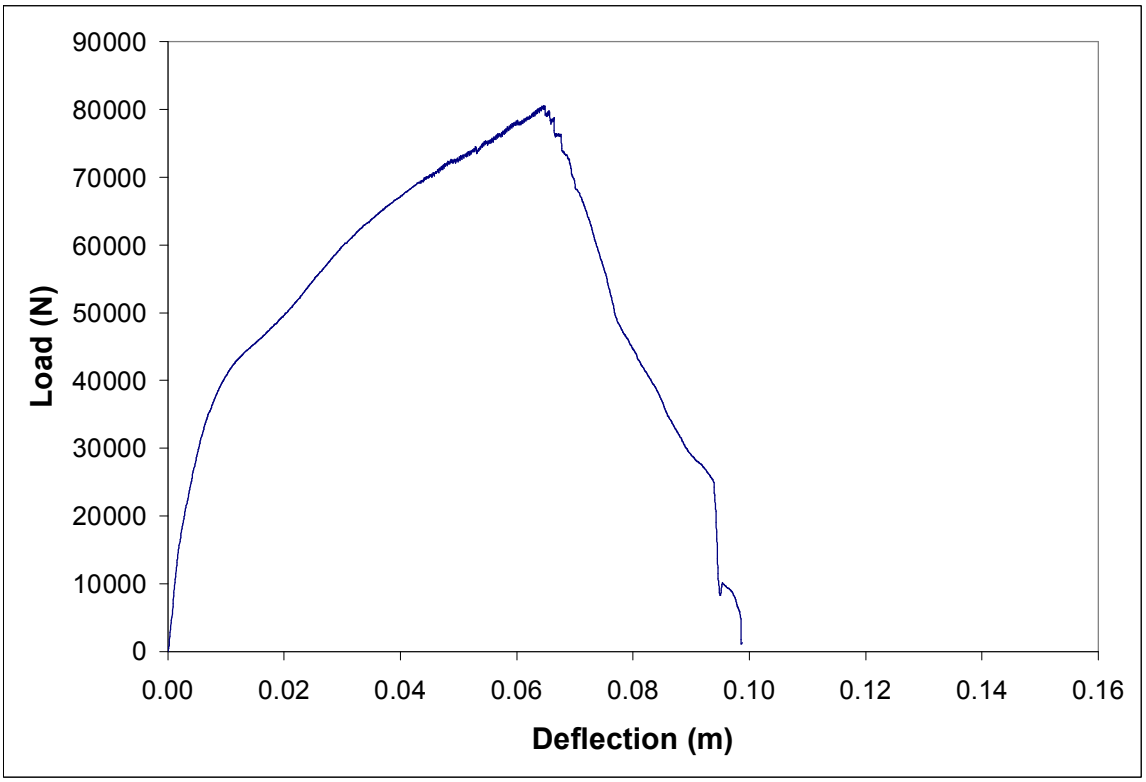

Figure 4A Typical Load versus deflection for 304 mm x 19.1 mm lag screw connections.

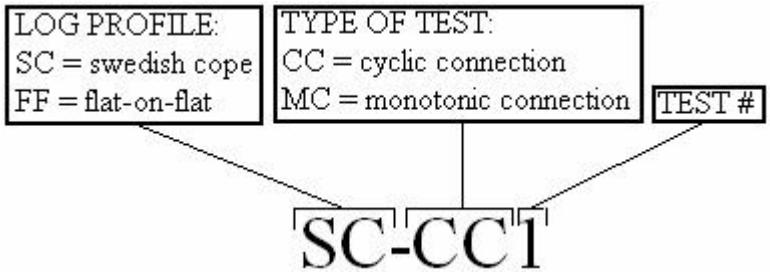

Figure 5A Nomenclature used for test specimen labeling.

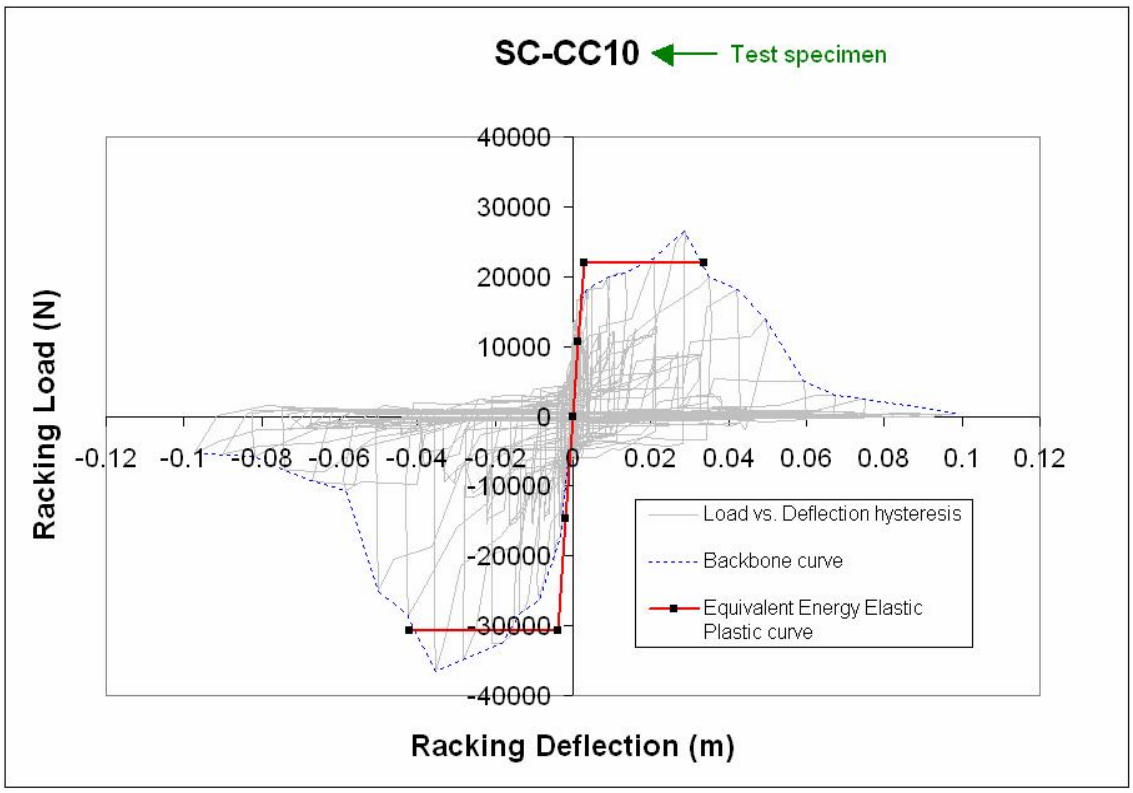

Figure 6A Load versus deflection hysteresis with typical test identification.

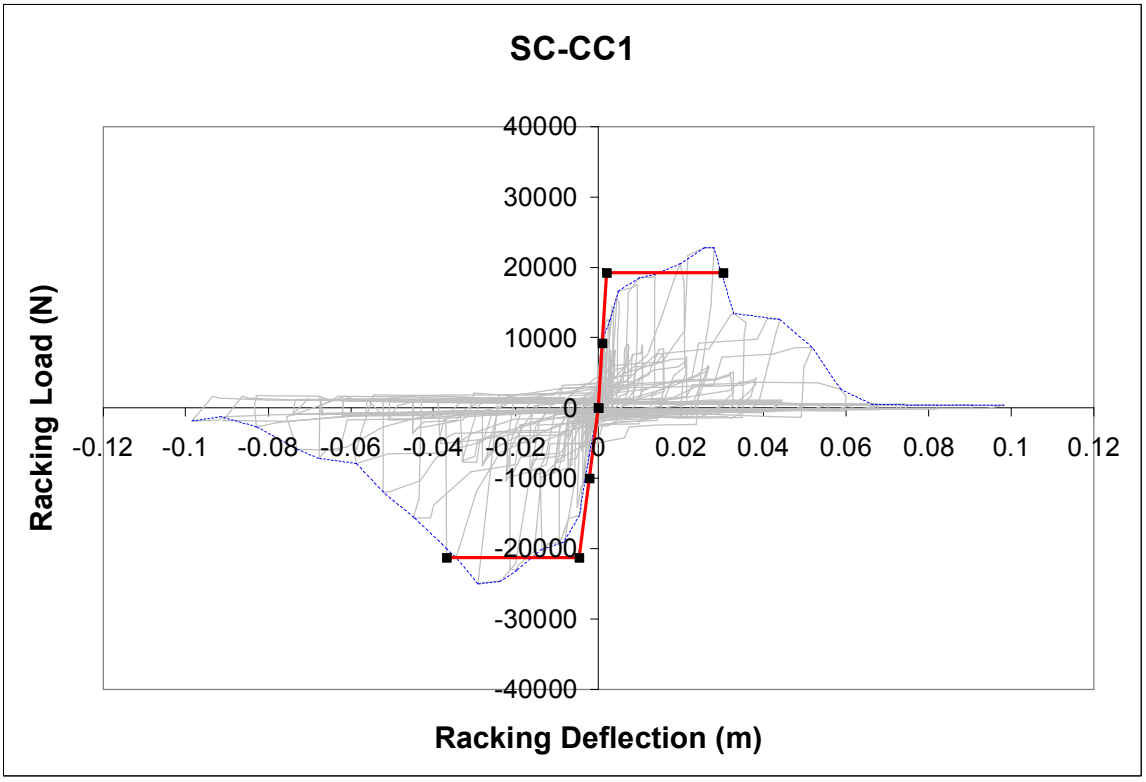

Figure 7A Load versus deflection hysteresis. Test SC-CC1.

Table 1A Calculated hysteretic parameters. Test SC-CC1.

Primary Cycle #	Δ_{max} (m)	Δ_{min} (m)	F @ Δ_{max} (N)	F @ Δ_{min} (N)	Strain Energy (N-m)	Hysteretic Energy (N-m)	ζ	Cyclic Stiffness (N/m)
2	0.0010	-0.0014	9808	-3456	8	6	0.119	5439921
4	0.0037	-0.0038	13794	-10502	46	24	0.085	3231629
6	0.0095	-0.0095	17493	-18773	172	108	0.100	1908792
8	0.0209	-0.0215	5842	-22916	307	219	0.114	679599
10	0.0329	-0.0368	13436	-20631	600	309	0.082	489143
12	0.0517	-0.0521	8604	-12007	536	312	0.093	198404
14	0.0679	-0.0677	565	-7149	261	146	0.089	56897
16	0.0822	-0.0828	486	-2679	131	118	0.143	19181
18	0.0982	-0.0985	373	-1845	109	108	0.158	11274

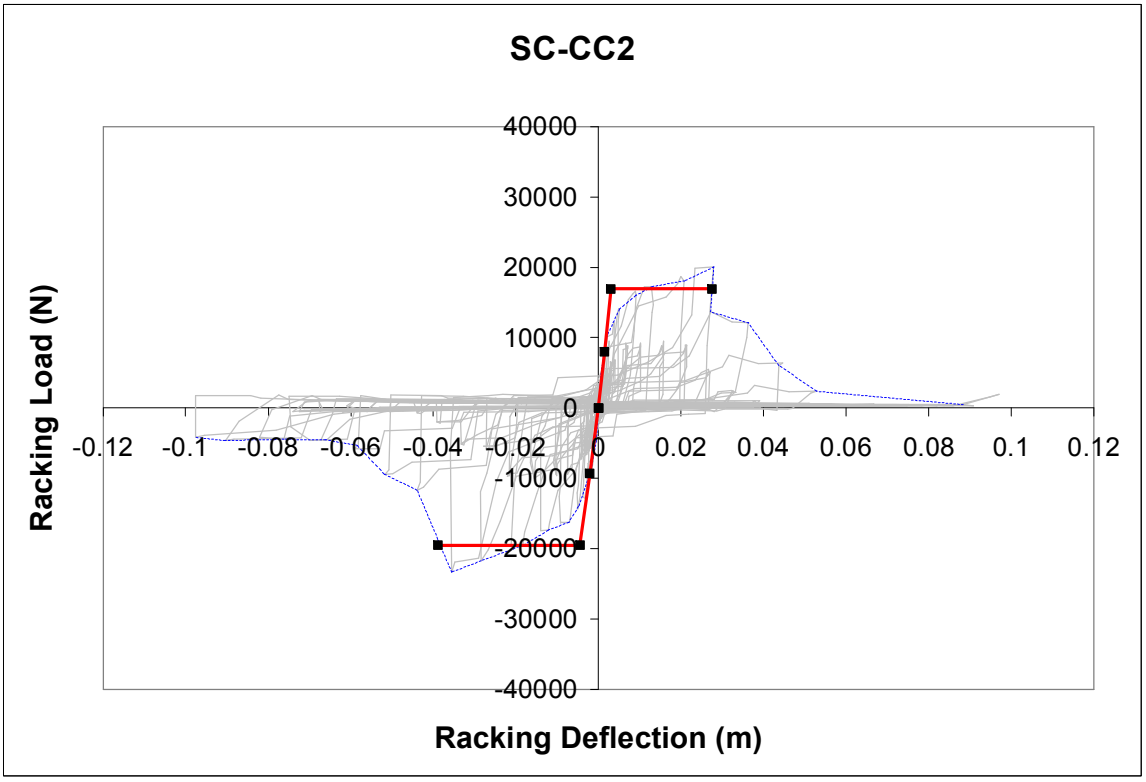

Figure 8A Load versus deflection hysteresis. Test SC-CC2.

Table 2A Calculated hysteretic parameters. Test SC-CC2.

Primary Cycle #	Δ_{max} (m)	Δ_{min} (m)	F @ Δ_{max} (N)	F @ Δ_{min} (N)	Strain Energy (N-m)	Hysteretic Energy (N-m)	ζ	Cyclic Stiffness (N/m)
2	0.0014	-0.0011	5656	-5785	7	5	0.109	4596059
4	0.0039	-0.0038	12084	-12601	47	26	0.088	3239553
6	0.0090	-0.0096	16013	-12660	133	86	0.103	1540053
8	0.0207	-0.0212	18635	-19395	399	229	0.091	907430
10	0.0362	-0.0359	12077	-5797	323	326	0.161	247602
12	0.0528	-0.0517	2365	-9450	307	160	0.083	113094
14	0.0671	-0.0671	379	-4510	164	55	0.054	36416
16	0.0820	-0.0762	331	-4466	184	68	0.059	30330
18	0.0970	-0.0976	1930	-4187	298	106	0.057	31437

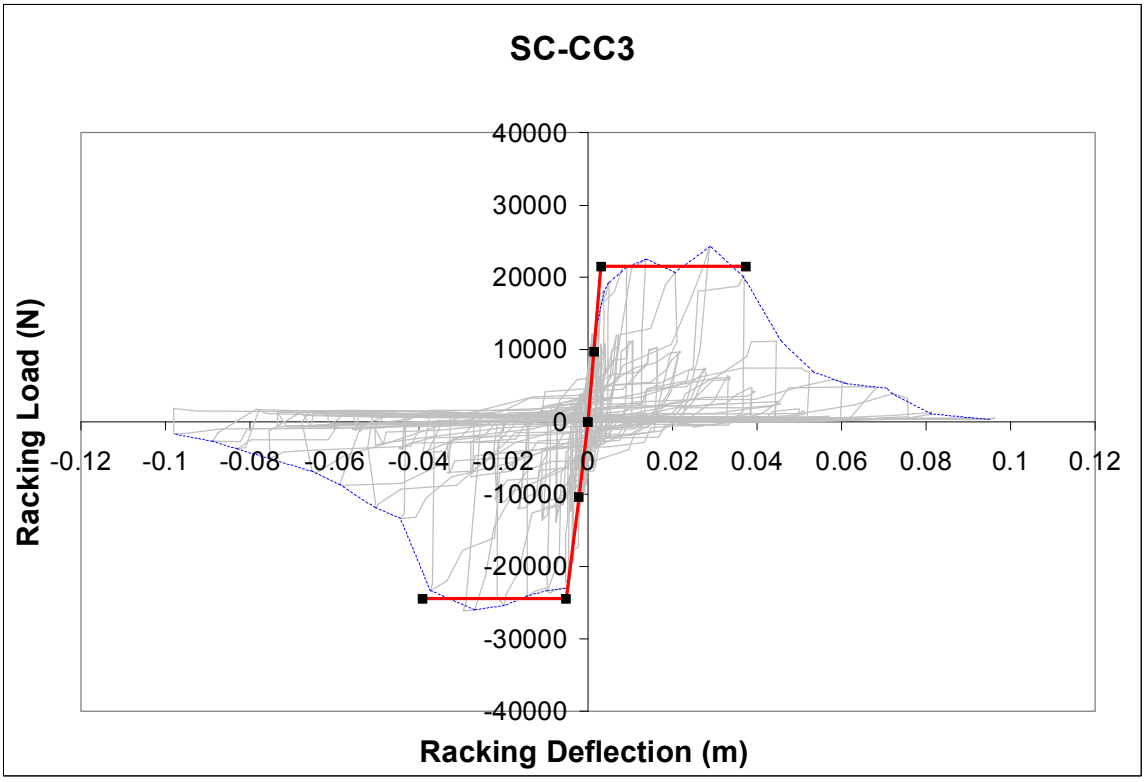

Figure 9A Load versus deflection hysteresis. Test SC-CC3.

Table 3A Calculated hysteretic parameters. Test SC-CC3.

Primary Cycle #	Δ_{max} (m)	Δ_{min} (m)	F @ Δ_{max} (N)	F @ Δ_{min} (N)	Strain Energy (N-m)	Hysteretic Energy (N-m)	ζ	Cyclic Stiffness (N/m)
2	0.0012	-0.0010	12055	-10106	12	12	0.154	9914436
4	0.0037	-0.0038	14455	-19623	64	52	0.128	4517327
6	0.0092	-0.0097	21380	-21519	202	151	0.119	2273131
8	0.0211	-0.0216	11050	-23825	373	313	0.133	818271
10	0.0370	-0.0373	20051	-23288	805	413	0.082	583736
12	0.0524	-0.0521	6966	-3455	272	359	0.210	99778
14	0.0682	-0.0644	4711	-7103	390	187	0.077	89038
16	0.0813	-0.0830	1459	-3726	214	84	0.063	31552
18	0.0962	-0.0981	551	-1640	107	74	0.110	11273

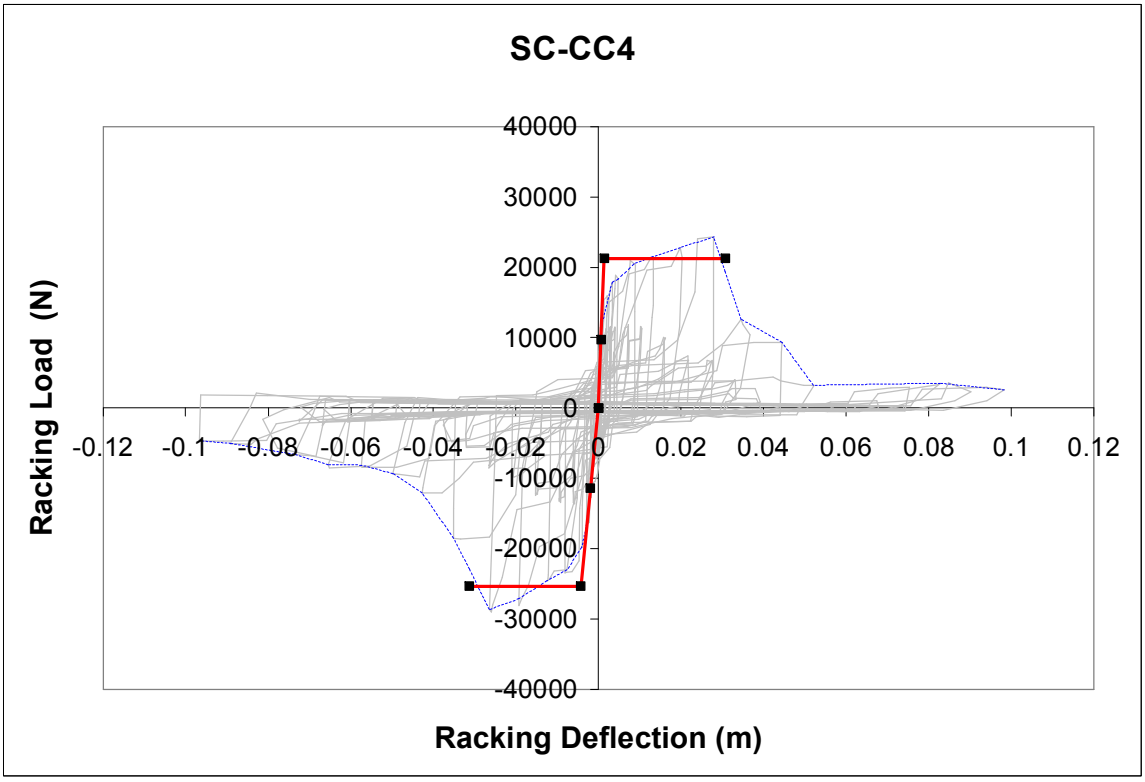

Figure 10A Load versus deflection hysteresis. Test SC-CC4.

Table 4A Calculated hysteretic parameters. Test SC-CC4.

Primary Cycle #	Δ_{max} (m)	Δ_{min} (m)	F @ Δ_{max} (N)	F @ Δ_{min} (N)	Strain Energy (N-m)	Hysteretic Energy (N-m)	ζ	Cyclic Stiffness (N/m)
2	0.0009	-0.0004	11639	-6725	6	6	0.143	14176357
4	0.0034	-0.0029	17825	-17031	55	36	0.103	5555823
6	0.0089	-0.0081	20276	-18623	166	146	0.141	2289157
8	0.0203	-0.0193	21410	-28080	489	322	0.105	1248209
10	0.0367	-0.0351	10399	-14276	442	331	0.119	343390
12	0.0521	-0.0499	3217	-9318	316	262	0.132	122888
14	0.0677	-0.0655	402	-8041	277	143	0.082	63366
16	0.0827	-0.0685	3512	-6864	380	147	0.062	68631
18	0.0983	-0.0967	2558	-4681	352	182	0.082	37133

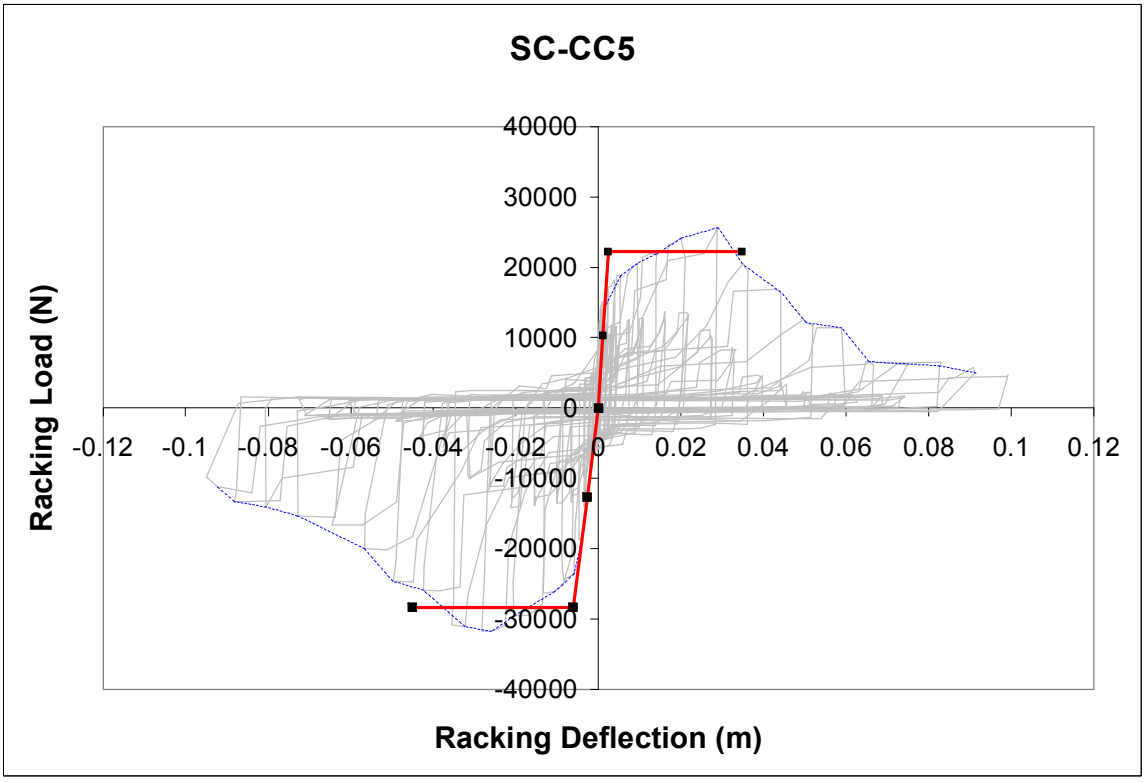

Figure 11A Load versus deflection hysteresis. Test SC-CC5.

Table 5A Calculated hysteretic parameters. Test SC-CC5.

Primary Cycle #	Δ_{max} (m)	Δ_{min} (m)	F @ Δ_{max} (N)	F @ Δ_{min} (N)	Strain Energy (N-m)	Hysteretic Energy (N-m)	ζ	Cyclic Stiffness (N/m)
2	0.0009	-0.0008	15125	-5781	9	9	0.154	12470985
4	0.0039	-0.0035	14443	-13820	52	43	0.132	3810719
6	0.0096	-0.0089	11218	-21195	148	162	0.175	1757742
8	0.0211	-0.0207	21116	-24738	478	366	0.122	1098777
10	0.0362	-0.0356	19300	-30848	899	485	0.086	697894
12	0.0518	-0.0497	11764	-24621	916	423	0.073	358472
14	0.0667	-0.0646	6112	-16673	742	271	0.058	173538
16	0.0831	-0.0807	6475	-88	272	302	0.176	40072
18	0.0992	-0.0950	4619	-9847	697	246	0.056	74516

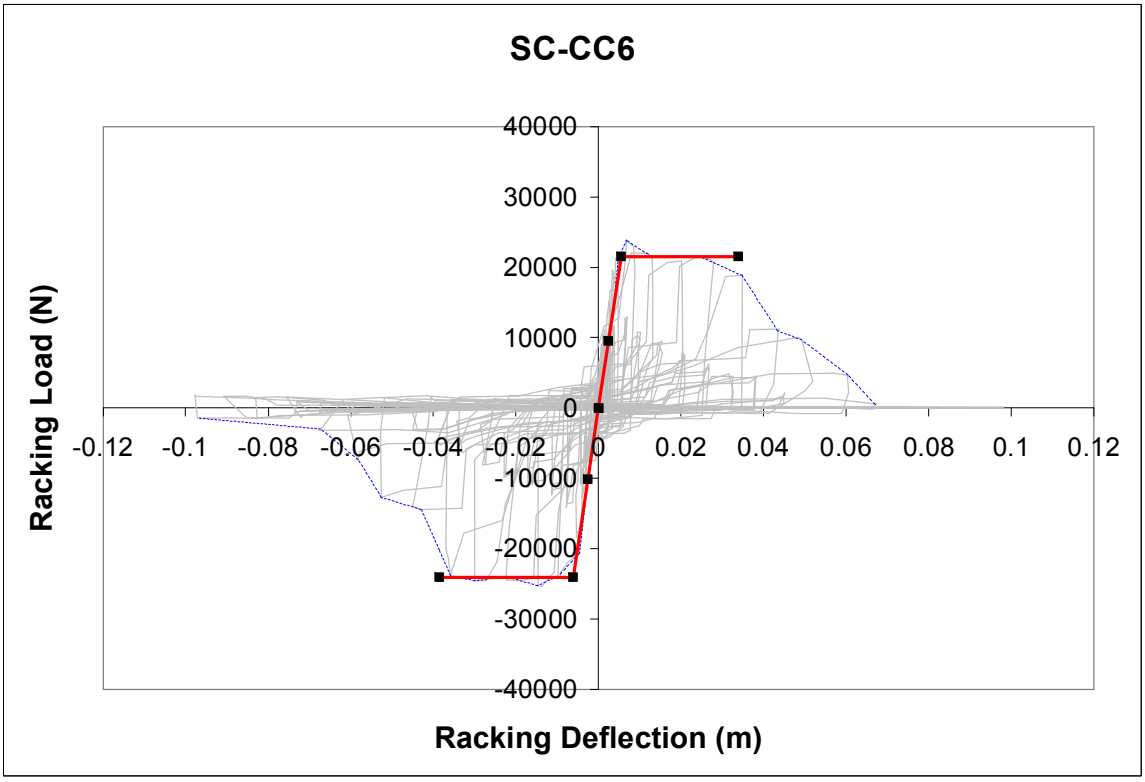

Figure 12A Load versus deflection hysteresis. Test SC-CC6.

Table 6A Calculated hysteretic parameters. Test SC-CC6.

Primary Cycle #	Δ_{max} (m)	Δ_{min} (m)	F @ Δ_{max} (N)	F @ Δ_{min} (N)	Strain Energy (N-m)	Hysteretic Energy (N-m)	ζ	Cyclic Stiffness (N/m)
2	0.0014	-0.0011	11128	-2793	9	6	0.100	5536011
4	0.0033	-0.0039	19575	-12563	57	26	0.074	4455161
6	0.0088	-0.0099	23824	-23302	220	160	0.116	2527727
8	0.0201	-0.0224	20861	-24452	484	288	0.095	1064425
10	0.0349	-0.0370	18128	-20021	686	366	0.085	531096
12	0.0493	-0.0526	9635	-12709	572	329	0.091	219158
14	0.0673	-0.0677	1373	-3165	153	116	0.120	33607
16	0.0826	-0.0831	104	-1492	66	48	0.116	9632
18	0.0981	-0.0977	128	-1457	77	54	0.110	8094

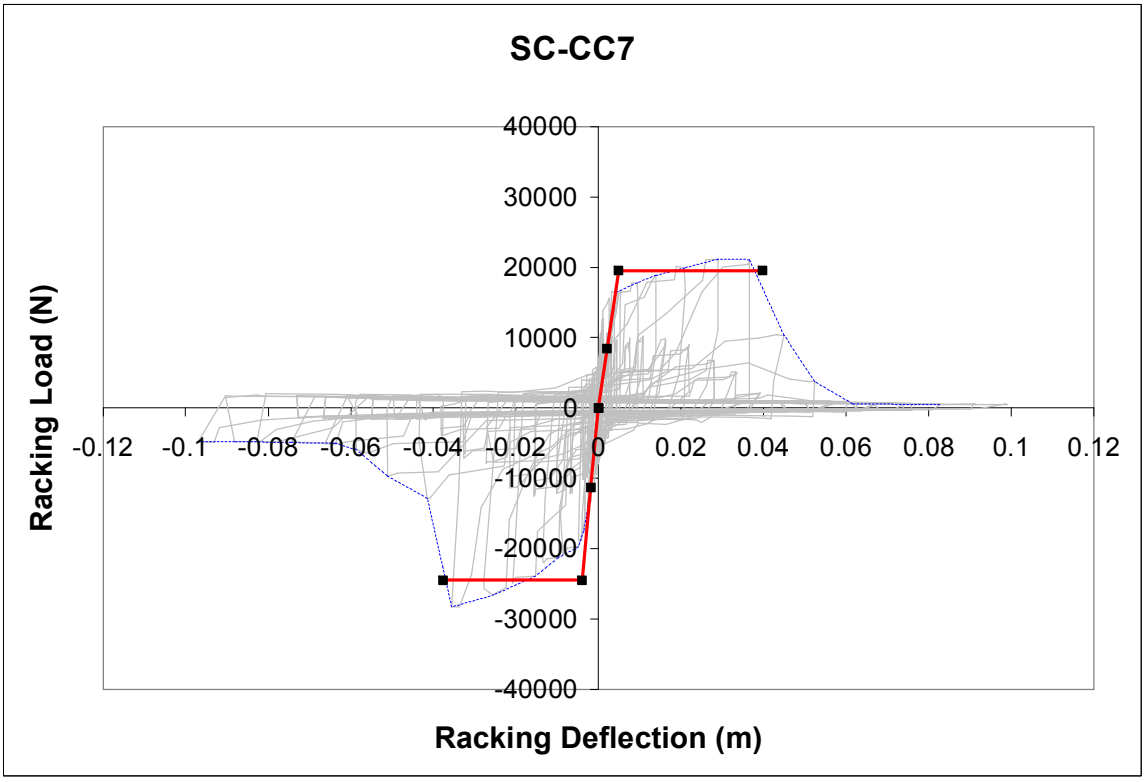

Figure 13A Load versus deflection hysteresis. Test SC-CC7.

Table 7A Calculated hysteretic parameters. Test SC-CC7.

Primary Cycle #	Δ_{max} (m)	Δ_{min} (m)	F @ Δ_{max} (N)	F @ Δ_{min} (N)	Strain Energy (N-m)	Hysteretic Energy (N-m)	ζ	Cyclic Stiffness (N/m)
2	0.0012	-0.0007	12763	-9338	11	10	0.146	11919469
4	0.0040	-0.0036	16368	-17559	64	47	0.116	4497335
6	0.0095	-0.0087	17777	-20832	175	136	0.124	2125905
8	0.0188	-0.0208	20100	-24860	448	299	0.106	1133208
10	0.0366	-0.0356	21070	-28268	889	427	0.076	682988
12	0.0524	-0.0510	3721	-9714	345	288	0.133	129928
14	0.0678	-0.0663	777	-5057	194	155	0.127	43497
16	0.0831	-0.0827	566	-4718	219	159	0.116	31871
18	0.0990	-0.0970	526	-4812	259	167	0.103	27236

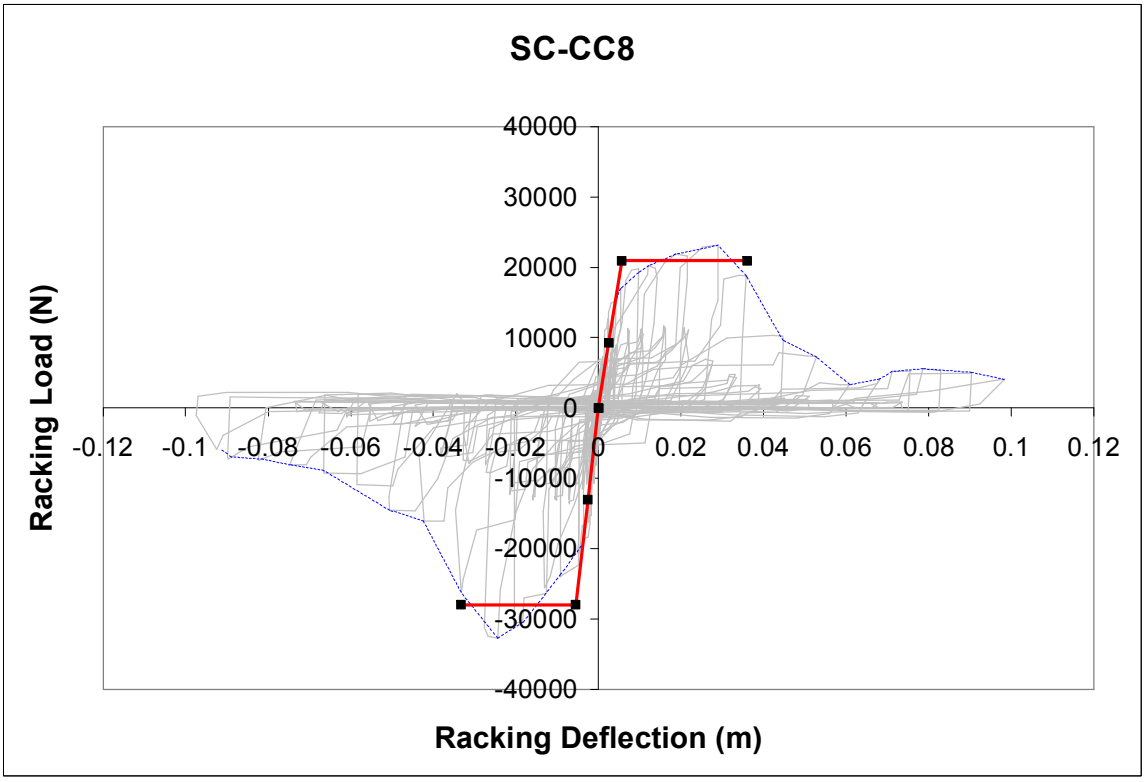

Figure 14A Load versus deflection hysteresis. Test SC-CC8.

Table 8A Calculated hysteretic parameters. Test SC-CC8.

Primary Cycle #	Δ_{max} (m)	Δ_{min} (m)	F @ Δ_{max} (N)	F @ Δ_{min} (N)	Strain Energy (N-m)	Hysteretic Energy (N-m)	ζ	Cyclic Stiffness (N/m)
2	0.0011	-0.0012	6549	-10687	10	8	0.128	7539976
4	0.0040	-0.0036	15214	-17513	62	26	0.068	4338242
6	0.0097	-0.0092	19246	-23675	202	134	0.106	2271211
8	0.0215	-0.0205	21627	-30534	546	342	0.100	1241581
10	0.0358	-0.0332	18785	-26201	772	365	0.075	651610
12	0.0529	-0.0507	7252	-12653	513	292	0.091	192121
14	0.0681	-0.0666	4108	-8875	436	201	0.073	96373
16	0.0830	-0.0824	5306	-7286	520	176	0.054	76163
18	0.0983	-0.0924	4076	-5925	474	161	0.054	52452

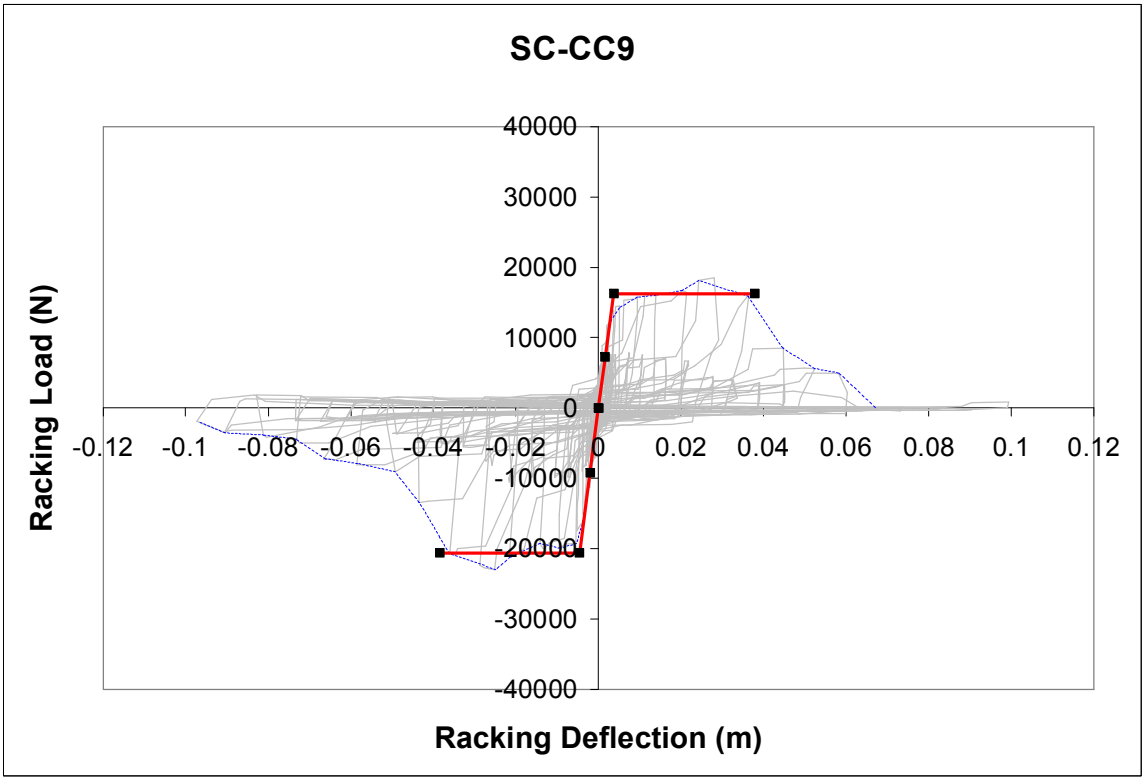

Figure 15A Load versus deflection hysteresis. Test SC-CC9.

Table 9A Calculated hysteretic parameters. Test SC-CC9.

Primary Cycle #	Δ_{max} (m)	Δ_{min} (m)	F @ Δ_{max} (N)	F @ Δ_{min} (N)	Strain Energy (N-m)	Hysteretic Energy (N-m)	ζ	Cyclic Stiffness (N/m)
2	0.0011	-0.0012	7898	-7639	9	9	0.155	6722054
4	0.0037	-0.0038	13826	-14903	54	34	0.101	3834152
6	0.0095	-0.0096	15762	-19936	170	99	0.093	1873892
8	0.0213	-0.0214	16386	-19951	388	279	0.114	850035
10	0.0363	-0.0360	15841	-20703	660	289	0.070	505354
12	0.0523	-0.0491	5606	-9079	370	269	0.116	144685
14	0.0670	-0.0666	23	-7237	242	194	0.128	54338
16	0.0840	-0.0803	52	-4152	169	106	0.100	25578
18	0.0993	-0.0904	875	-3552	204	123	0.096	23328

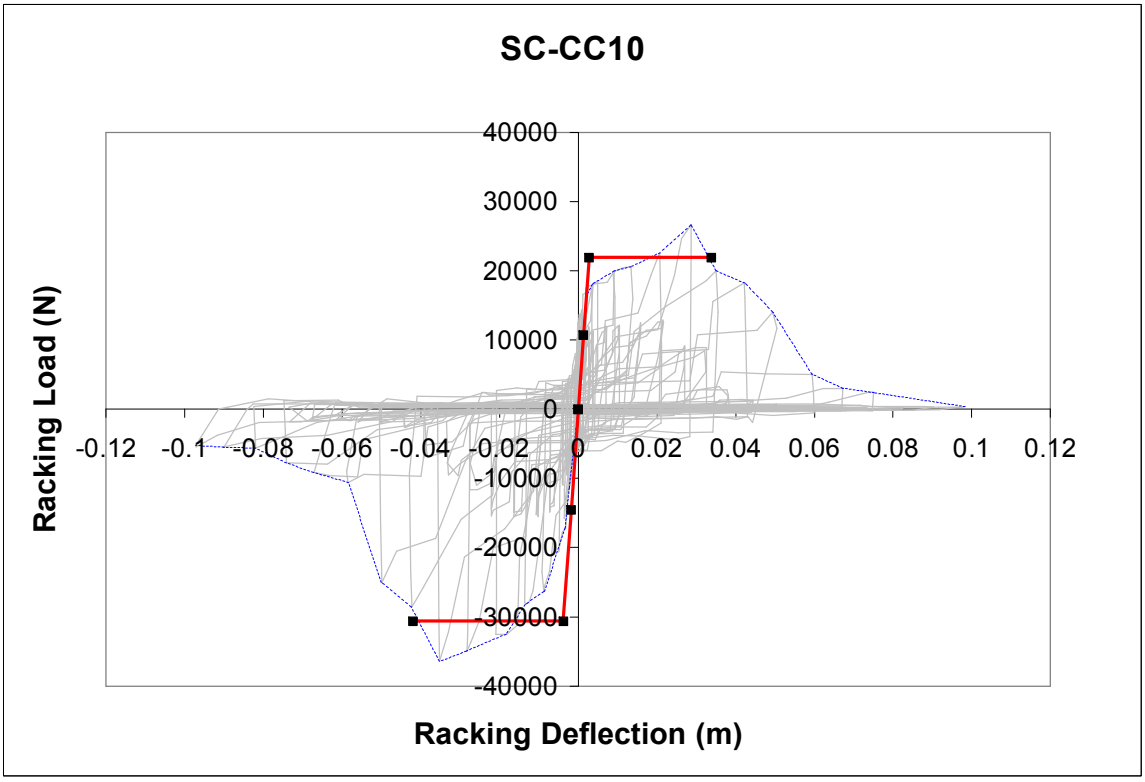

Figure 16A Load versus deflection hysteresis. Test SC-CC10.

Table 10A Calculated hysteretic parameters. Test SC-CC10.

Primary Cycle #	Δ_{max} (m)	Δ_{min} (m)	F @ Δ_{max} (N)	F @ Δ_{min} (N)	Strain Energy (N-m)	Hysteretic Energy (N-m)	ζ	Cyclic Stiffness (N/m)
2	0.0008	-0.0012	14372	-7582	10	14	0.211	10803967
4	0.0035	-0.0035	17881	-15842	59	45	0.121	4810526
6	0.0093	-0.0092	19690	-23491	200	169	0.135	2335182
8	0.0208	-0.0210	22604	-32475	575	401	0.111	1319019
10	0.0351	-0.0353	19985	-36450	993	565	0.091	802687
12	0.0494	-0.0499	13990	-24991	969	460	0.075	392404
14	0.0672	-0.0672	3024	-9163	410	169	0.066	90643
16	0.0826	-0.0820	227	-5650	241	89	0.059	35718
18	0.0982	-0.0973	372	-5249	274	115	0.067	28742

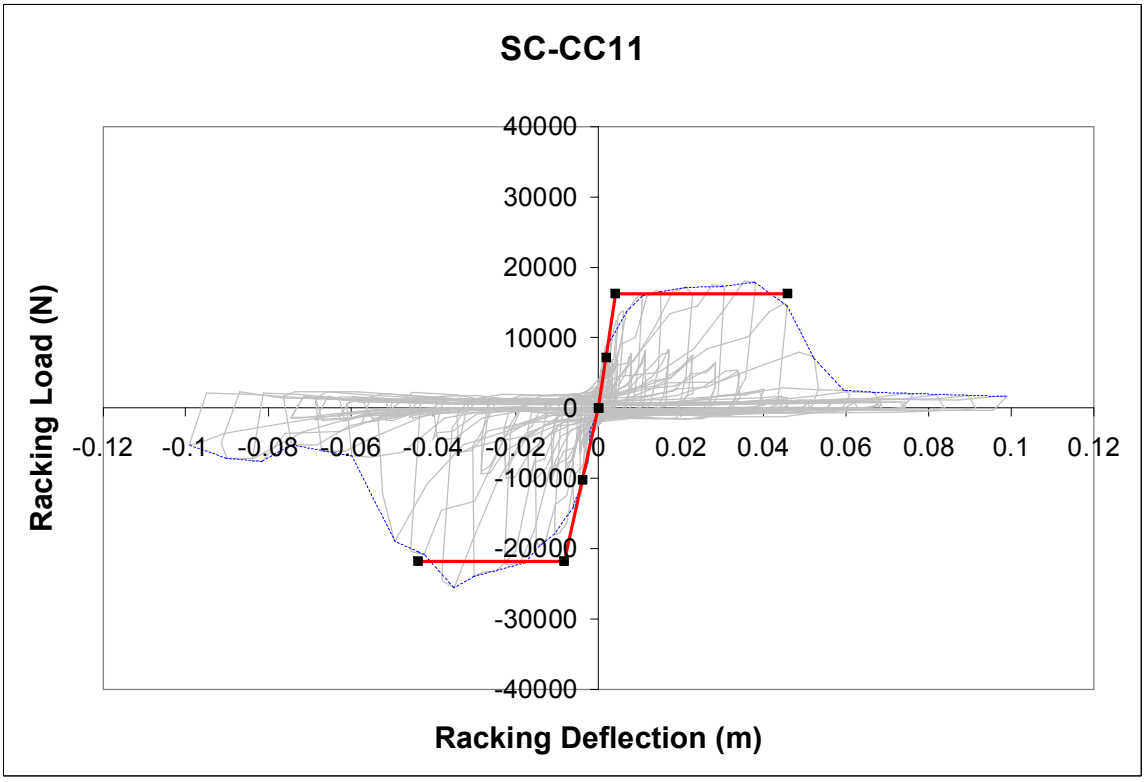

Figure 17A Load versus deflection hysteresis. Test SC-CC11.

Table 11A Calculated hysteretic parameters. Test SC-CC11.

Primary Cycle #	Δ_{max} (m)	Δ_{min} (m)	F @ Δ_{max} (N)	F @ Δ_{min} (N)	Strain Energy (N-m)	Hysteretic Energy (N-m)	ζ	Cyclic Stiffness (N/m)
2	0.0015	-0.0014	7569	-3984	9	7	0.137	3887675
4	0.0046	-0.0046	12226	-12274	56	31	0.089	2679283
6	0.0107	-0.0107	15962	-17901	181	104	0.091	1587116
8	0.0228	-0.0228	15722	-20731	415	257	0.099	800424
10	0.0379	-0.0379	17869	-24535	804	358	0.071	559290
12	0.0522	-0.0493	7170	-18950	654	315	0.077	257343
14	0.0601	-0.0615	2288	-6115	257	177	0.109	69085
16	0.0818	-0.0840	1827	-7505	390	182	0.074	56288
18	0.0990	-0.0992	1615	-5237	340	170	0.080	34584

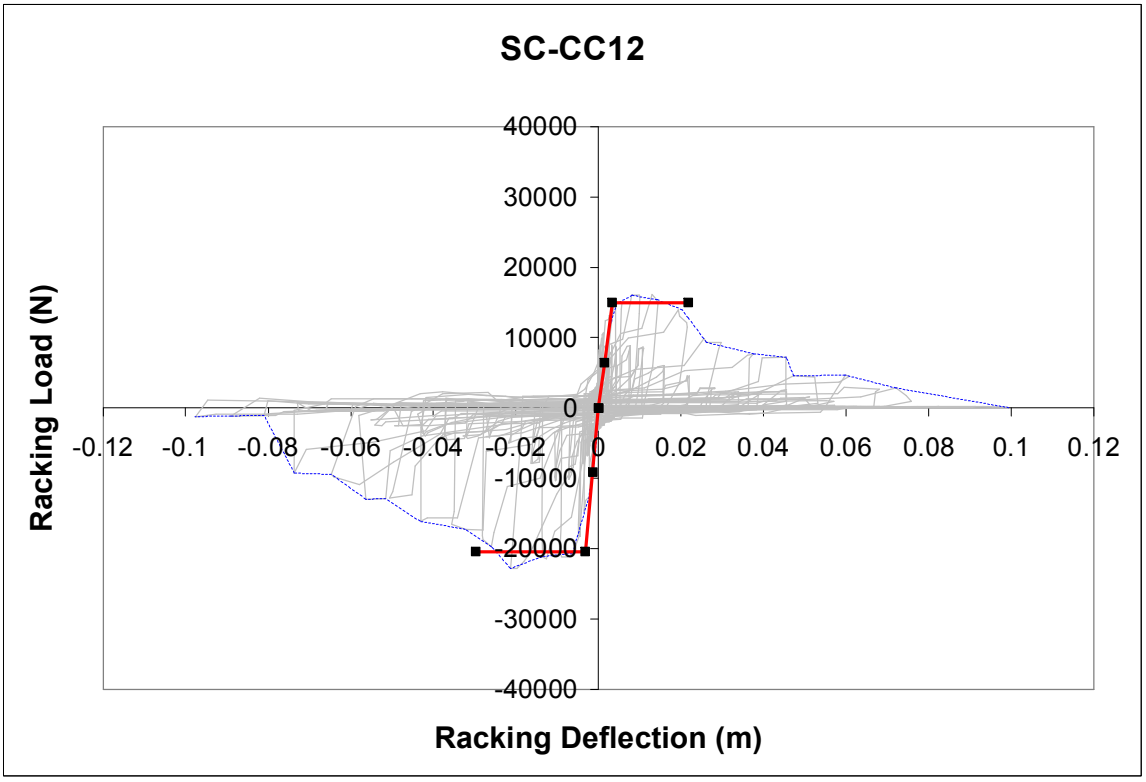

Figure 18A Load versus deflection hysteresis. Test SC-CC12.

Table 12A Calculated hysteretic parameters. Test SC-CC12.

Primary Cycle #	Δ_{max} (m)	Δ_{min} (m)	F @ Δ_{max} (N)	F @ Δ_{min} (N)	Strain Energy (N-m)	Hysteretic Energy (N-m)	ζ	Cyclic Stiffness (N/m)
2	0.0012	-0.0010	10662	-4178	9	8	0.150	6639049
4	0.0042	-0.0034	14702	-14511	56	34	0.098	3833742
6	0.0101	-0.0093	15831	-20609	175	116	0.106	1885164
8	0.0214	-0.0213	13039	-22822	383	242	0.101	839372
10	0.0375	-0.0357	7683	-16494	438	228	0.083	330384
12	0.0523	-0.0506	4437	-12785	440	175	0.063	167204
14	0.0680	-0.0648	2279	-9437	383	224	0.093	88210
16	0.0824	-0.0826	174	-1063	51	35	0.110	7495
18	0.0992	-0.0977	46	-1254	64	50	0.125	6604

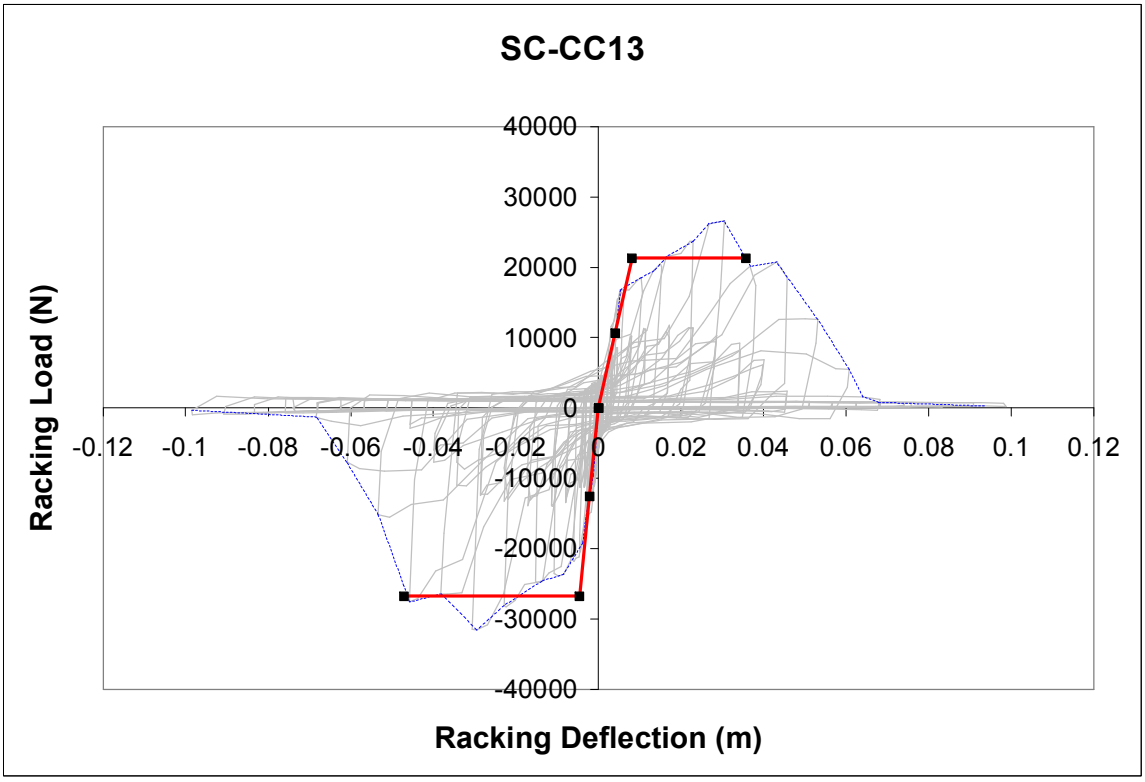

Figure 19A Load versus deflection hysteresis. Test SC-CC13.

Table 13A Calculated hysteretic parameters. Test SC-CC13.

Primary Cycle #	Δ_{max} (m)	Δ_{min} (m)	F @ Δ_{max} (N)	F @ Δ_{min} (N)	Strain Energy (N-m)	Hysteretic Energy (N-m)	ζ	Cyclic Stiffness (N/m)
2	0.0015	-0.0014	4432	-12122	12	11	0.152	5667298
4	0.0046	-0.0046	15494	-20237	82	44	0.086	3896791
6	0.0107	-0.0107	16294	-23514	213	152	0.113	1861315
8	0.0229	-0.0229	23650	-28306	595	362	0.097	1133864
10	0.0381	-0.0381	17414	-26421	835	487	0.093	575272
12	0.0532	-0.0534	12634	-15180	741	423	0.091	260968
14	0.0683	-0.0684	1239	-1314	87	122	0.223	18686
16	0.0833	-0.0833	727	-796	63	87	0.218	9136
18	0.0987	-0.0983	243	-980	60	102	0.269	6209

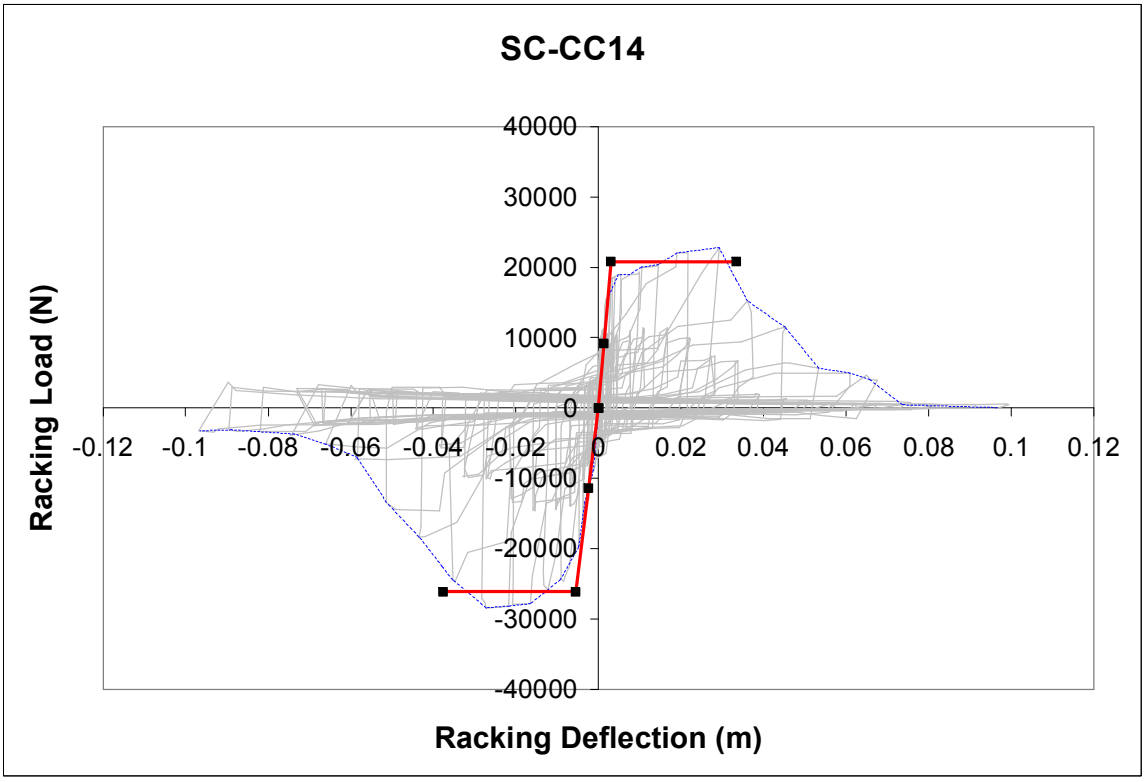

Figure 20A Load versus deflection hysteresis. Test SC-CC14.

Table 14A Calculated hysteretic parameters. Test SC-CC14.

Primary Cycle #	Δ_{max} (m)	Δ_{min} (m)	F @ Δ_{max} (N)	F @ Δ_{min} (N)	Strain Energy (N-m)	Hysteretic Energy (N-m)	ζ	Cyclic Stiffness (N/m)
2	0.0012	-0.0005	7553	-6916	7	10	0.249	8137607
4	0.0040	-0.0036	18540	-15741	65	45	0.109	4528962
6	0.0099	-0.0084	19280	-24622	198	151	0.121	2410655
8	0.0217	-0.0209	22053	-27902	531	388	0.117	1173478
10	0.0361	-0.0348	15214	-24691	704	445	0.101	562901
12	0.0533	-0.0490	5631	-14465	505	332	0.105	196318
14	0.0649	-0.0661	4656	-5132	321	212	0.105	74724
16	0.0830	-0.0825	478	-3333	157	178	0.180	23038
18	0.0993	-0.0969	502	-3254	182	187	0.163	19145

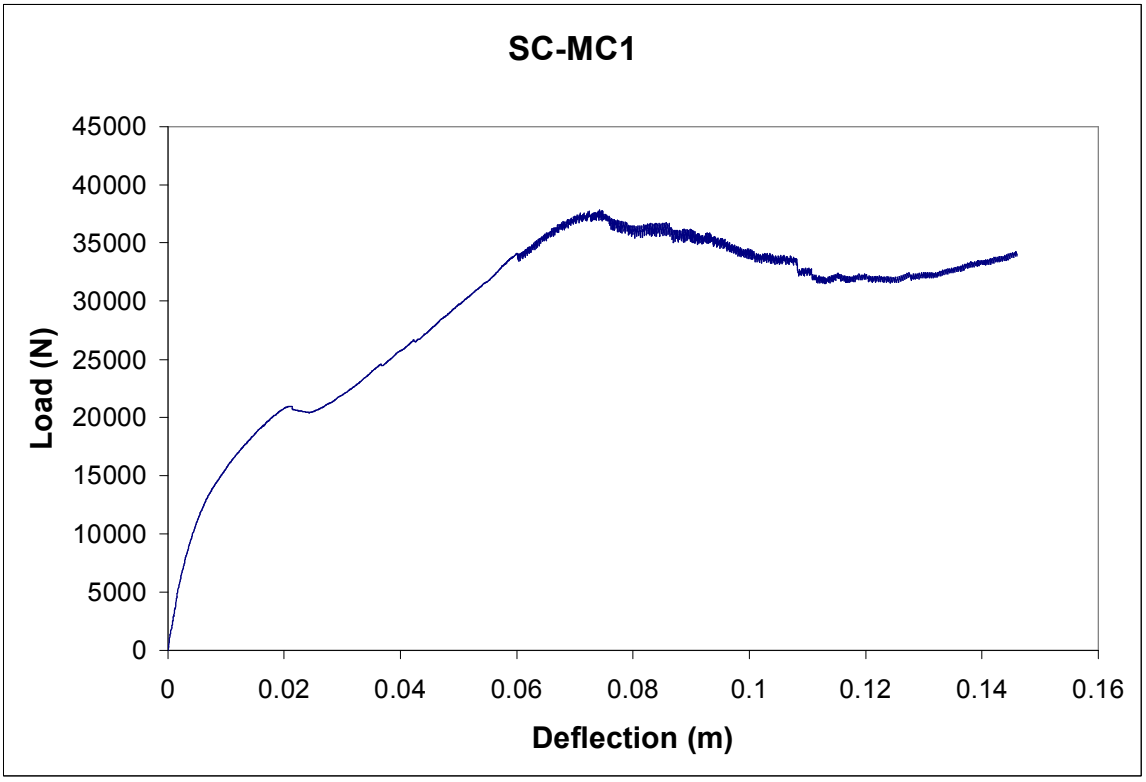

Figure 21A Load versus deflection plot. Test SC-MC1.

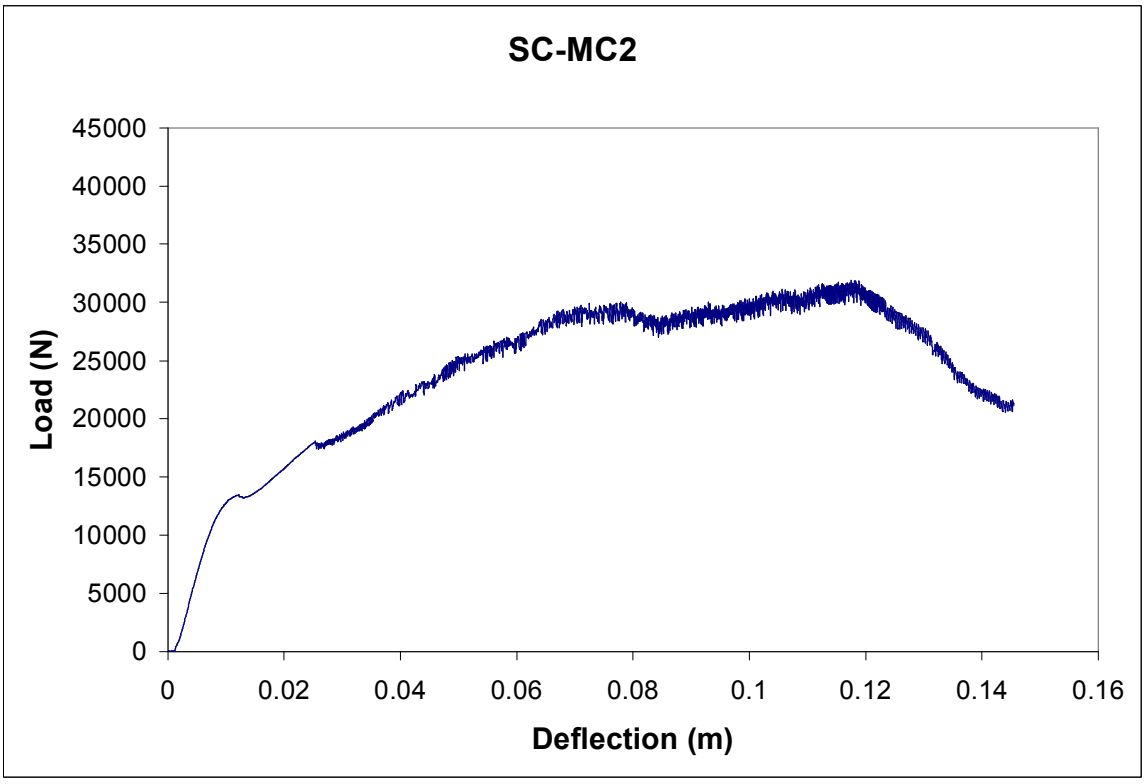

Figure 22A Load versus deflection plot. Test SC-MC2.

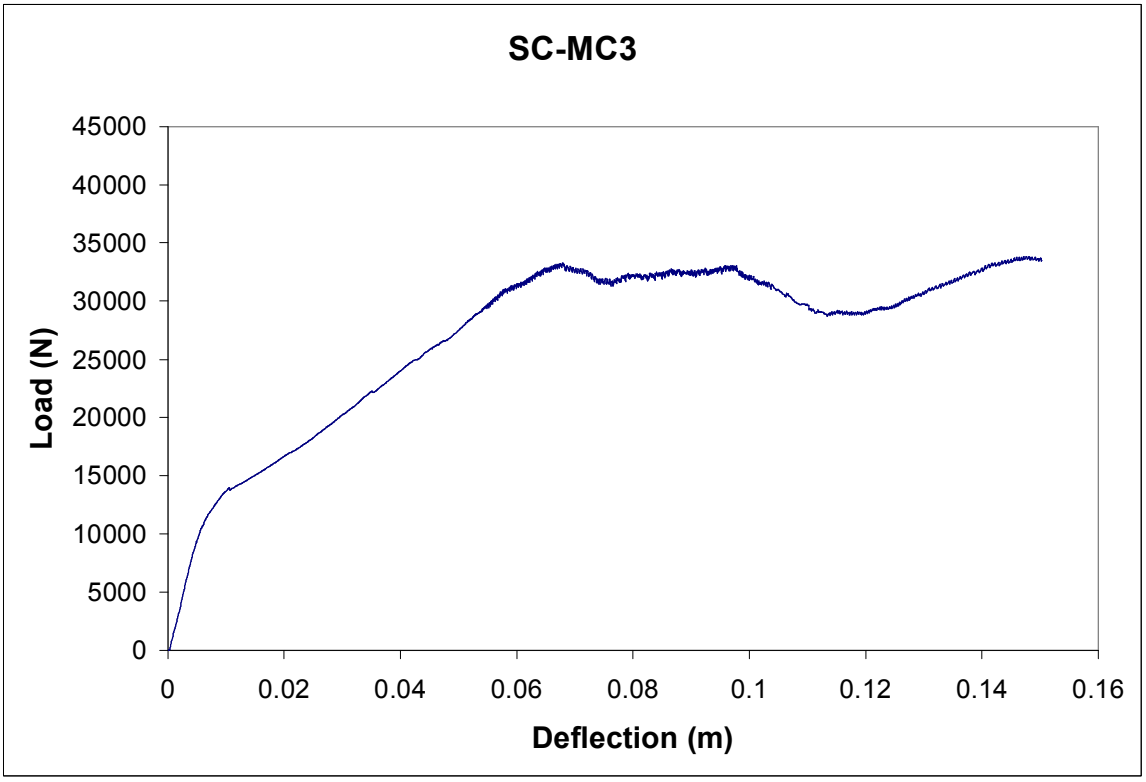

Figure 23A Load versus deflection plot. Test SC-MC3.

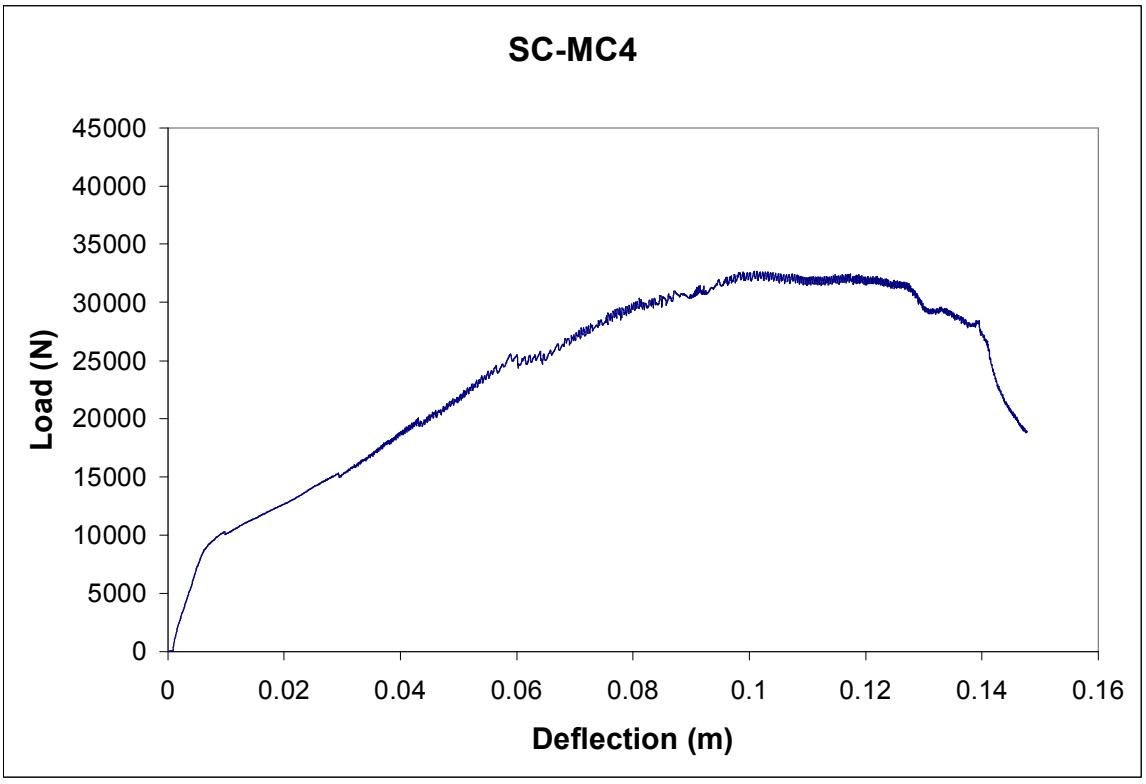

Figure 24A Load versus deflection plot. Test SC-MC4.

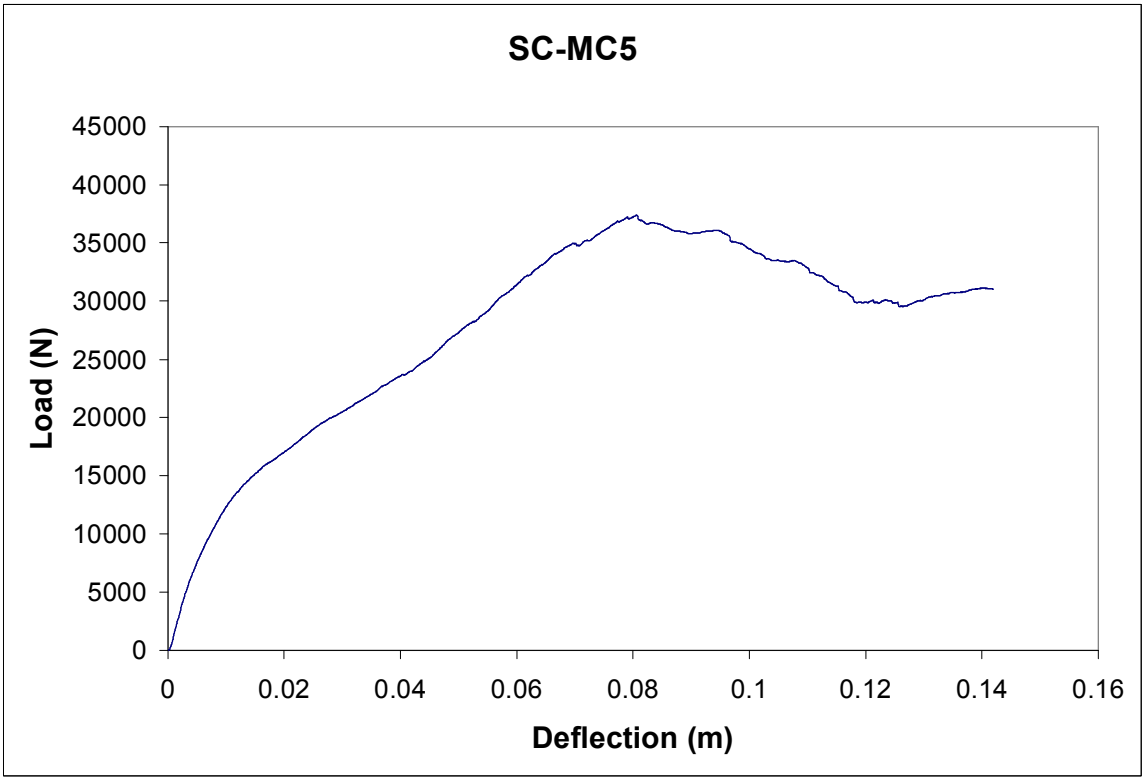

Figure 25A Load versus deflection plot. Test SC-MC5.

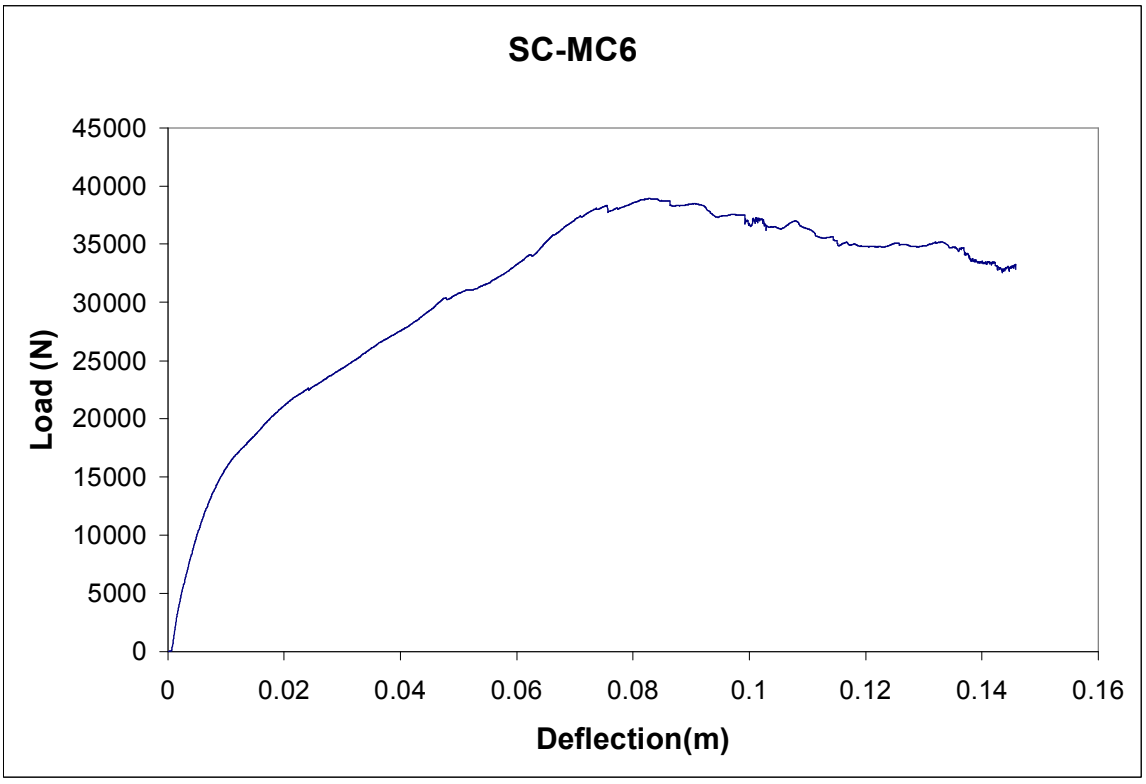

Figure 26A Load versus deflection plot. Test SC-MC6.

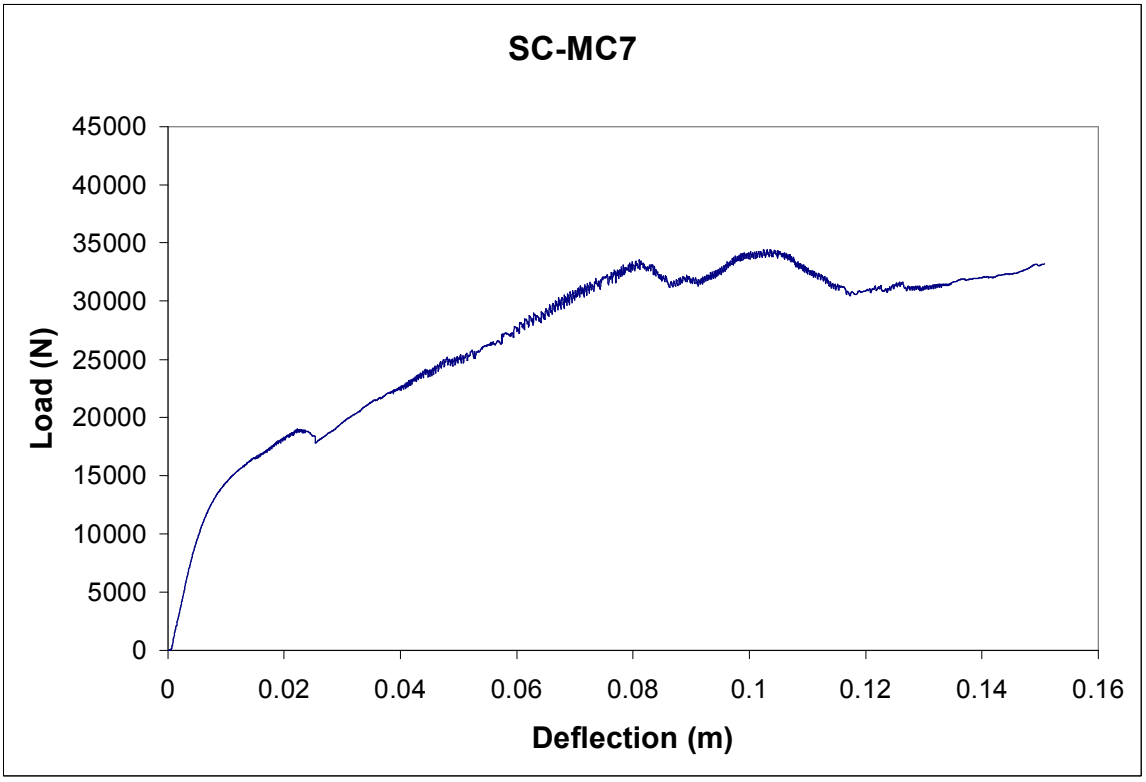

Figure 27A Load versus deflection plot. Test SC-MC7.

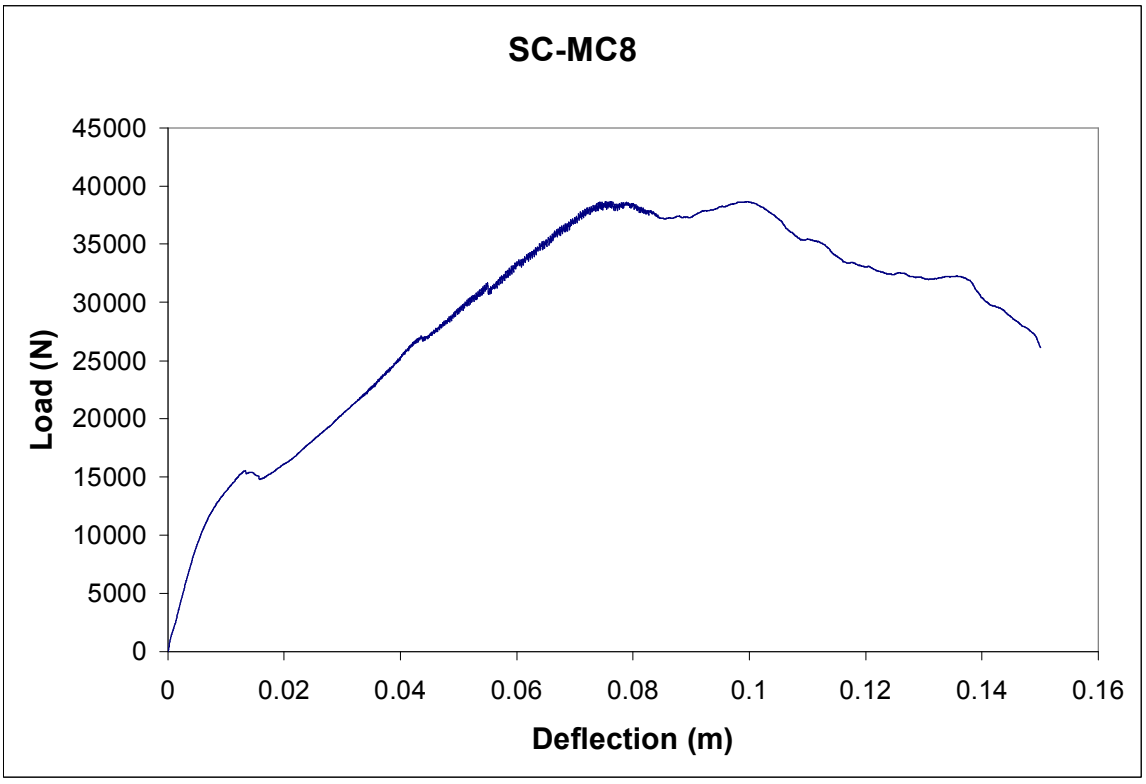

Figure 28A Load versus deflection plot. Test SC-MC8.

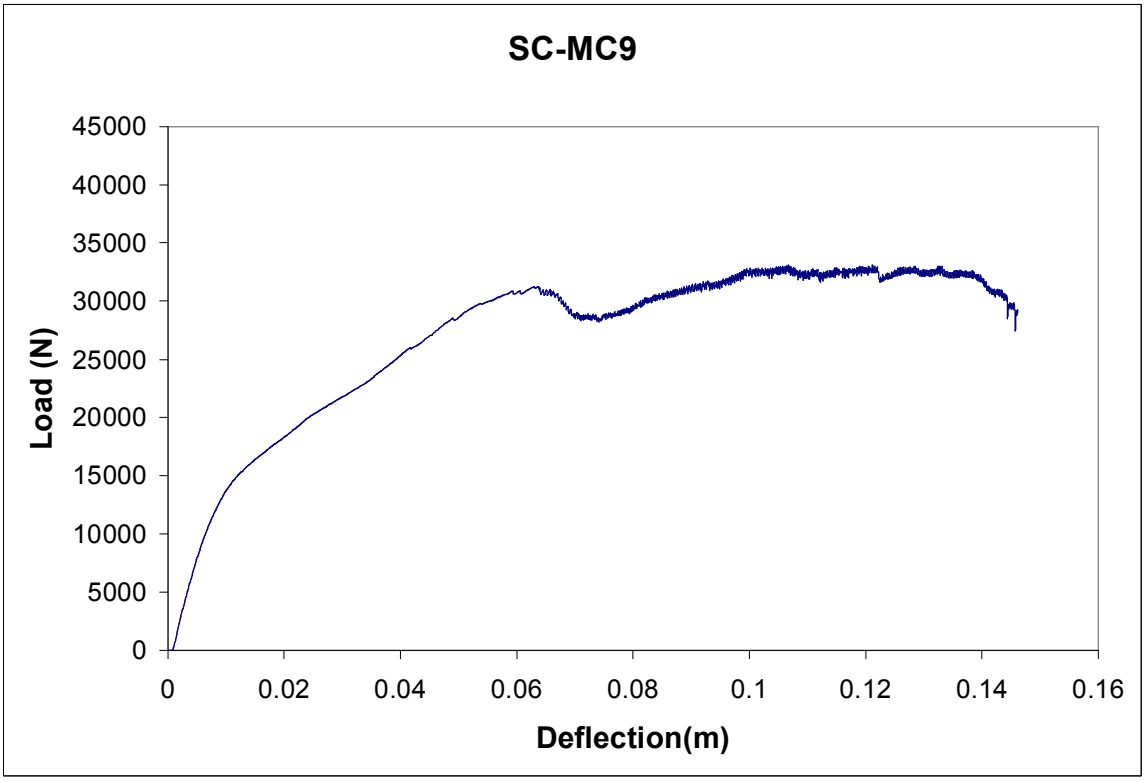

Figure 29A Load versus deflection plot. Test SC-MC9.

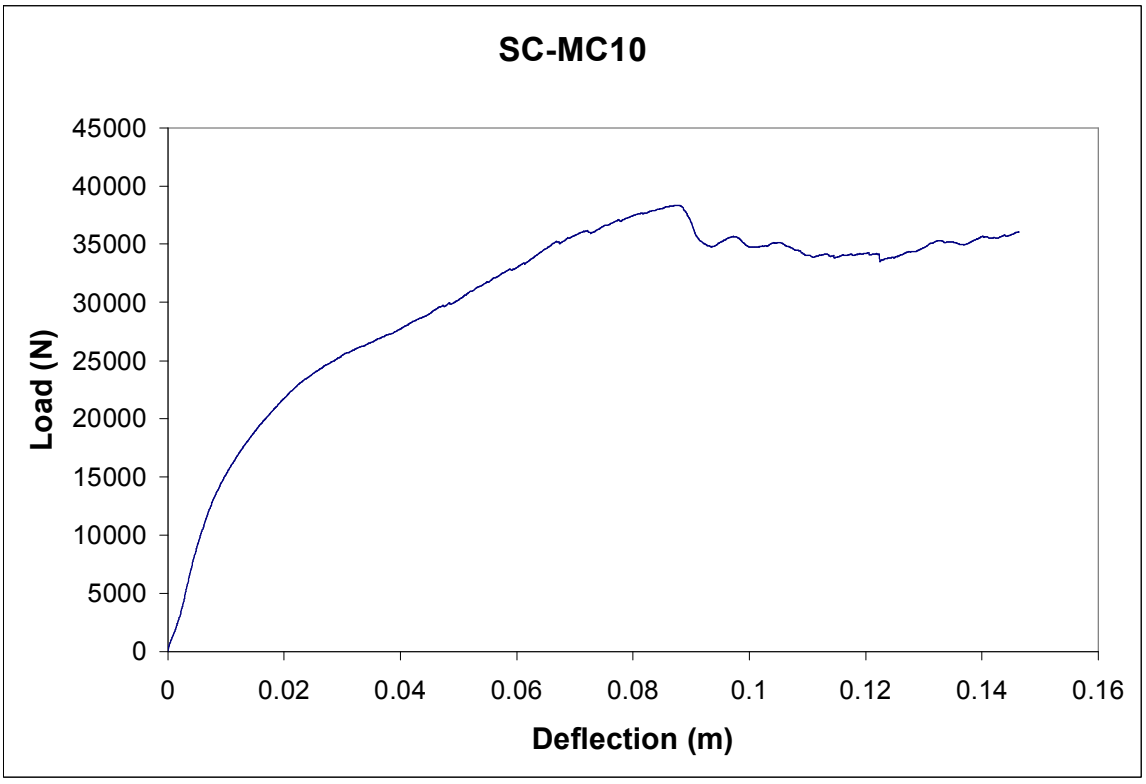

Figure 30A Load versus deflection plot. Test SC-MC10.

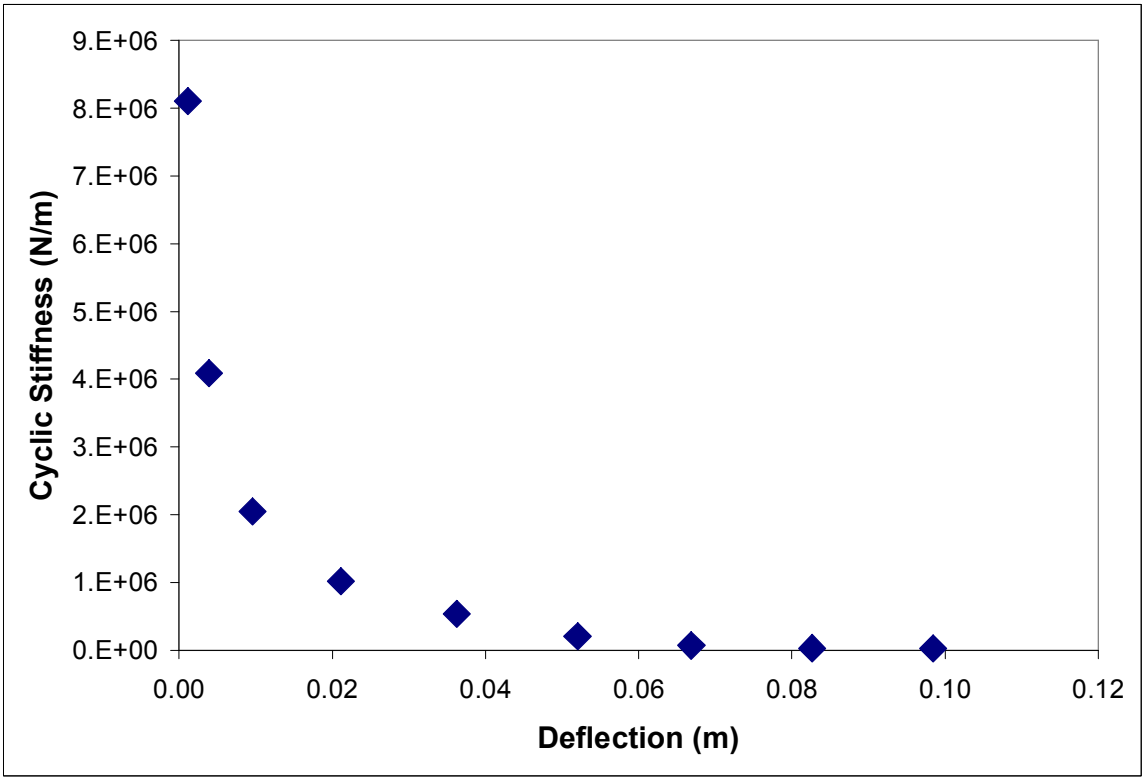

Figure 31A Average Cyclic Stiffness vs. Deflection plot showing stiffness degradation.

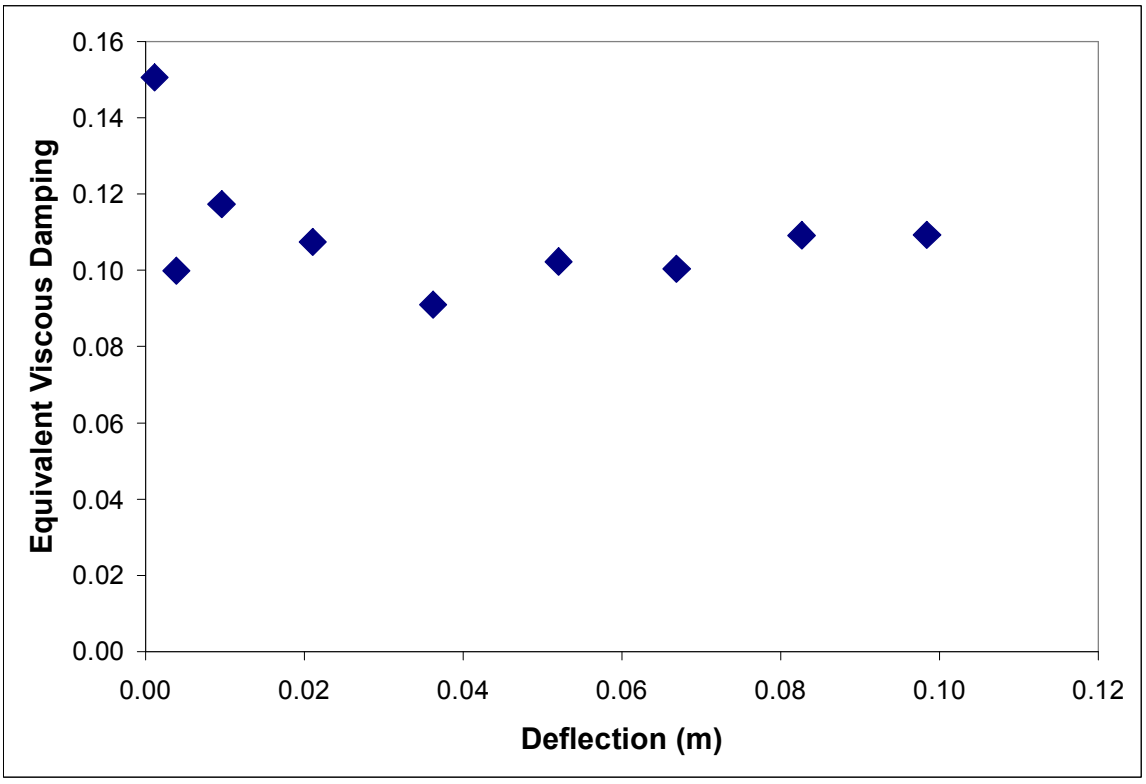

Figure 32A Average Equivalent Viscous Damping vs. Deflection.

APPENDIX B – LOG SHEAR WALL TEST RESULTS

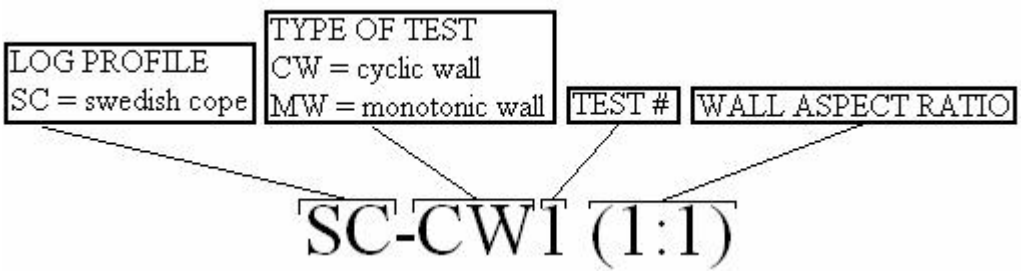

Figure 1B Nomenclature used for test specimen labeling.

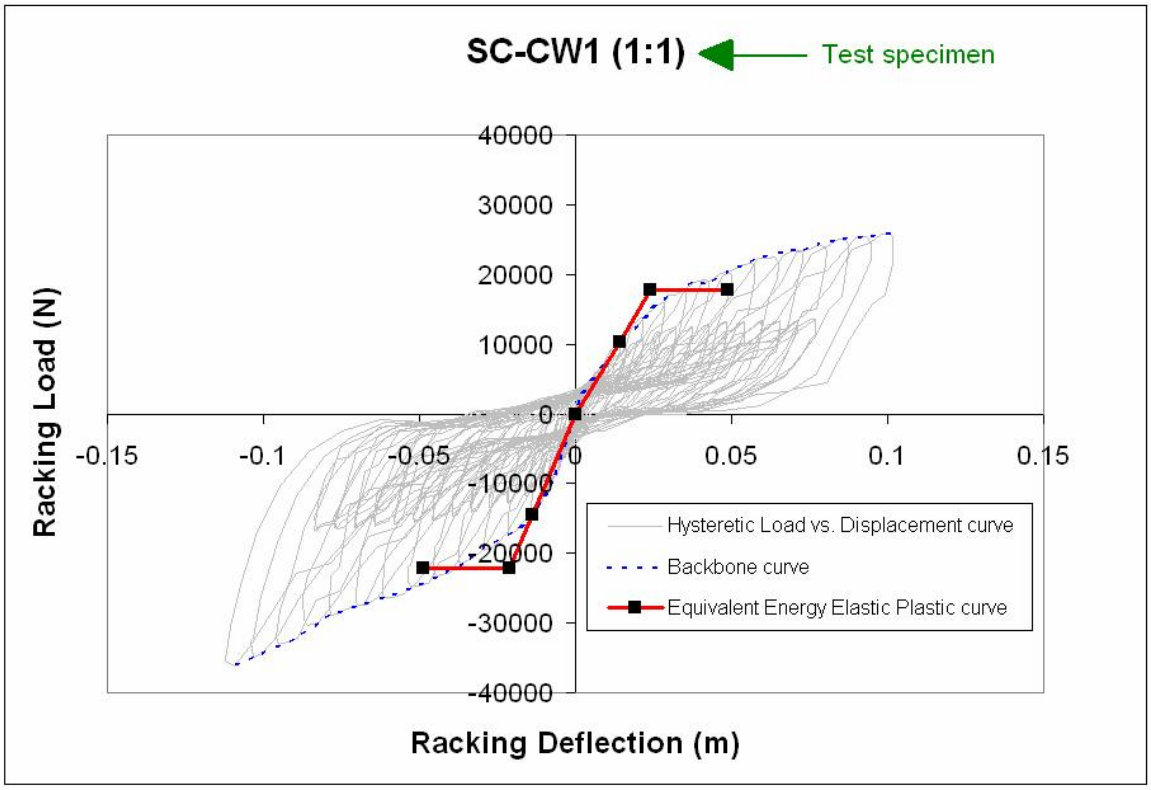

Figure 2B Load versus deflection hysteresis with typical test identification.

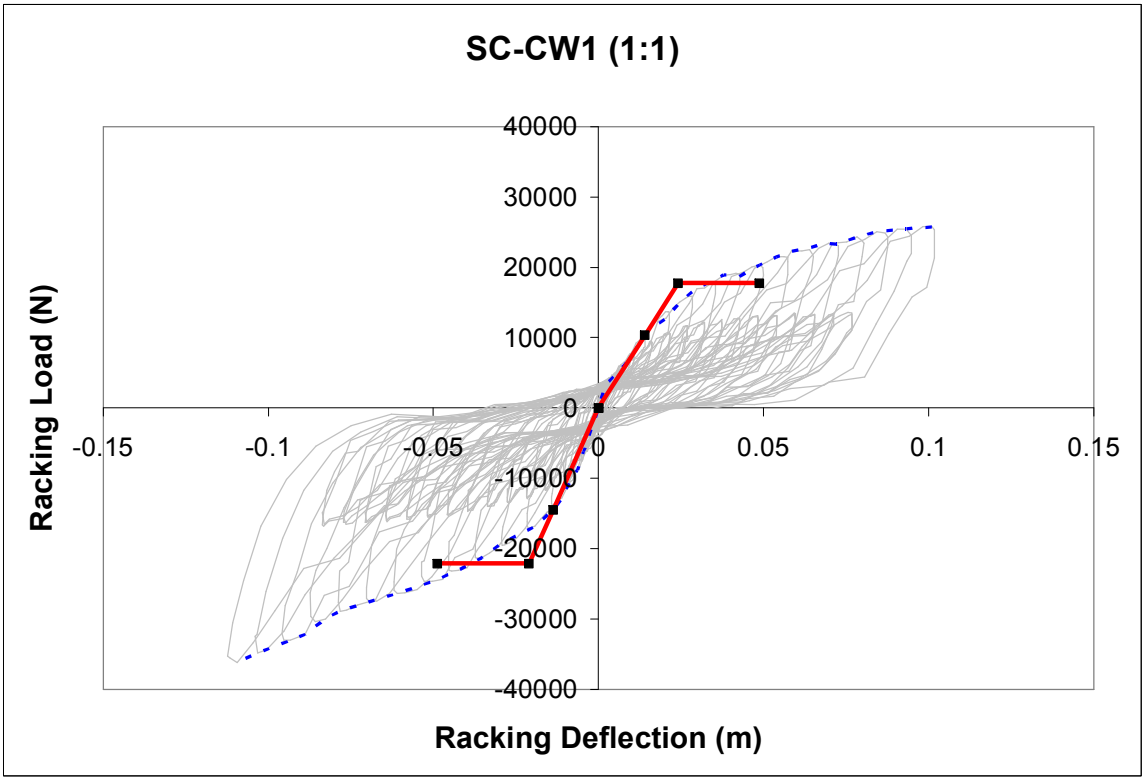

Figure 3B Load versus deflection hysteresis. Test SC-CW1 (1:1).

Table 1B Calculated hysteretic parameters. Test SC-CW1 (1:1).

Primary Cycle #	Δ_{max} (m)	Δ_{min} (m)	F @ Δ_{max} (N)	F @ Δ_{min} (N)	Strain Energy (N-m)	Hysteretic Energy (N-m)	ζ	Cyclic Stiffness (N/m)
1	0.001	-0.001	1612	-2012	2	1	0.116	1902622
3	0.003	-0.002	3395	-4261	9	4	0.070	1603334
5	0.005	-0.005	4982	-7471	33	12	0.056	1172933
7	0.014	-0.014	10364	-12589	163	68	0.066	807578
9	0.028	-0.029	15392	-18406	489	209	0.068	584380
11	0.043	-0.045	18691	-22198	903	345	0.061	464057
13	0.057	-0.062	20809	-24711	1362	516	0.060	381466
15	0.073	-0.079	23001	-27611	1924	645	0.053	334106
17	0.088	-0.096	24360	-32062	2603	796	0.049	307667
19	0.102	-0.112	25338	-35296	3271	923	0.045	283276

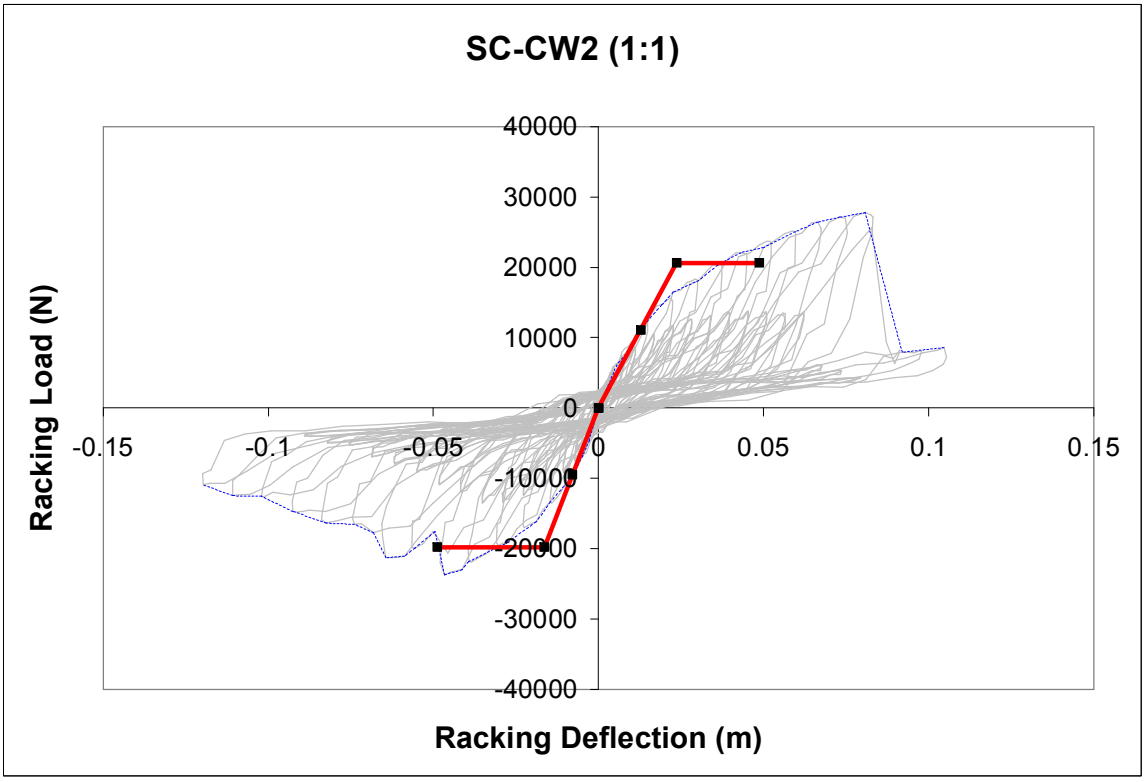

Figure 4B Load versus deflection hysteresis. Test SC-CW2 (1:1). (Note: check opened up vertically causing this wall to fail and uplift considerably)

Table 2B Calculated hysteretic parameters. Test SC-CW2 (1:1).

Primary Cycle #	Δ_{max} (m)	Δ_{min} (m)	F @ Δ_{max} (N)	F @ Δ_{min} (N)	Strain Energy (N-m)	Hysteretic Energy (N-m)	ζ	Cyclic Stiffness (N/m)
1	0.001	-0.001	1683	-1395	2	1	0.109	1425710
3	0.003	-0.002	3720	-3311	9	4	0.067	1383878
5	0.006	-0.005	5841	-6231	33	14	0.064	1090035
7	0.015	-0.015	12041	-13273	186	72	0.062	859884
9	0.030	-0.031	17988	-18976	563	205	0.058	607131
11	0.045	-0.048	20658	-22015	991	353	0.057	460029
13	0.060	-0.065	24250	-16421	1262	455	0.057	324786
15	0.075	-0.084	24900	-15443	1585	474	0.048	253561
17	0.091	-0.102	8230	-12574	1016	490	0.077	107697
19	0.105	-0.120	7230	-9382	943	242	0.041	73776

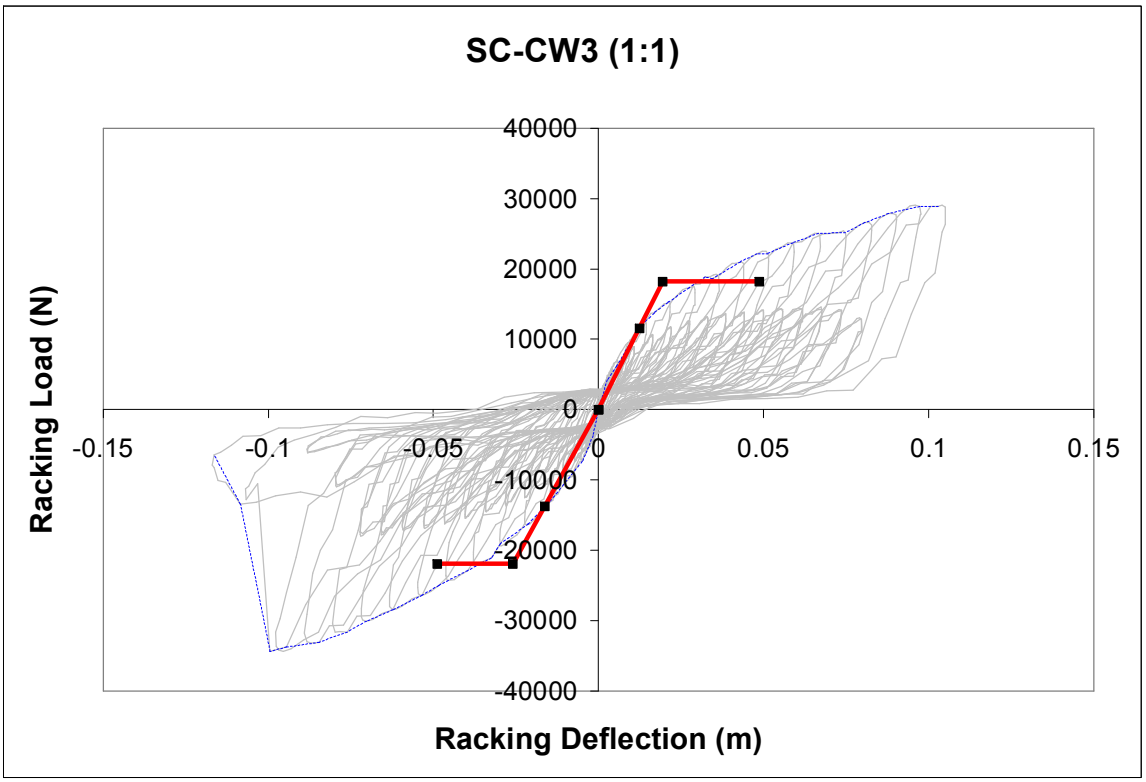

Figure 5B Load versus deflection hysteresis. Test SC-CW3 (1:1).

Table 3B Calculated hysteretic parameters. Test SC-CW3 (1:1).

Primary Cycle #	Δ_{max} (m)	Δ_{min} (m)	F @ Δ_{max} (N)	F @ Δ_{min} (N)	Strain Energy (N-m)	Hysteretic Energy (N-m)	ζ	Cyclic Stiffness (N/m)
1	0.001	-0.001	2549	-1904	3	1	0.088	1992022
3	0.003	-0.002	4134	-3745	10	4	0.066	1590658
5	0.006	-0.005	6993	-6323	37	15	0.064	1207888
7	0.014	-0.015	11664	-11851	171	70	0.065	810676
9	0.029	-0.030	16560	-18452	517	205	0.063	593626
11	0.044	-0.046	18219	-23539	946	358	0.060	462453
13	0.059	-0.063	22455	-26491	1504	537	0.057	399380
15	0.075	-0.081	24530	-30335	2142	697	0.052	352657
17	0.090	-0.098	27077	-31630	2767	868	0.050	312334
19	0.105	-0.117	26325	-7892	1844	735	0.063	154170

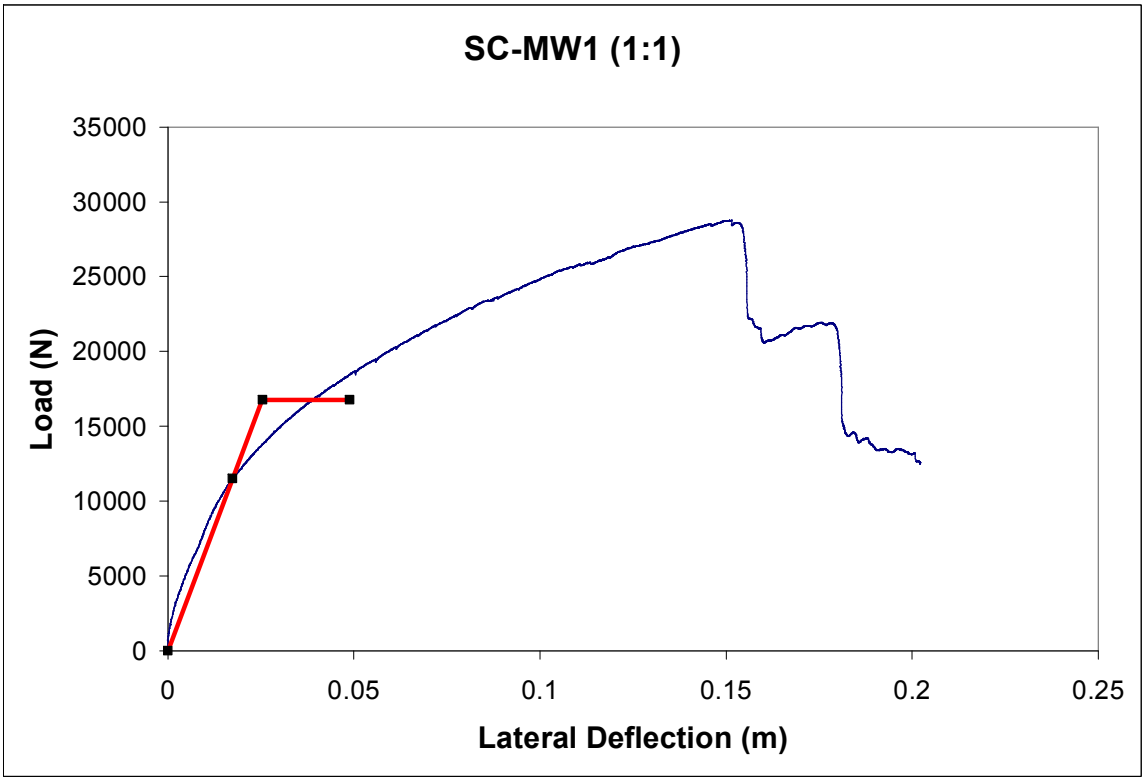

Figure 6B Load versus deflection. Test SC-MW1 (1:1).

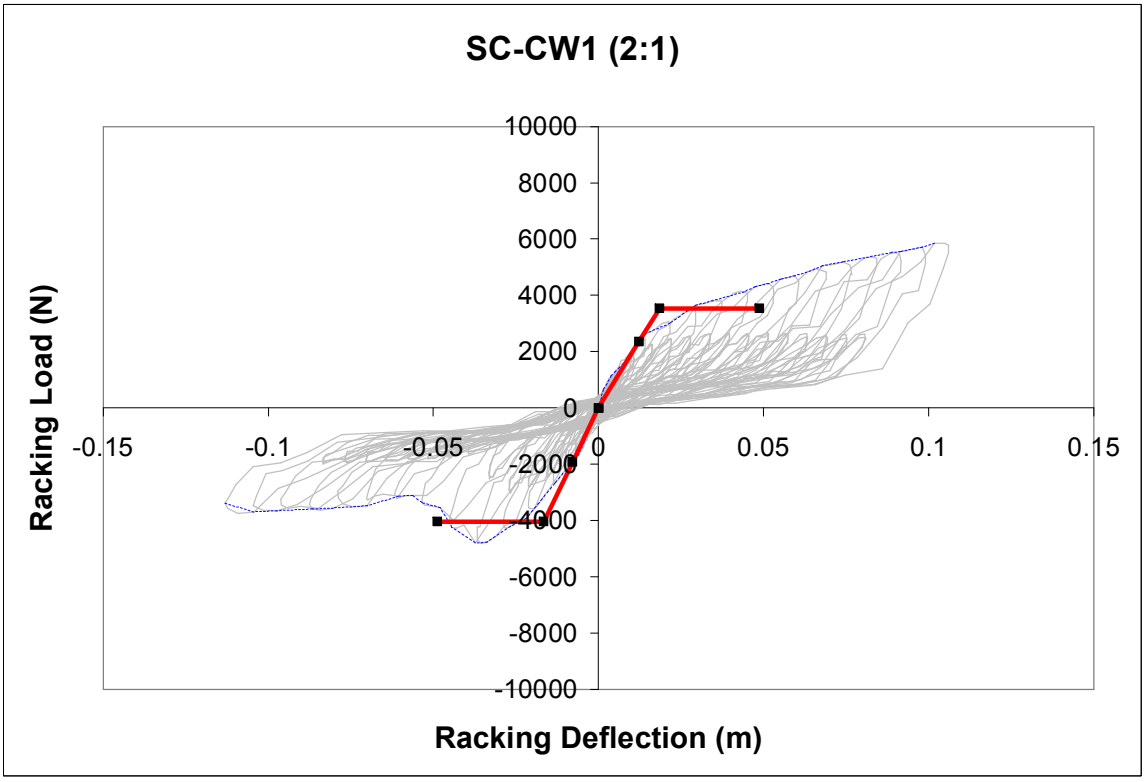

Figure 7B Load versus deflection hysteresis. Test SC-CW1 (2:1).

Table 4B Calculated hysteretic parameters. Test SC-CW1 (2:1).

Primary Cycle #	Δ_{max} (m)	Δ_{min} (m)	F @ Δ_{max} (N)	F @ Δ_{min} (N)	Strain Energy (N-m)	Hysteretic Energy (N-m)	ζ	Cyclic Stiffness (N/m)
1	0.001	-0.001	246	-390	0.31	0.36	0.185	317115
3	0.003	-0.002	633	-611	1.50	0.93	0.099	257729
5	0.006	-0.005	1245	-1308	6.74	2.72	0.064	241689
7	0.014	-0.014	2403	-2505	34.17	10.91	0.051	176118
9	0.029	-0.029	3238	-4030	105.62	35.99	0.054	124838
11	0.045	-0.045	3760	-3881	172.39	62.71	0.058	84668
13	0.061	-0.062	4393	-3073	228.09	52.14	0.036	61010
15	0.077	-0.079	4736	-2947	297.73	68.88	0.037	49403
17	0.092	-0.096	5209	-3244	394.61	83.29	0.034	45019
19	0.106	-0.113	5795	-3384	498.65	86.29	0.028	41876

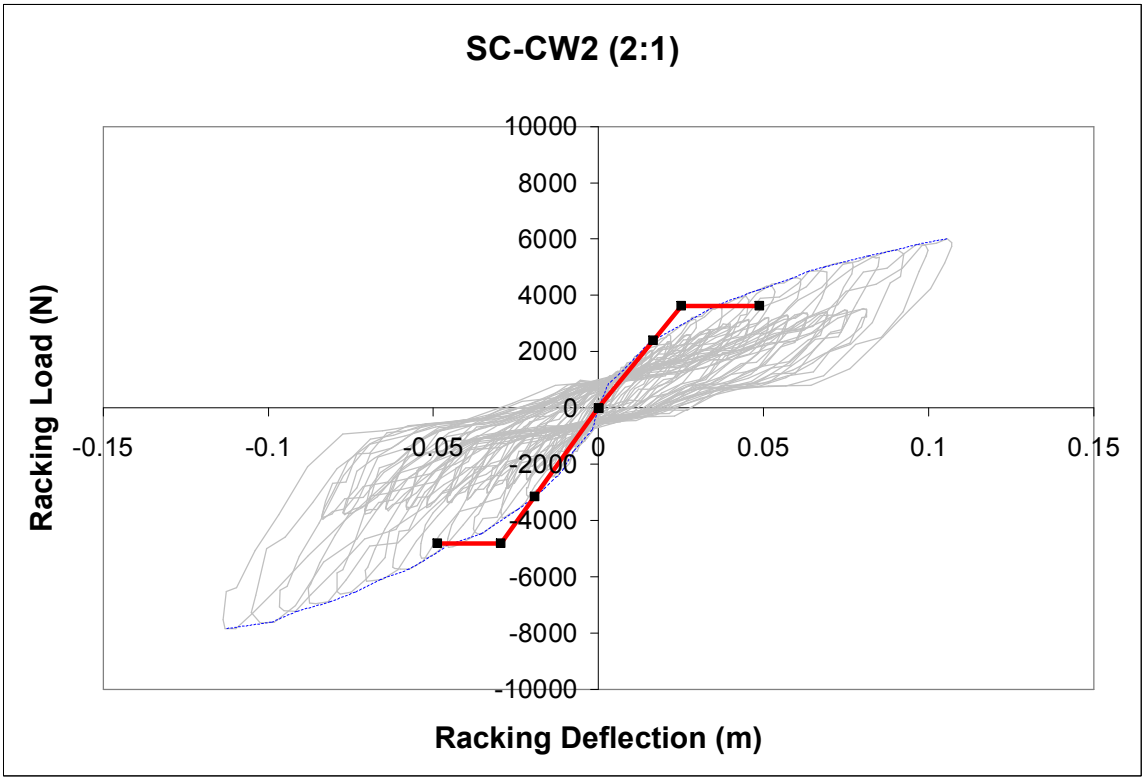

Figure 8B Load versus deflection hysteresis. Test SC-CW2 (2:1).

Table 5B Calculated hysteretic parameters. Test SC-CW2 (2:1).

Primary Cycle #	Δ_{max} (m)	Δ_{min} (m)	F @ Δ_{max} (N)	F @ Δ_{min} (N)	Strain Energy (N-m)	Hysteretic Energy (N-m)	ζ	Cyclic Stiffness (N/m)
1	0.001	-0.001	180	-239	0.21	0.26	0.199	203716
3	0.003	-0.002	509	-570	1.31	0.73	0.089	221294
5	0.005	-0.005	1038	-1156	5.83	1.89	0.052	206156
7	0.014	-0.014	1987	-2206	29.89	10.21	0.054	146996
9	0.030	-0.029	3063	-3703	99.95	35.06	0.056	114462
11	0.046	-0.046	3842	-4868	199.02	67.65	0.054	95333
13	0.061	-0.062	4397	-5668	310.97	106.06	0.054	81511
15	0.077	-0.079	5043	-6524	452.70	132.83	0.047	74027
17	0.092	-0.097	5442	-7061	592.83	171.59	0.046	66106
19	0.107	-0.114	5730	-7512	733.38	194.72	0.042	60022

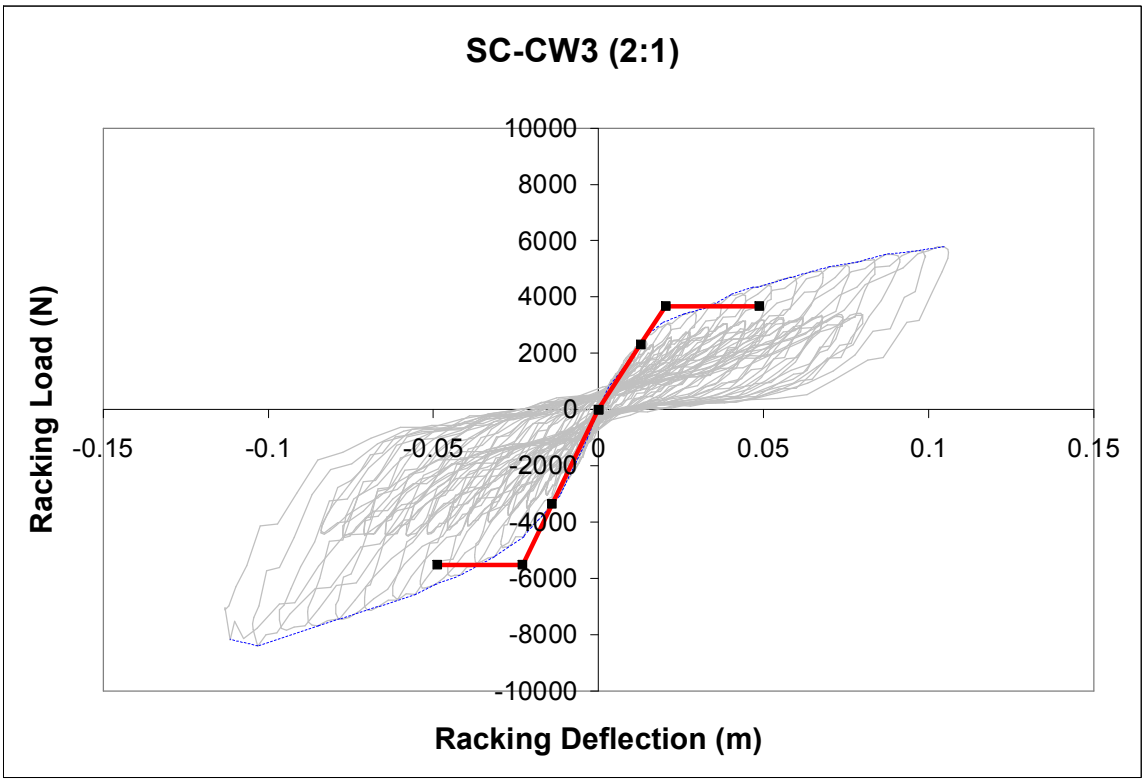

Figure 9B Load versus deflection hysteresis. Test SC-CW3 (2:1).

Table 6B Calculated hysteretic parameters. Test SC-CW3 (2:1).

Primary Cycle #	Δ_{max} (m)	Δ_{min} (m)	F @ Δ_{max} (N)	F @ Δ_{min} (N)	Strain Energy (N-m)	Hysteretic Energy (N-m)	ζ	Cyclic Stiffness (N/m)
1	0.002	-0.001	282	-239	0.29	0.30	0.166	244158
3	0.003	-0.002	723	-745	1.77	1.59	0.143	302549
5	0.006	-0.005	1298	-1441	7.24	5.46	0.120	257953
7	0.015	-0.014	2333	-3117	38.86	29.43	0.121	190568
9	0.030	-0.029	3355	-4802	120.34	69.18	0.091	138182
11	0.045	-0.046	3920	-5571	214.48	71.01	0.053	105192
13	0.060	-0.062	4495	-6616	341.23	107.53	0.050	90775
15	0.076	-0.079	4816	-7239	470.28	148.67	0.050	77598
17	0.091	-0.097	5231	-7122	582.62	177.73	0.049	65767
19	0.106	-0.113	5576	-7042	693.46	214.03	0.049	57609

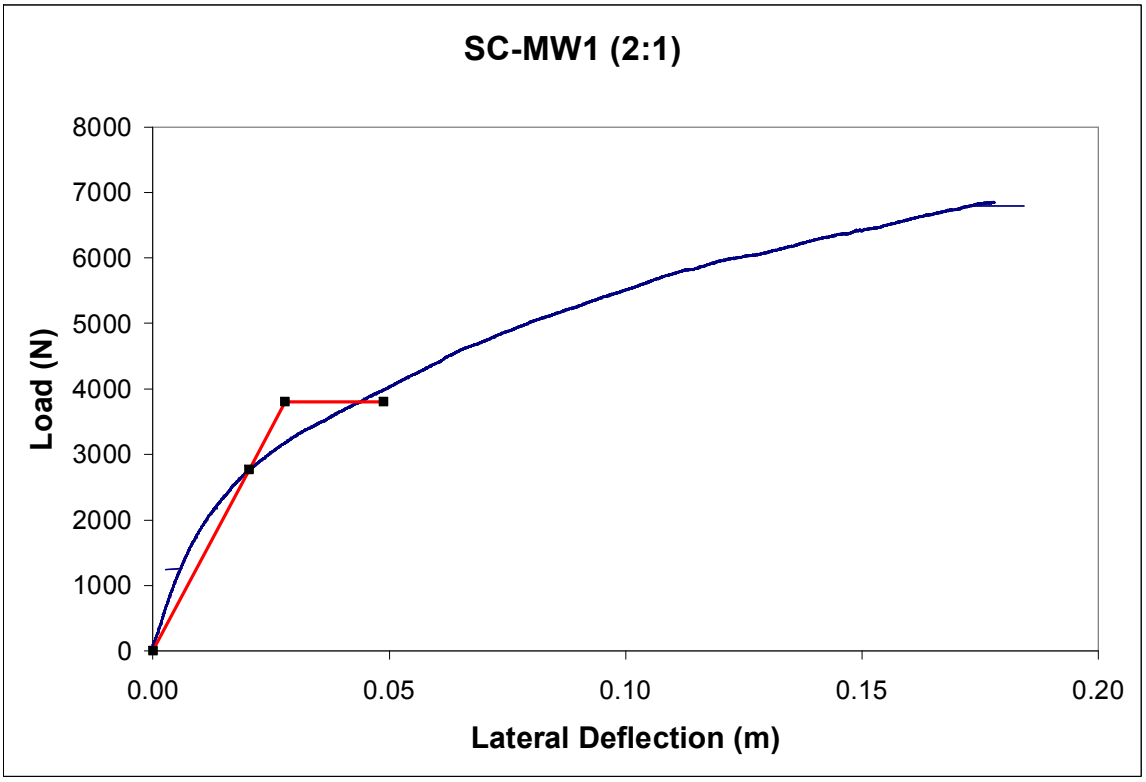

Figure 10B Load versus deflection. Test SC-MW1 (2:1).

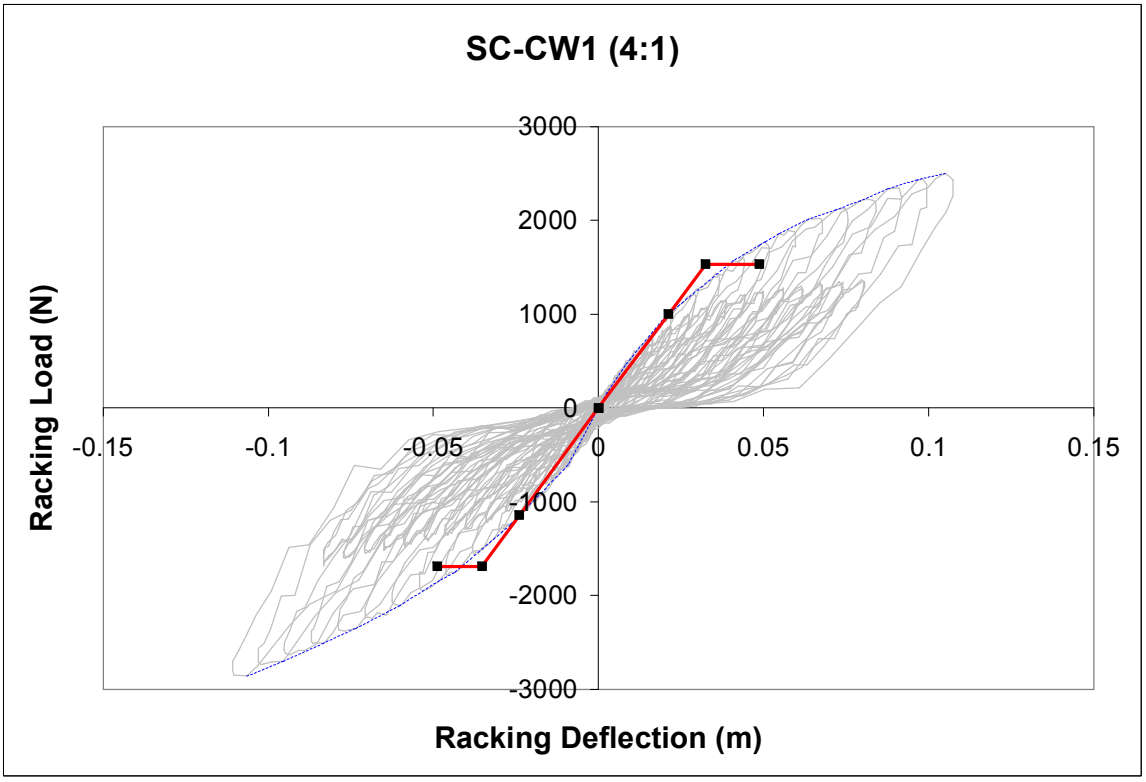

Figure 11B Load versus deflection hysteresis. Test SC-CW1 (4:1).

Table 7B Calculated hysteretic parameters. Test SC-CW1 (4:1).

Primary Cycle #	Δ_{max} (m)	Δ_{min} (m)	F @ Δ_{max} (N)	F @ Δ_{min} (N)	Strain Energy (N-m)	Hysteretic Energy (N-m)	ζ	Cyclic Stiffness (N/m)
1	0.001	0.000	66	-95	0.04	0.05	0.192	154791
3	0.003	-0.002	166	-212	0.46	0.23	0.082	77998
5	0.006	-0.005	343	-361	1.90	0.63	0.052	65081
7	0.014	-0.014	687	-730	10.15	2.51	0.039	49409
9	0.029	-0.030	1195	-1307	37.17	8.47	0.036	42100
11	0.044	-0.046	1587	-1722	74.75	16.08	0.034	36655
13	0.060	-0.063	1868	-2057	119.97	25.21	0.033	32138
15	0.075	-0.079	2011	-2301	166.81	34.93	0.033	27906
17	0.092	-0.095	2243	-2578	225.63	42.80	0.030	25784
19	0.107	-0.111	2357	-2796	281.31	53.12	0.030	23633

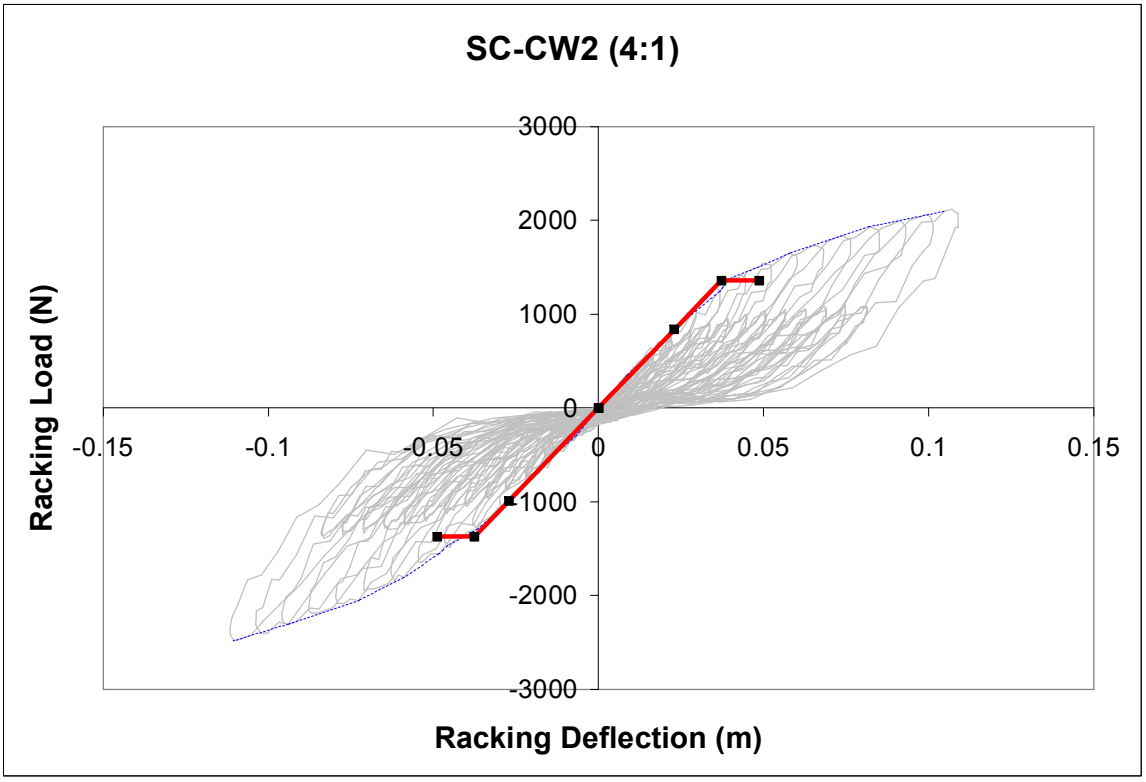

Figure 12B Load versus deflection hysteresis. Test SC-CW2 (4:1).

Table 8B Calculated hysteretic parameters. Test SC-CW2 (4:1).

Primary Cycle #	Δ_{max} (m)	Δ_{min} (m)	F @ Δ_{max} (N)	F @ Δ_{min} (N)	Strain Energy (N-m)	Hysteretic Energy (N-m)	ζ	Cyclic Stiffness (N/m)
1	0.001	-0.001	39	-115	0.05	0.07	0.204	93529
3	0.003	-0.002	83	-141	0.25	0.19	0.118	48188
5	0.006	-0.005	187	-236	1.12	0.48	0.068	39418
7	0.015	-0.014	506	-492	7.17	1.87	0.042	34732
9	0.030	-0.030	1025	-999	30.14	6.31	0.033	33987
11	0.045	-0.047	1356	-1430	63.47	13.84	0.035	30598
13	0.060	-0.063	1568	-1738	101.81	20.15	0.032	26860
15	0.076	-0.080	1758	-2002	146.88	29.26	0.032	24099
17	0.093	-0.096	1929	-2250	197.50	35.81	0.029	22137
19	0.109	-0.112	2074	-2338	243.43	43.15	0.028	20004

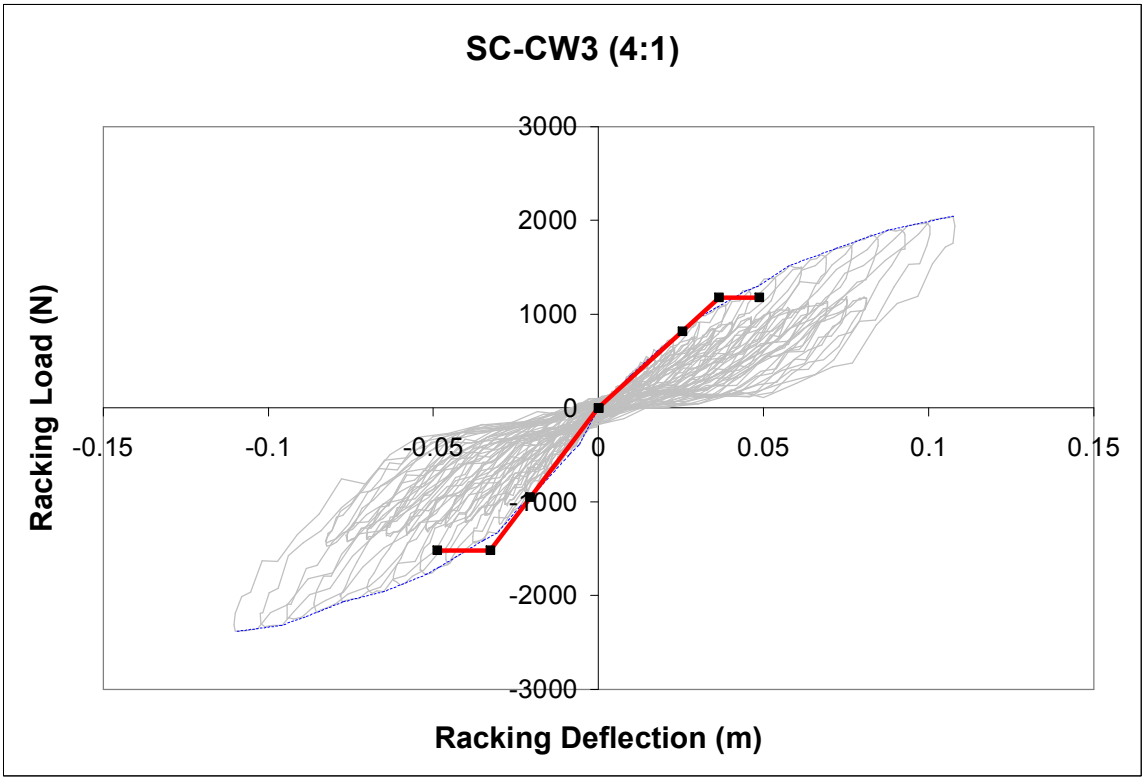

Figure 13B Load versus deflection hysteresis. Test SC-CW3 (4:1).

Table 9B Calculated hysteretic parameters. Test SC-CW3 (4:1).

Primary Cycle #	Δ_{max} (m)	Δ_{min} (m)	F @ Δ_{max} (N)	F @ Δ_{min} (N)	Strain Energy (N-m)	Hysteretic Energy (N-m)	ζ	Cyclic Stiffness (N/m)
1	0.001	0.000	54	-70	0.05	0.05	0.185	77409
3	0.003	-0.002	88	-127	0.24	0.16	0.106	46874
5	0.006	-0.005	176	-260	1.15	0.50	0.069	40493
7	0.015	-0.014	518	-592	8.06	4.31	0.085	38125
9	0.031	-0.030	893	-1171	31.28	7.20	0.037	33990
11	0.046	-0.046	1152	-1490	60.94	15.31	0.040	28639
13	0.061	-0.062	1502	-1790	101.64	22.08	0.035	26667
15	0.077	-0.078	1714	-2006	144.13	30.55	0.034	24014
17	0.093	-0.094	1848	-2092	184.28	39.26	0.034	21071
19	0.108	-0.110	1943	-2313	232.34	45.18	0.031	19507

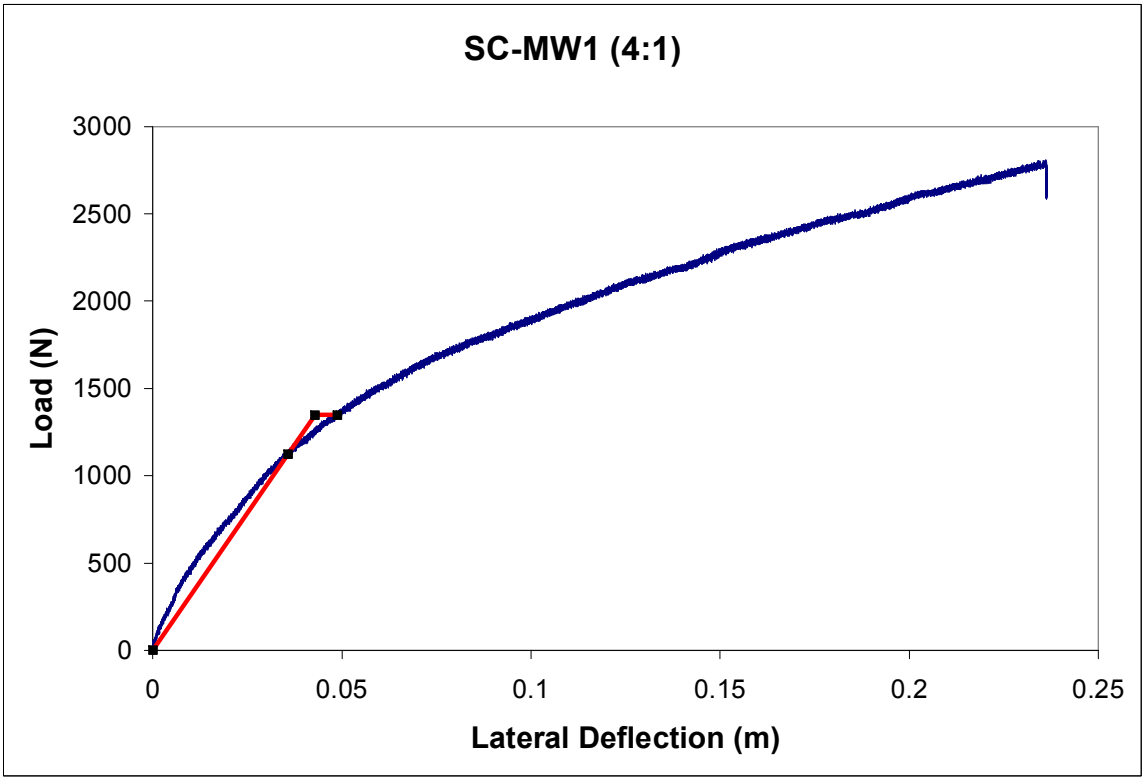

Figure 14B Load versus deflection. Test SC-MW1 (4:1).

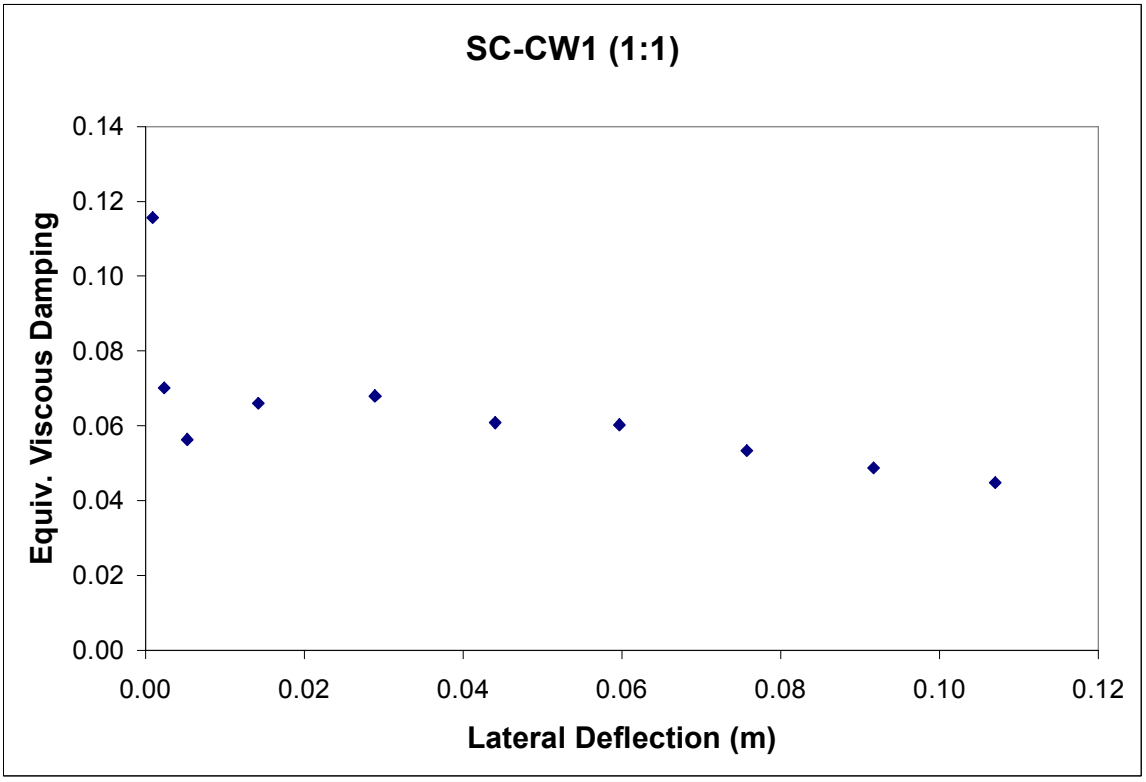

Figure 15B Equivalent viscous damping vs. Lateral deflection. Test SC-CW1 (1:1).

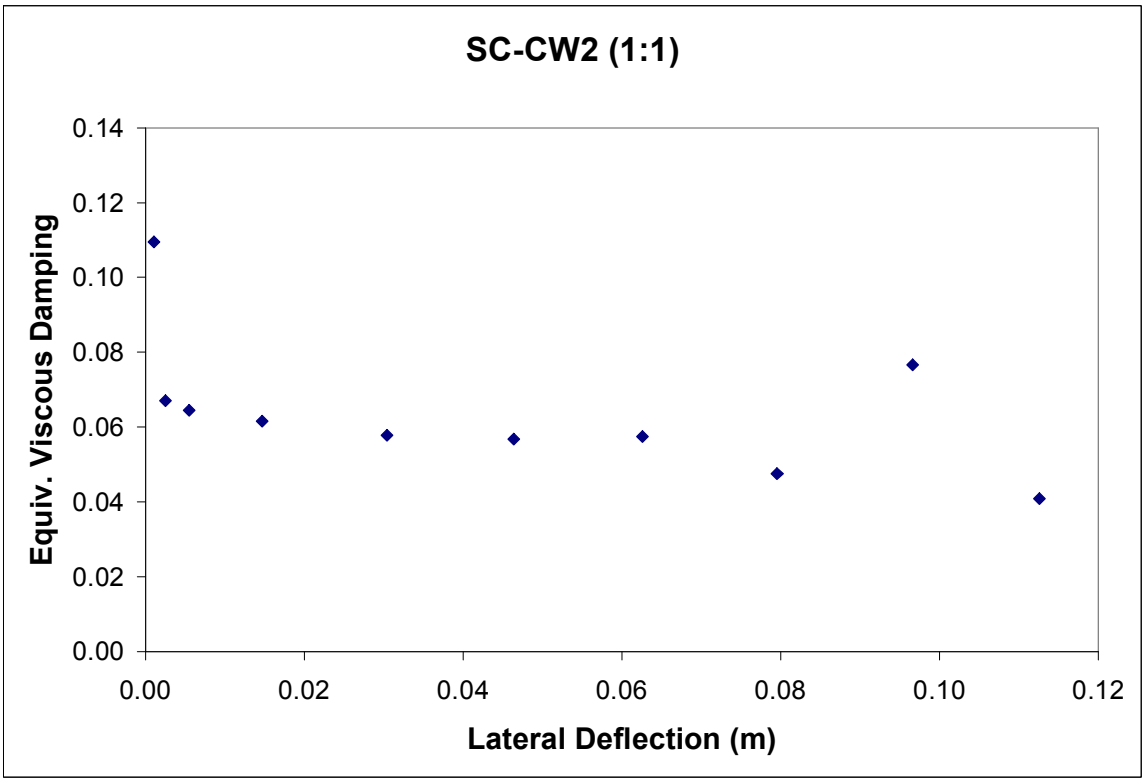

Figure 16B Equivalent viscous damping vs. Lateral deflection. Test SC-CW2 (1:1).

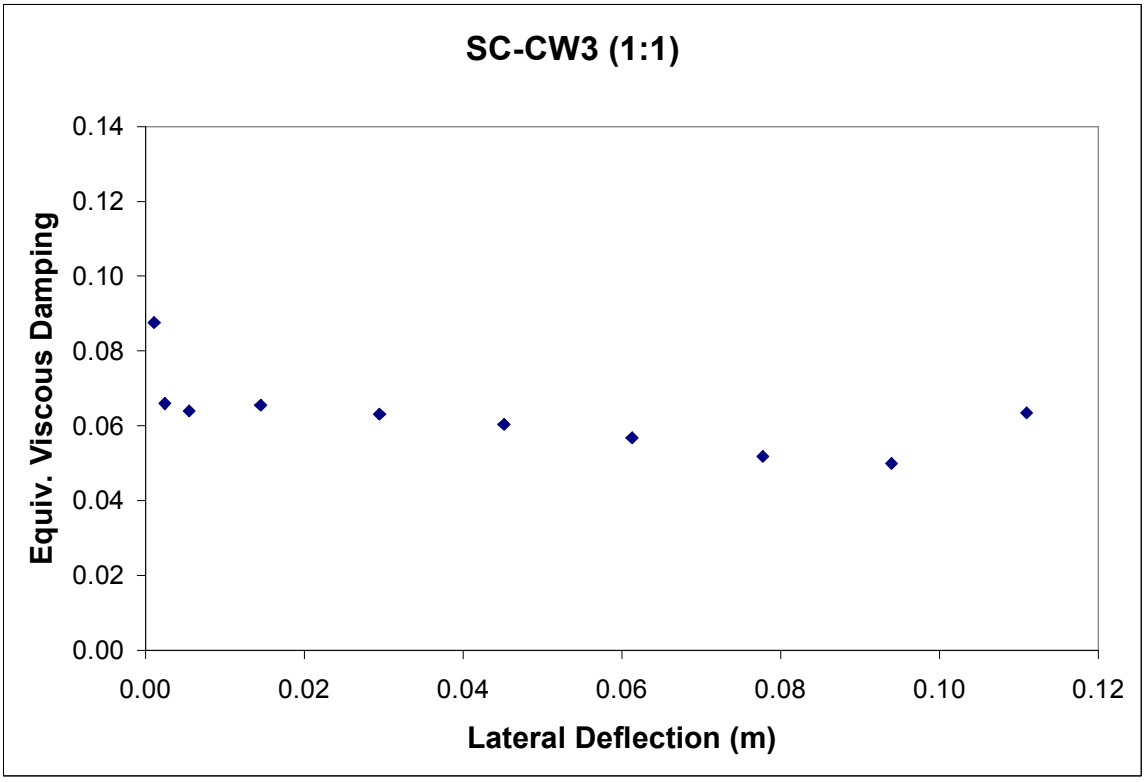

Figure 17B Equivalent viscous damping vs. Lateral deflection. Test SC-CW3 (1:1).

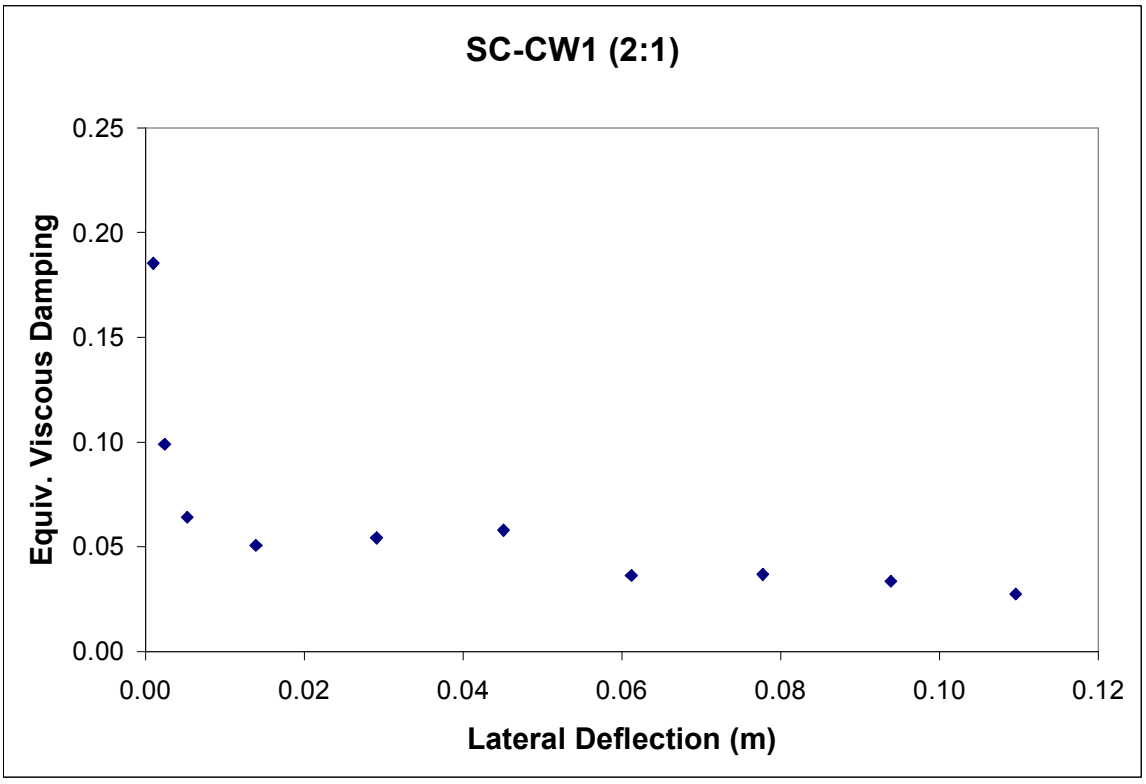

Figure 18B Equivalent viscous damping vs. Lateral deflection. Test SC-CW1 (2:1).

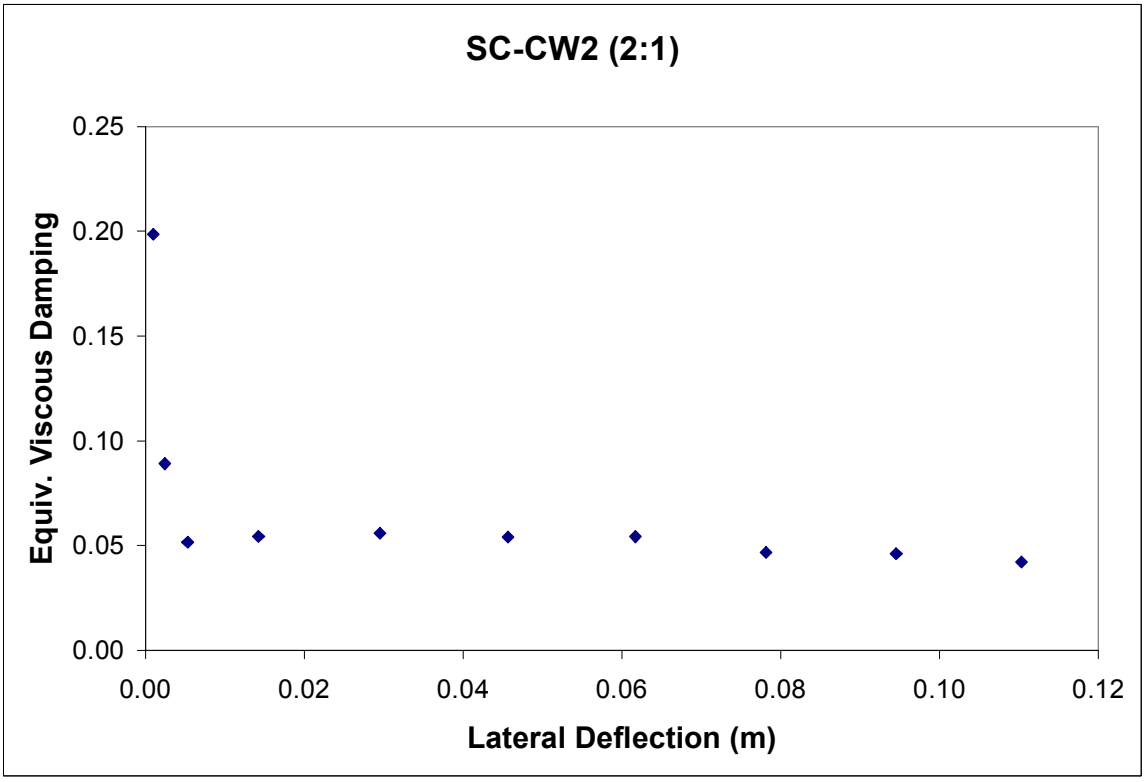

Figure 19B Equivalent viscous damping vs. Lateral deflection. Test SC-CW2 (2:1).

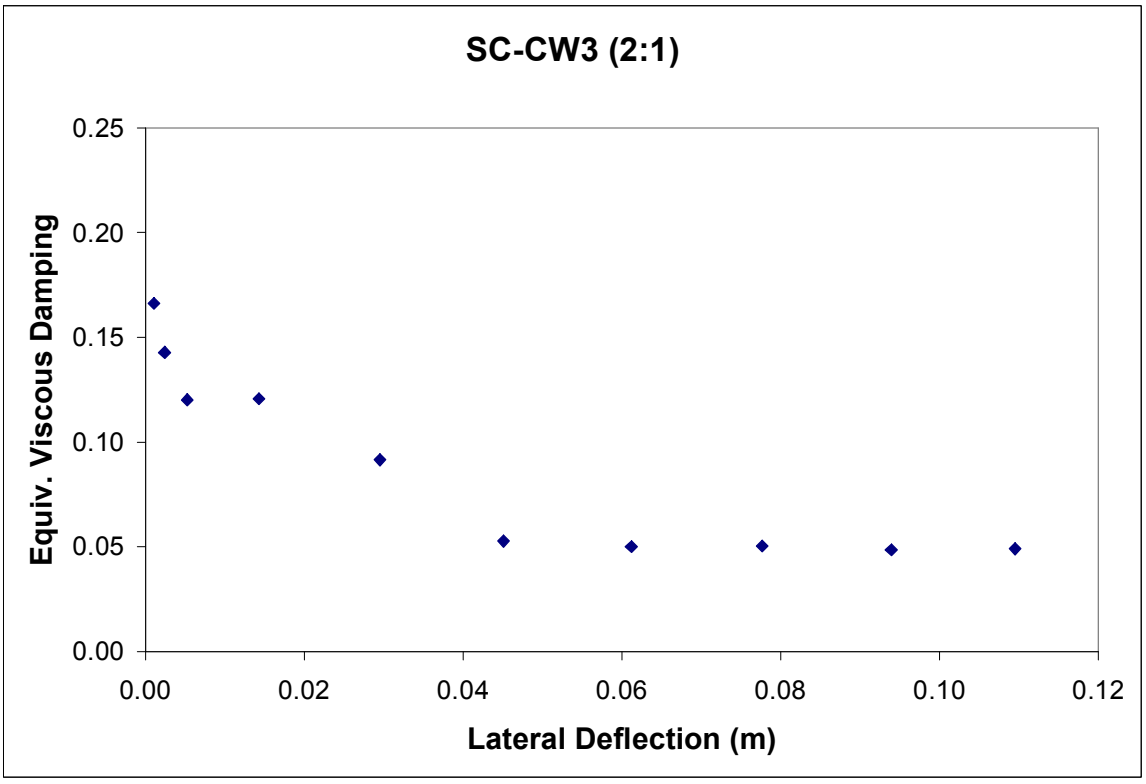

Figure 20B Equivalent viscous damping vs. Lateral deflection. Test SC-CW3 (2:1).

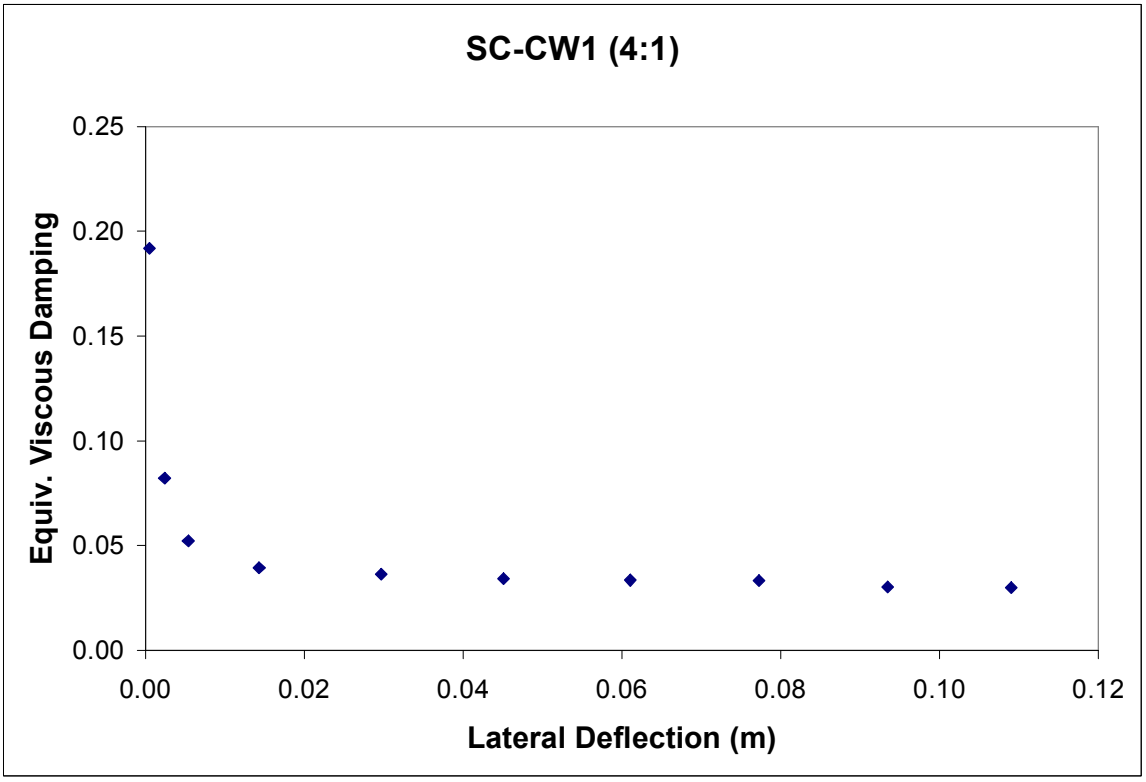

Figure 21B Equivalent viscous damping vs. Lateral deflection. Test SC-CW1 (4:1).

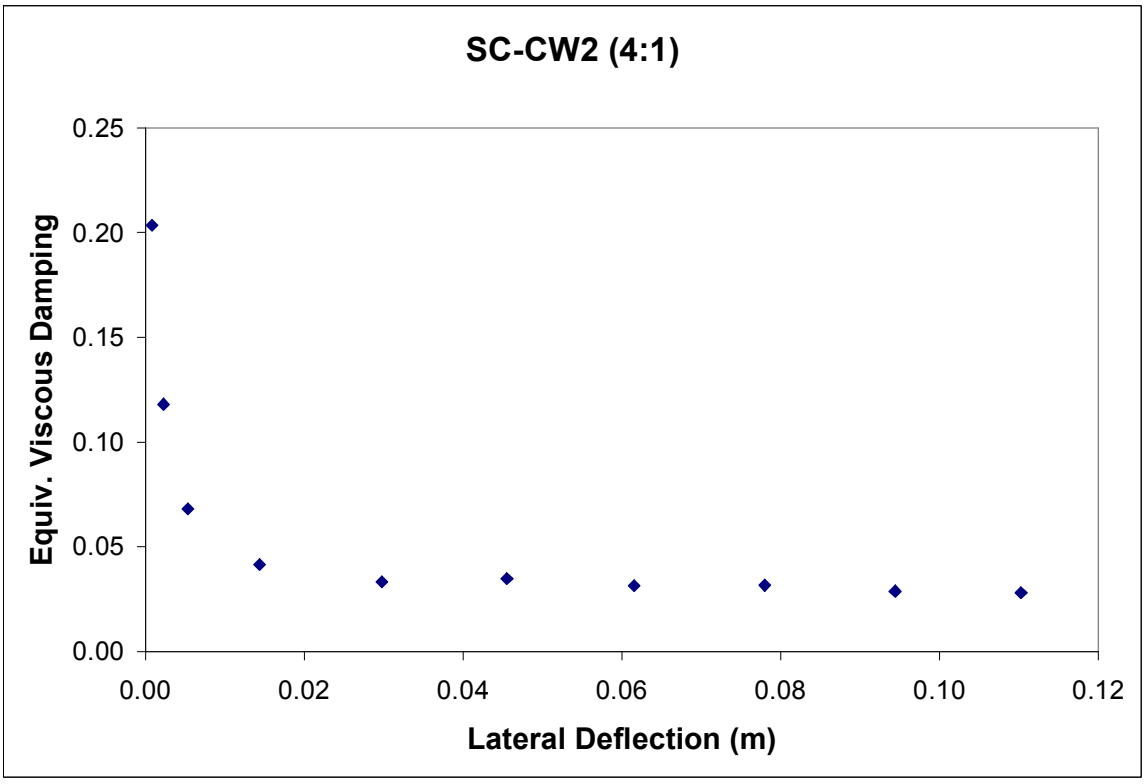

Figure 22B Equivalent viscous damping vs. Lateral deflection. Test SC-CW2 (4:1).

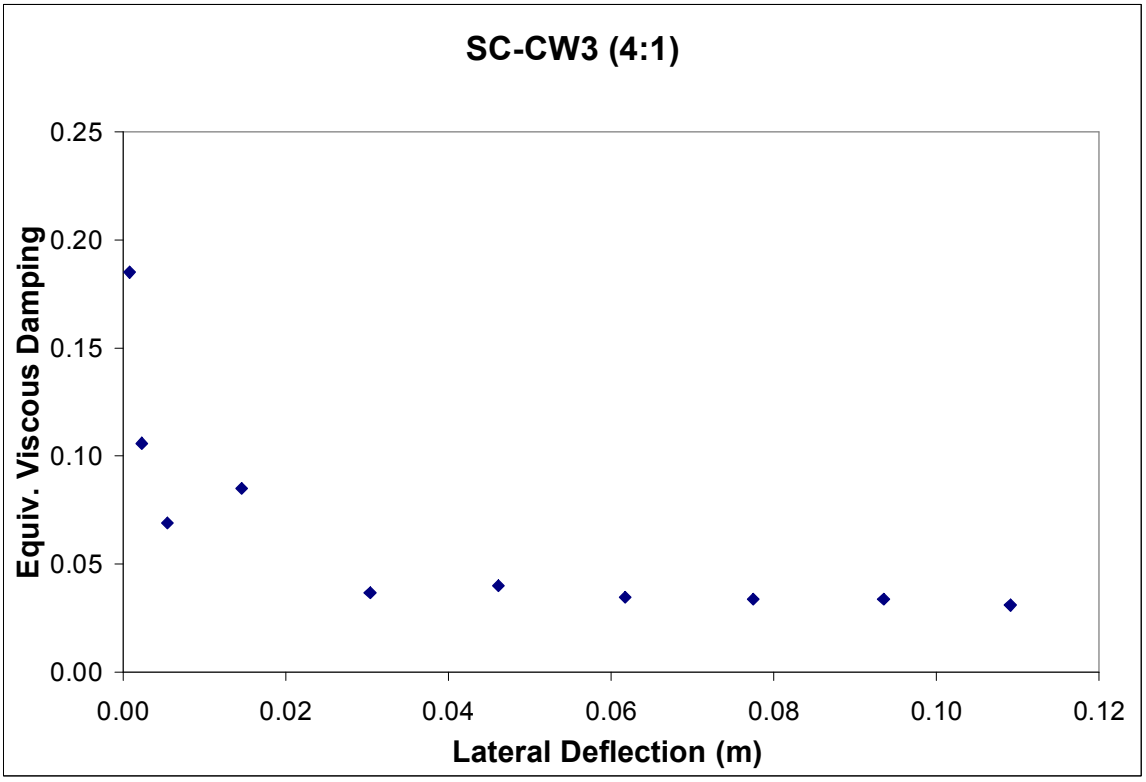

Figure 23B Equivalent viscous damping vs. Lateral deflection. Test SC-CW3 (4:1).

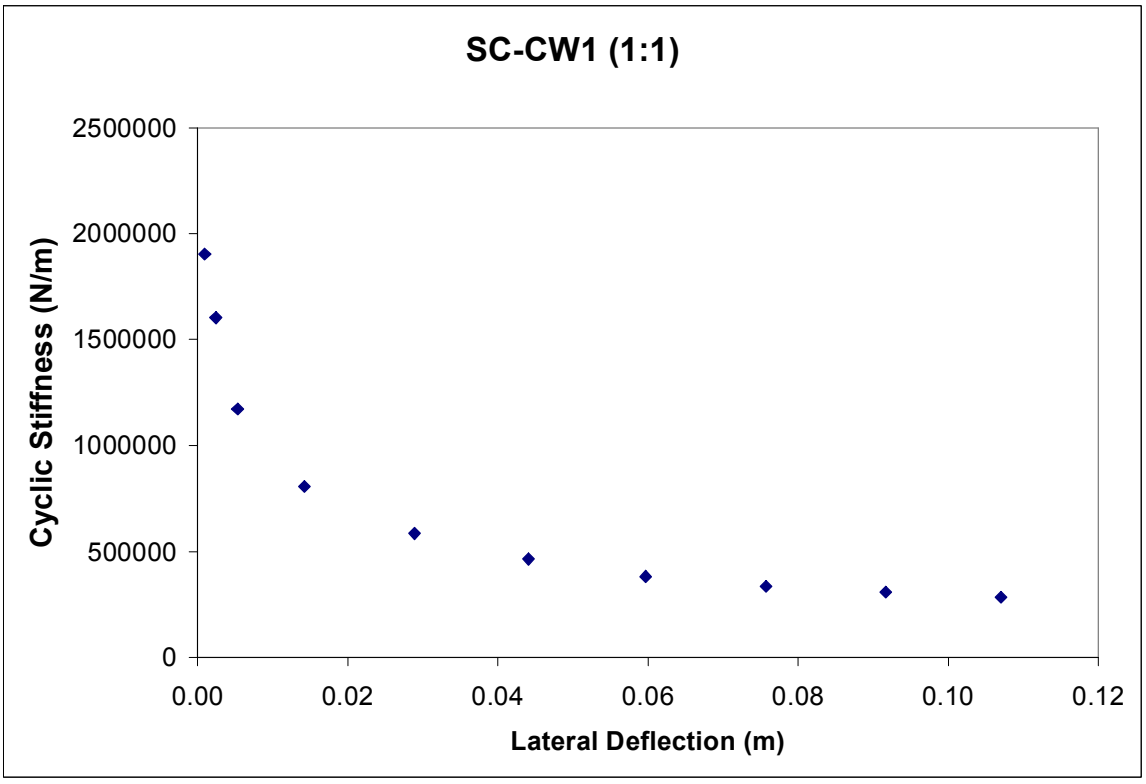

Figure 24B Cyclic stiffness vs. Lateral deflection. Test SC-CW1 (1:1).

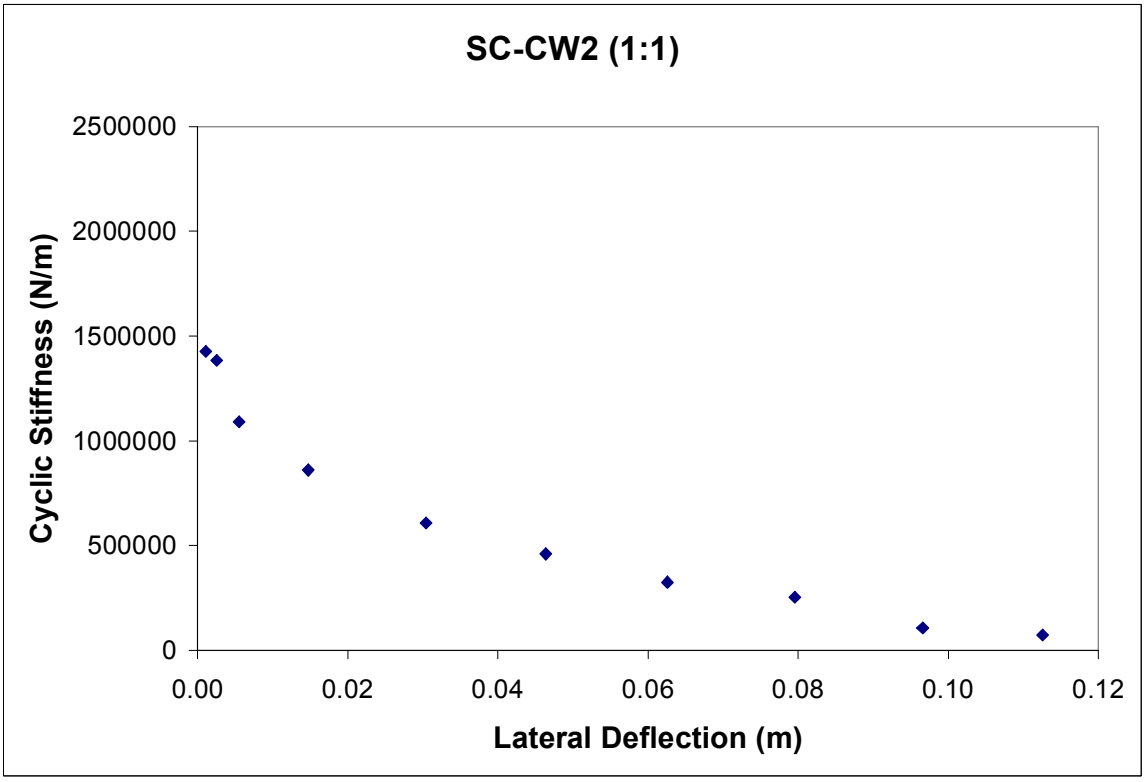

Figure 25B Cyclic stiffness vs. Lateral deflection. Test SC-CW2 (1:1).

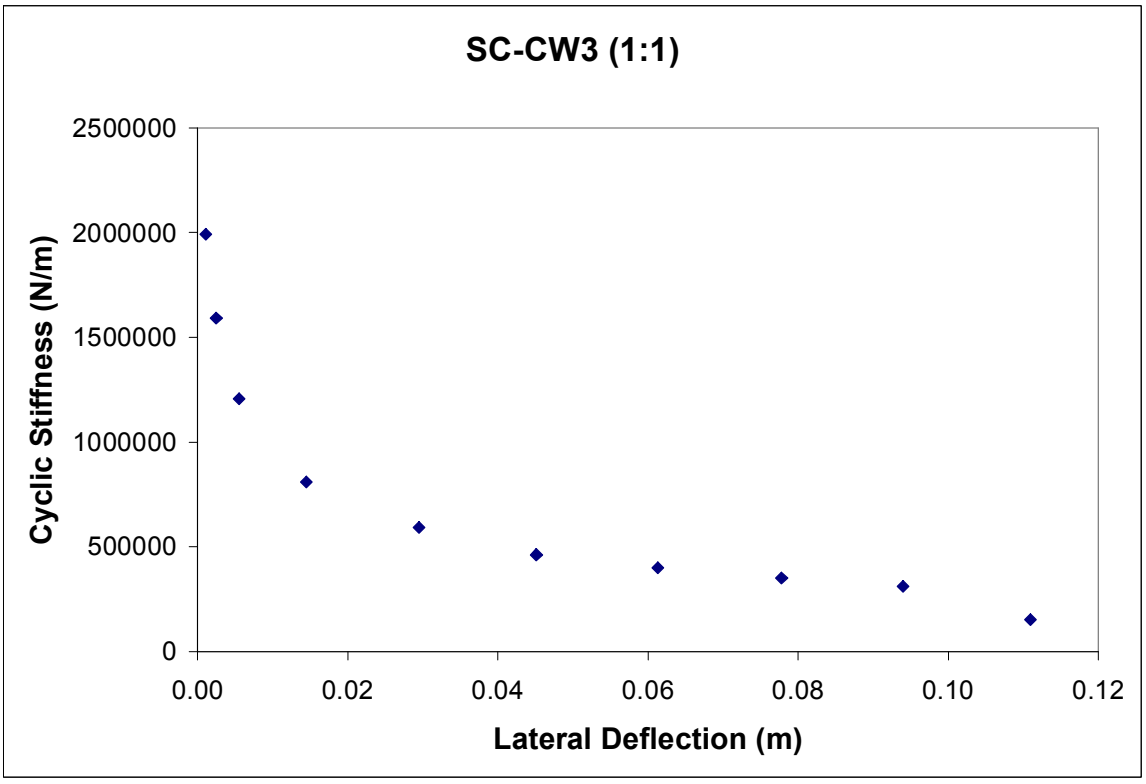

Figure 26B Cyclic stiffness vs. Lateral deflection. Test SC-CW3 (1:1).

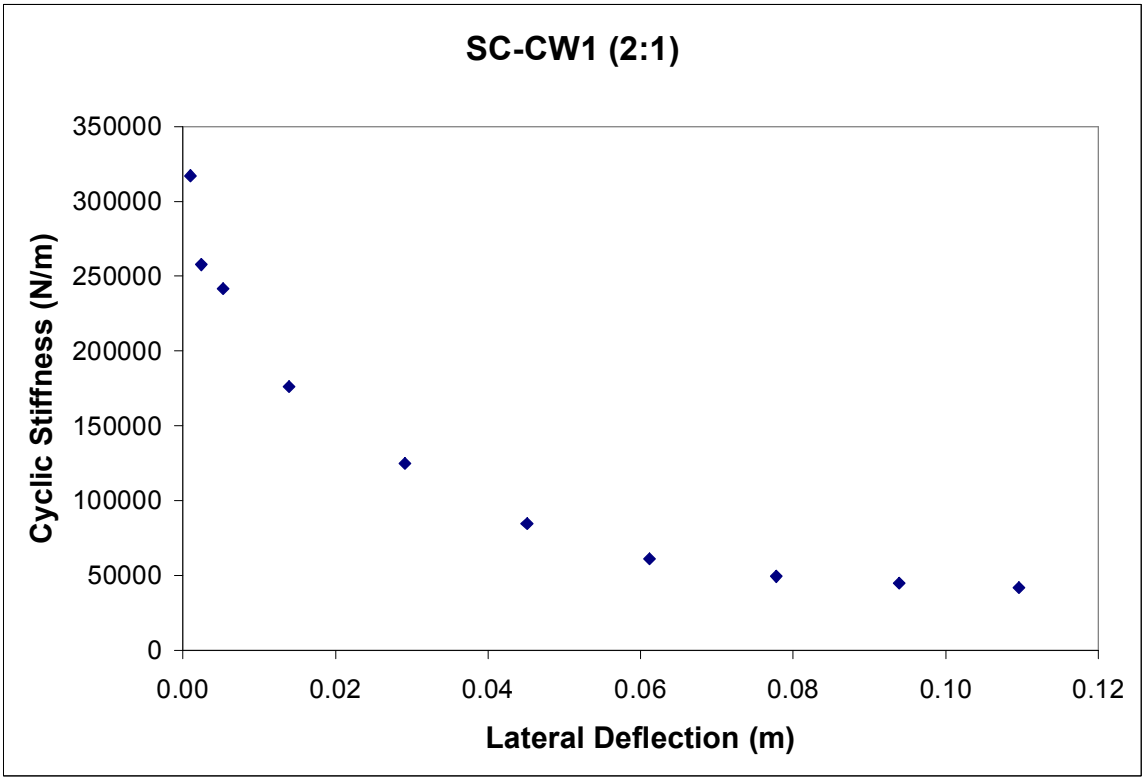

Figure 27B Cyclic stiffness vs. Lateral deflection. Test SC-CW1 (2:1).

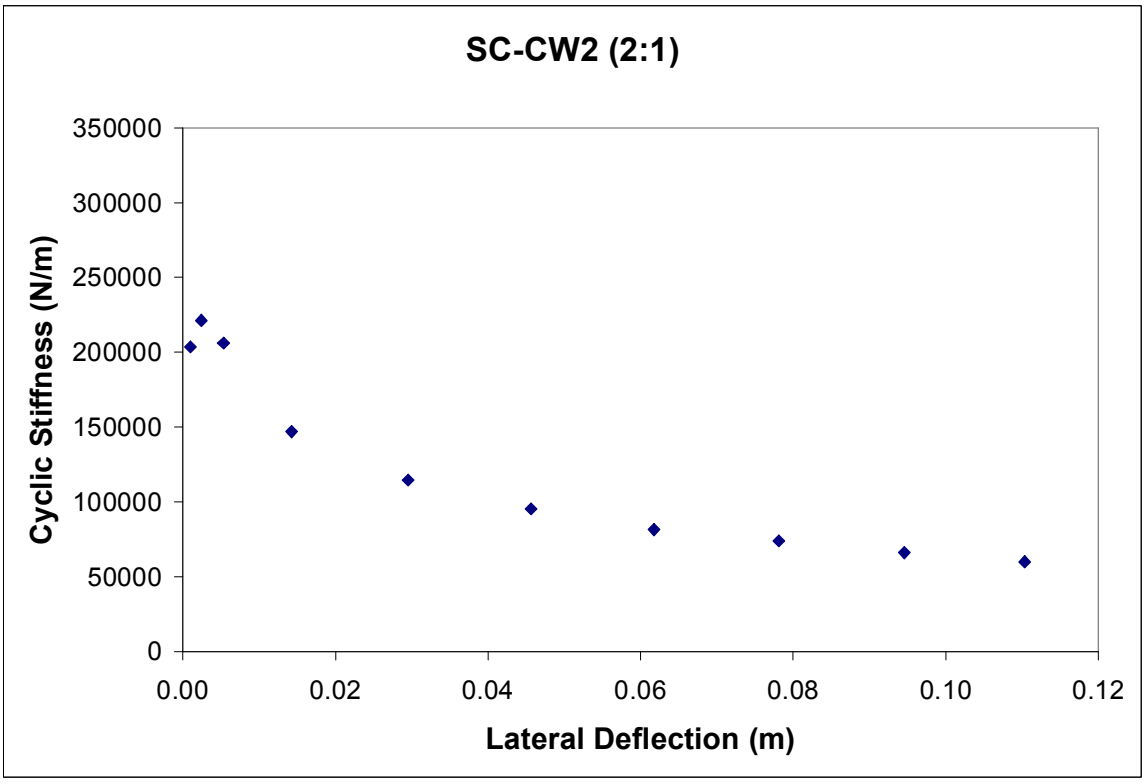

Figure 28B Cyclic stiffness vs. Lateral deflection. Test SC-CW2 (2:1).

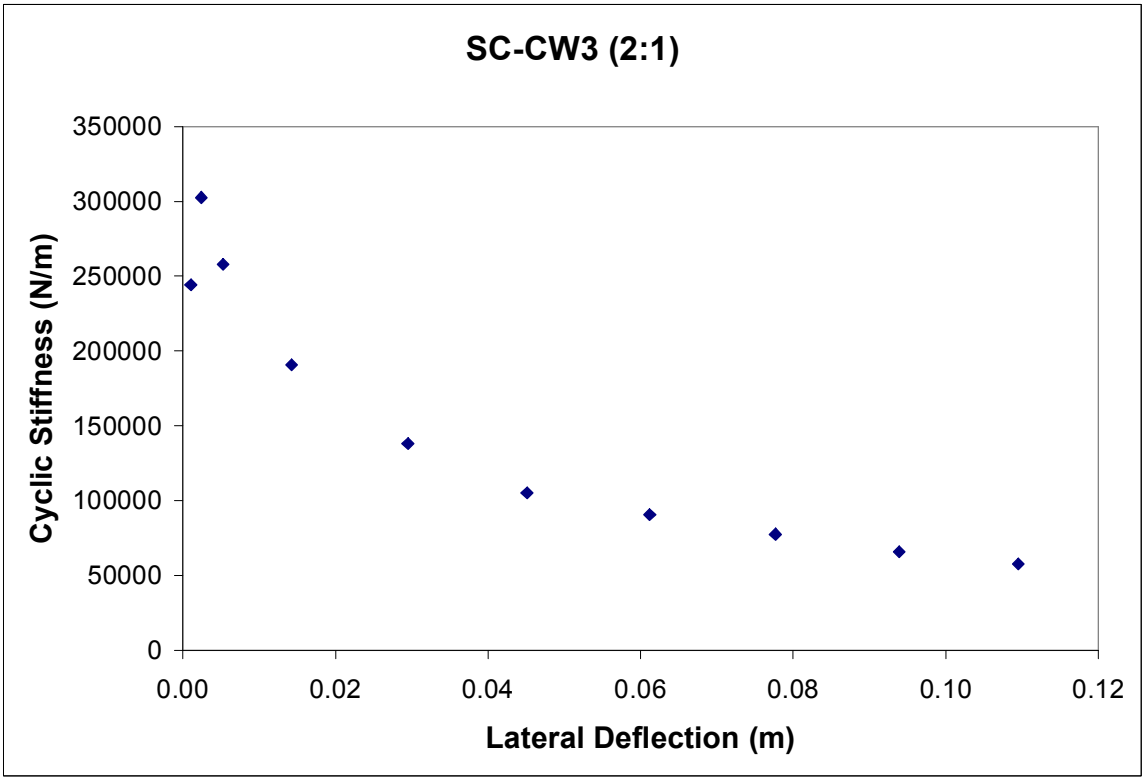

Figure 29B Cyclic stiffness vs. Lateral deflection. Test SC-CW3 (2:1).

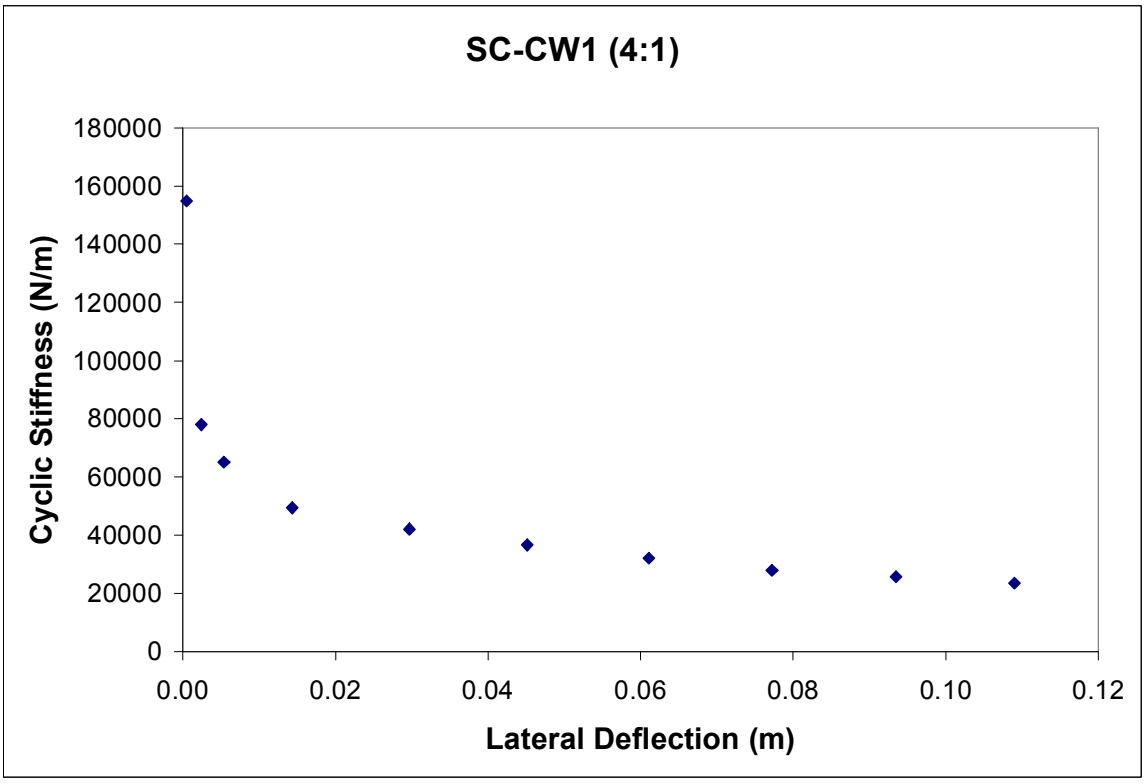

Figure 30B Cyclic stiffness vs. Lateral deflection. Test SC-CW1 (4:1).

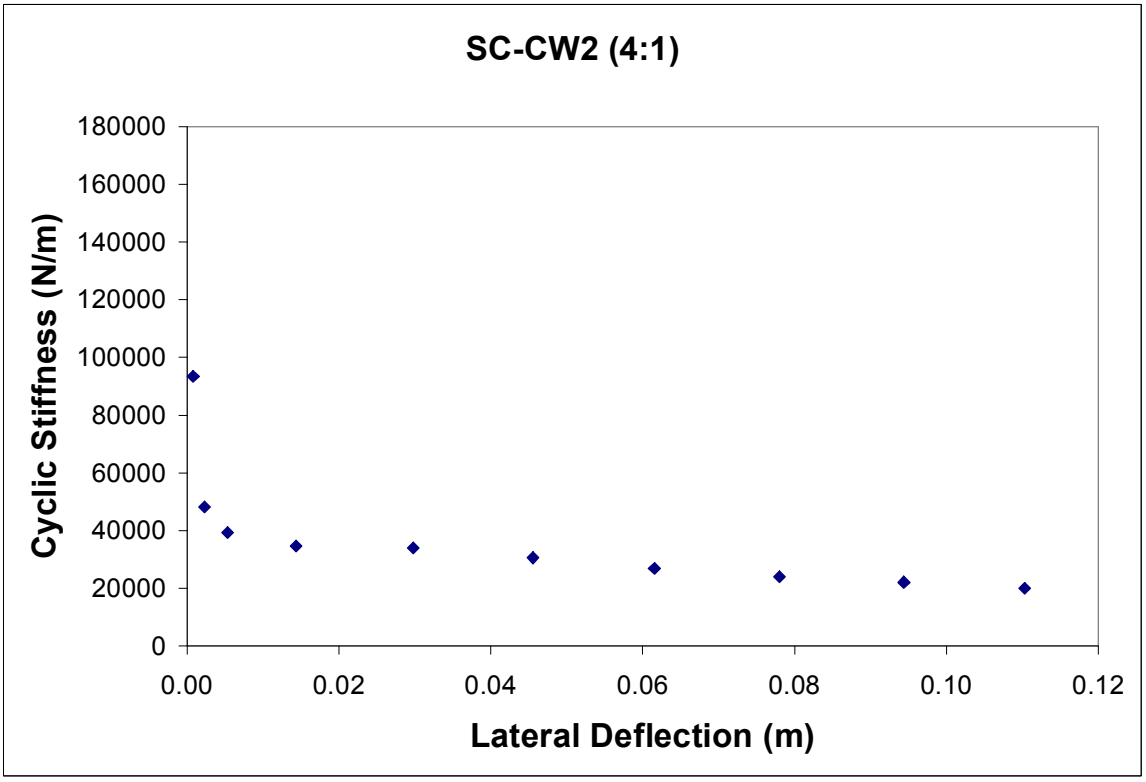

Figure 31B Cyclic stiffness vs. Lateral deflection. Test SC-CW2 (4:1).

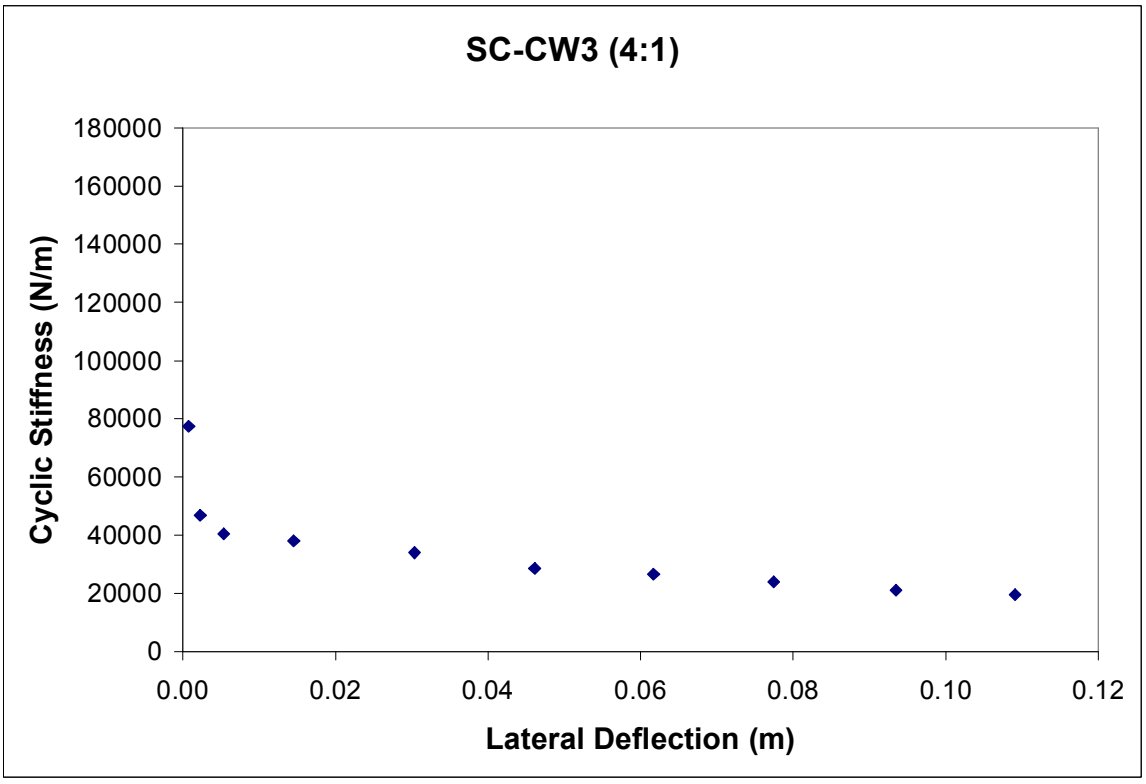

Figure 32B Cyclic stiffness vs. Lateral deflection. Test SC-CW3 (4:1).

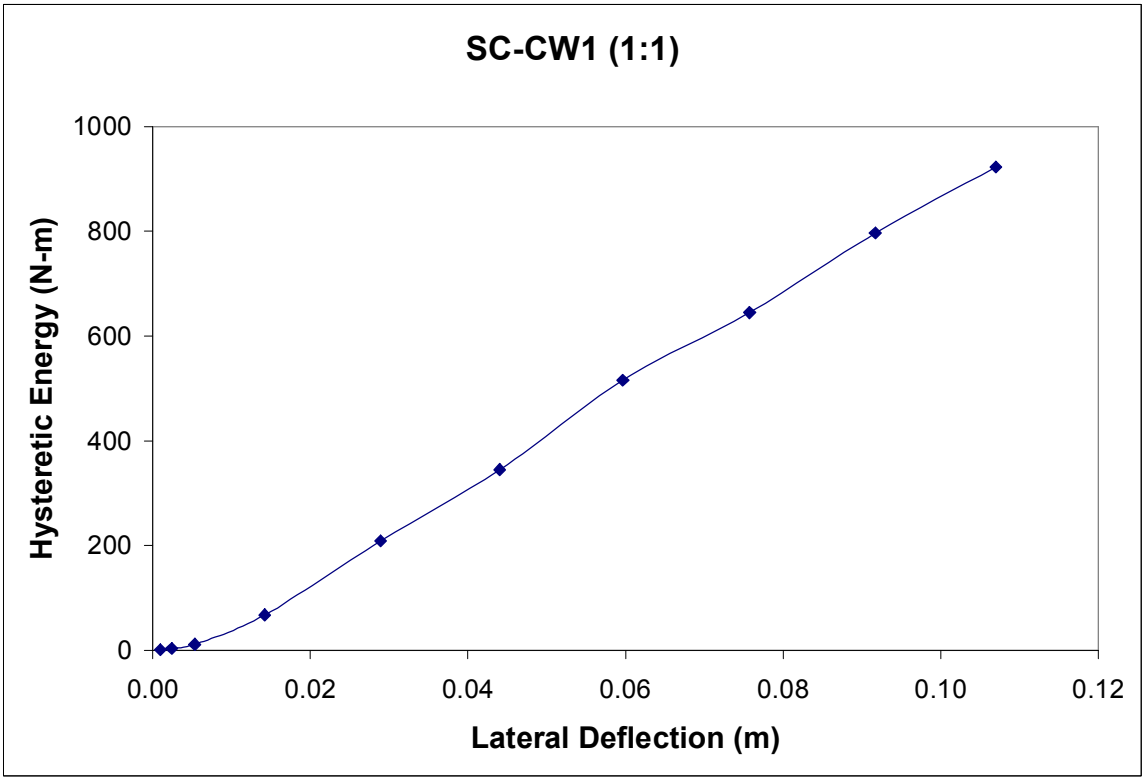

Figure 33B Hysteretic Energy vs. Lateral deflection. Test SC-CW1 (1:1).

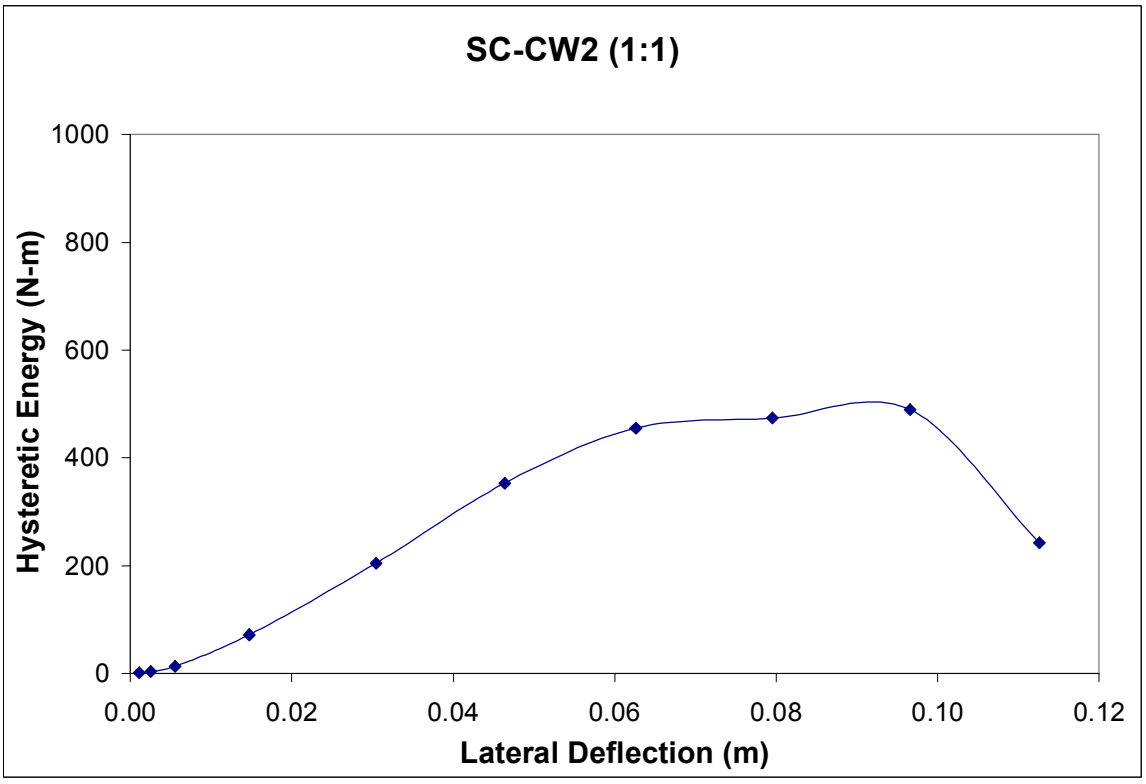

Figure 34B Hysteretic Energy vs. Lateral deflection. Test SC-CW2 (1:1).

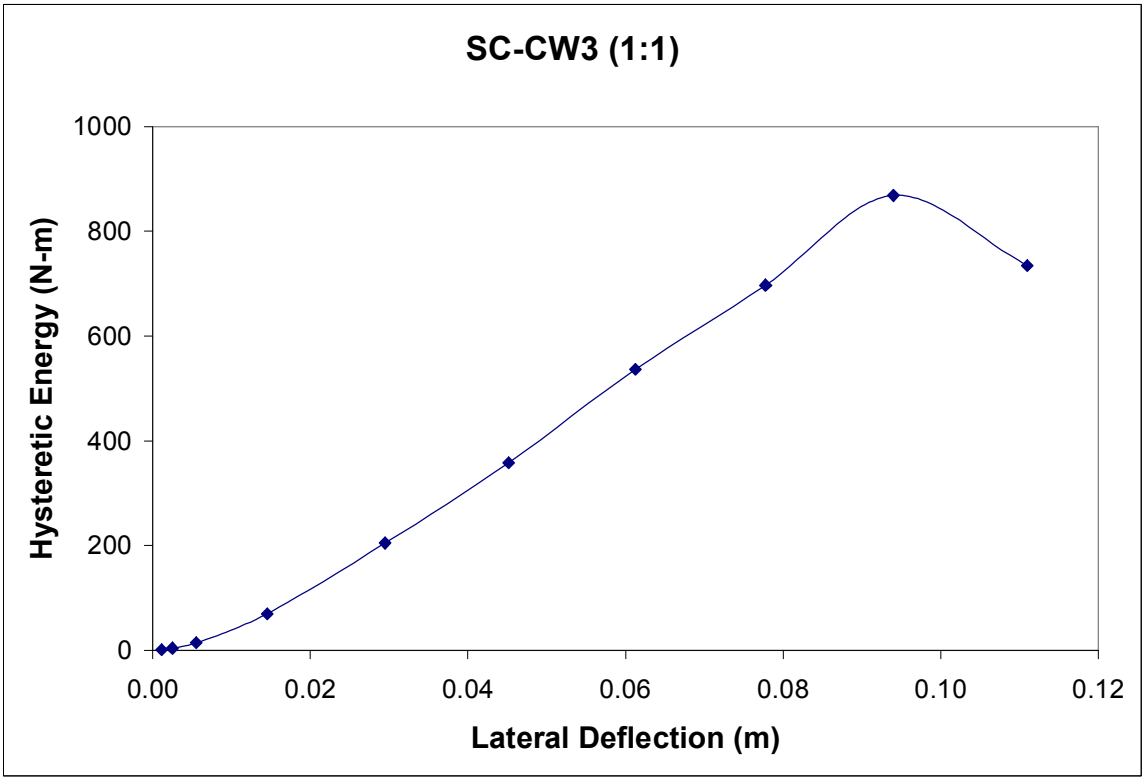

Figure 35B Hysteretic Energy vs. Lateral deflection. Test SC-CW3 (1:1).

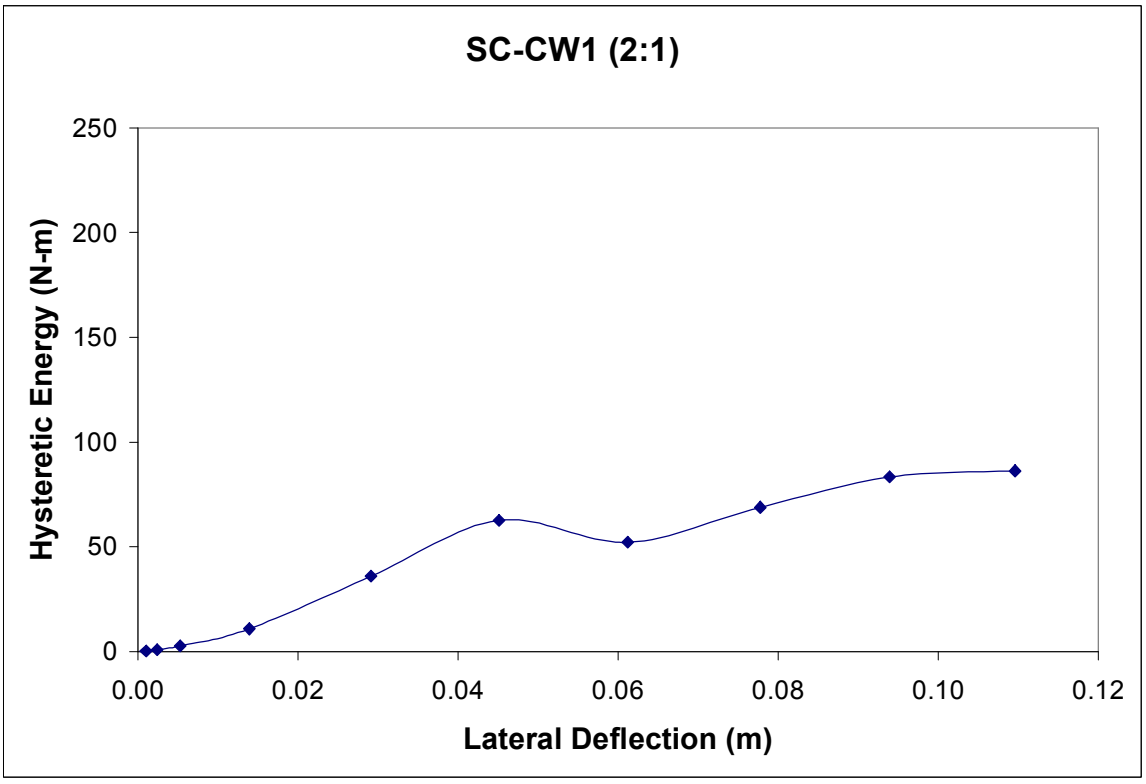

Figure 36B Hysteretic Energy vs. Lateral deflection. Test SC-CW1 (2:1).

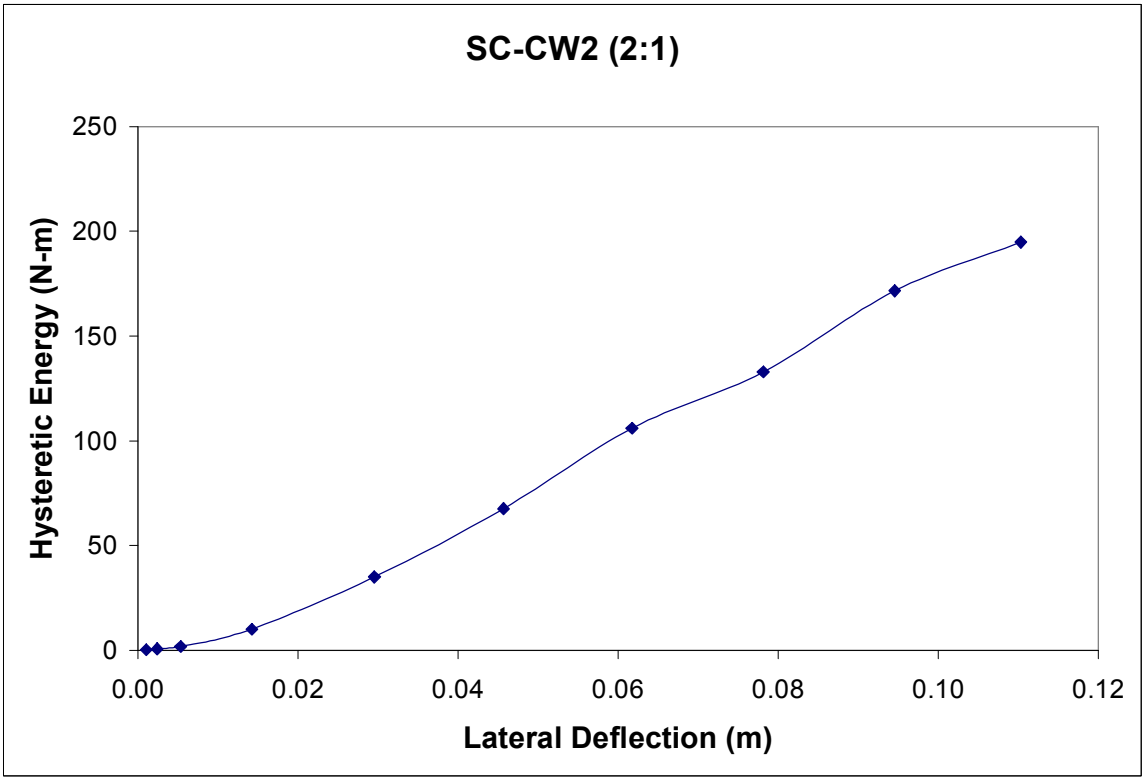

Figure 37B Hysteretic Energy vs. Lateral deflection. Test SC-CW2 (2:1).

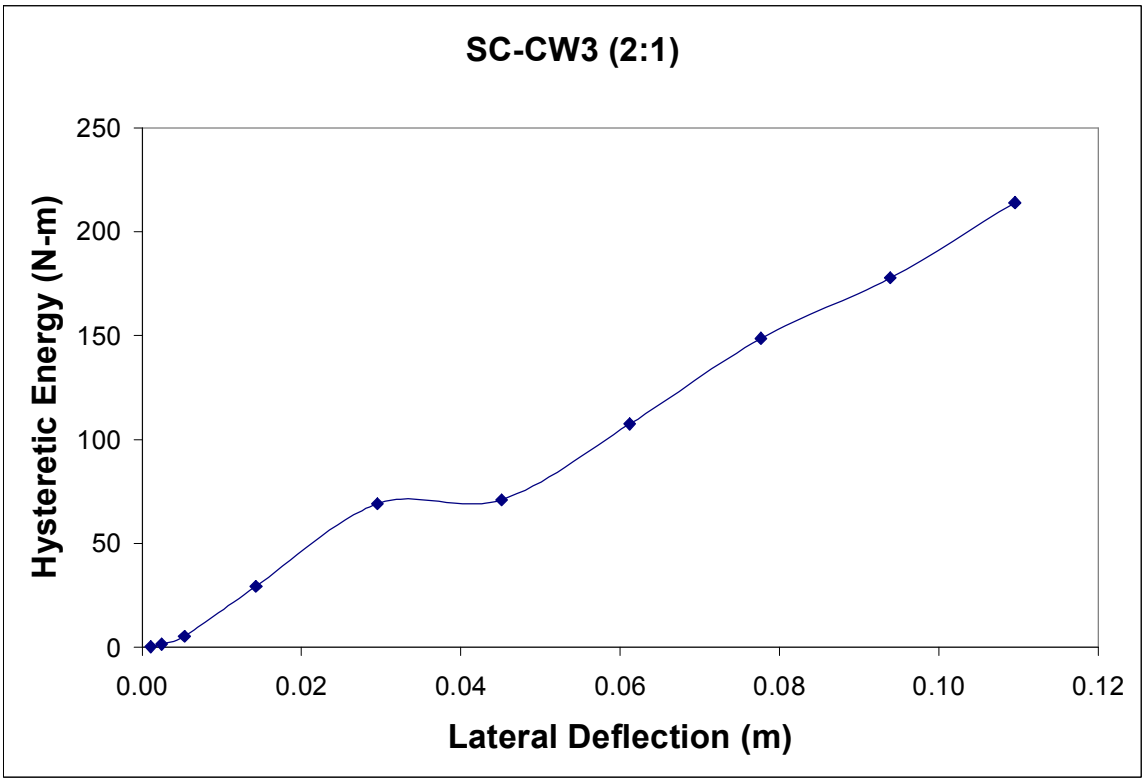

Figure 38B Hysteretic Energy vs. Lateral deflection. Test SC-CW3 (2:1).

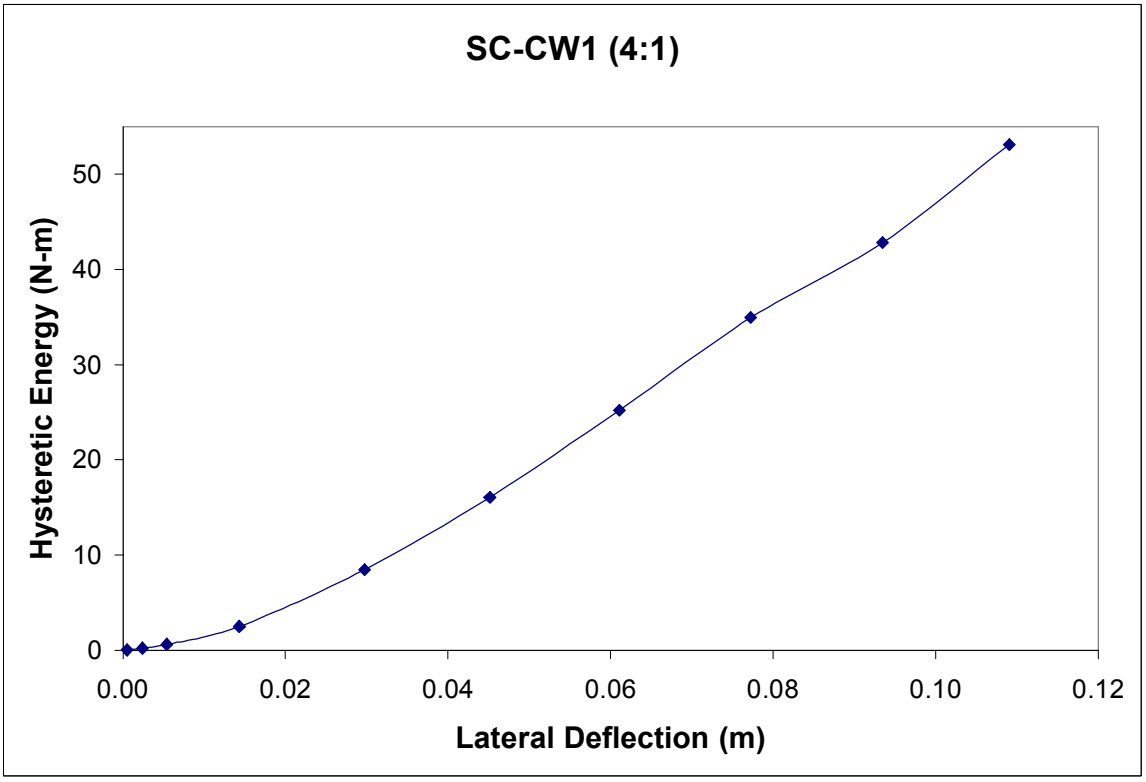

Figure 39B Hysteretic Energy vs. Lateral deflection. Test SC-CW1 (4:1).

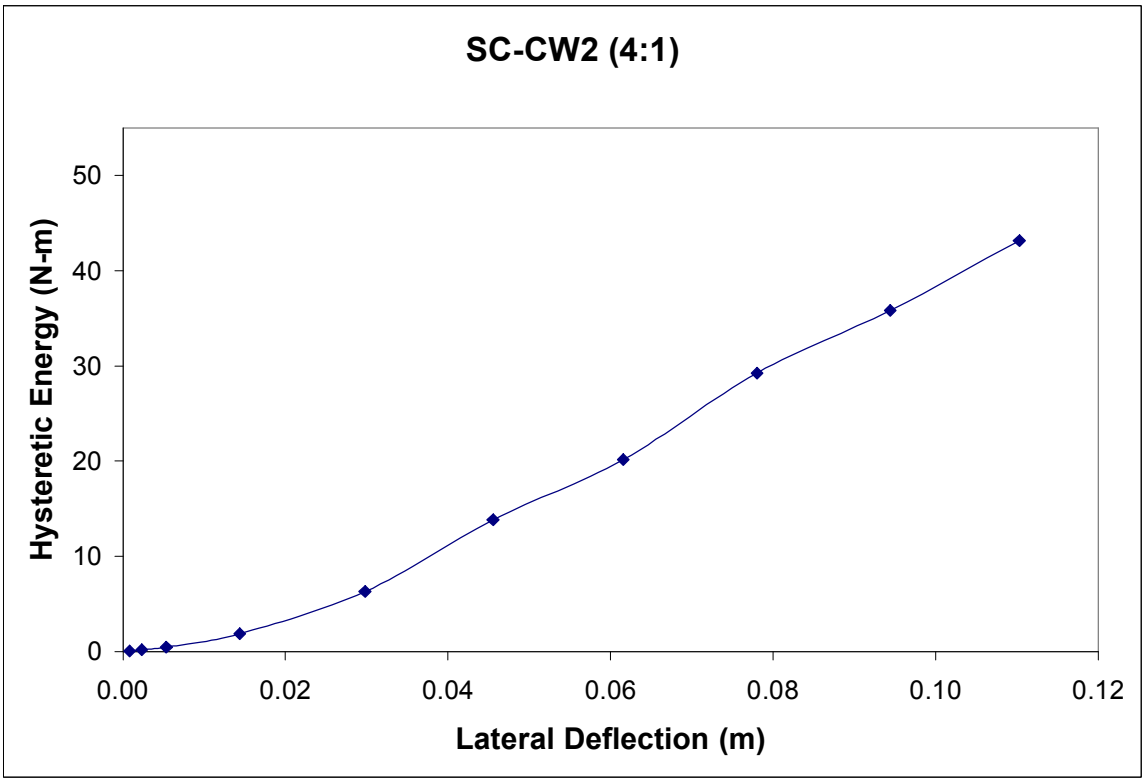

Figure 40B Hysteretic Energy vs. Lateral deflection. Test SC-CW2 (4:1).

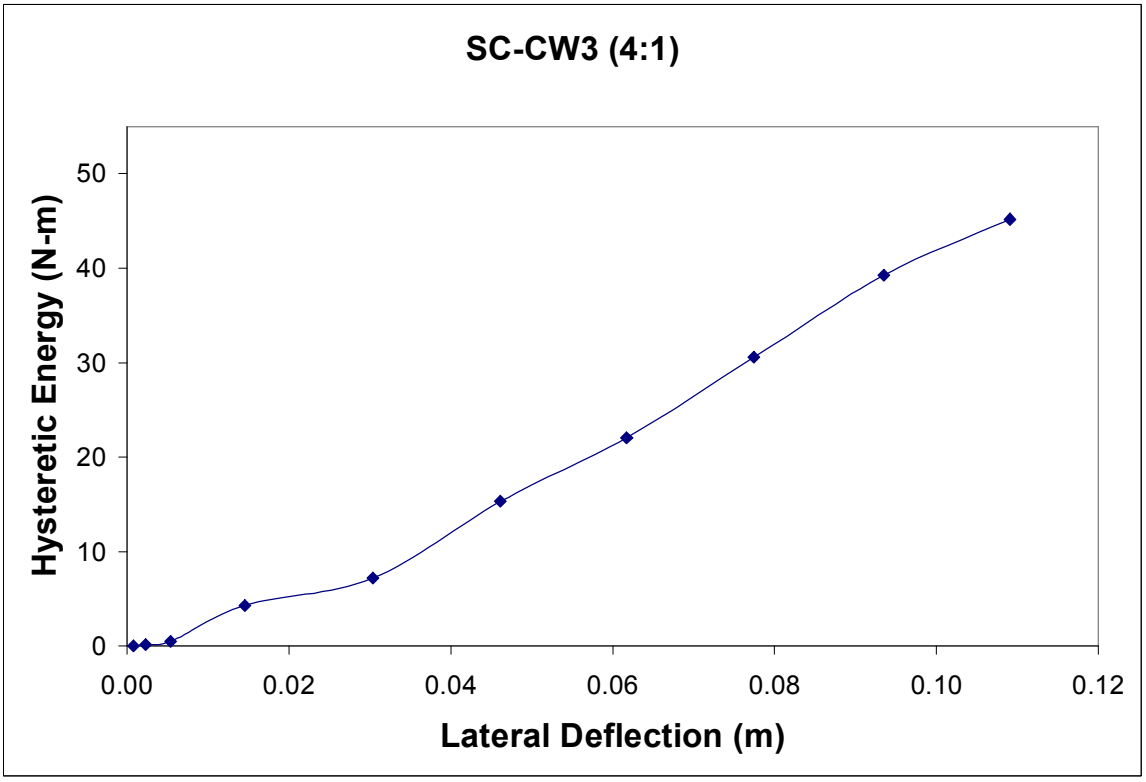

Figure 41B Hysteretic Energy vs. Lateral deflection. Test SC-CW3 (4:1).

Table 10B Basic parameters obtained from each log shear wall test as well as EEEP parameters.

Aspect ratio	Test	F_{peak} (N)	Δ @ F_{peak} (m)	$0.4F_{peak}$ (N)	Δ @ $0.4F_{peak}$ (m)	$F_{failure}$ (N)	$F_{EEEP\ yield}$ (N)	$\Delta_{EEEP\ yield}$ (m)	k_e (N/m)	EEEP (N-m)	D	V_{peak} (N/m)	$V_{failure}$ (N/m)
1:1	SC-CW1	30,946	0.1047	12,378	0.0139	22,487	19,938	0.0226	894,899	749	2.16	12,683	9,216
	SC-CW2	25,726	0.0637	10,291	0.0103	22,591	20,222	0.0200	1,043,888	783	2.44	10,543	9,259
	SC-CW3	31,644	0.1011	12,657	0.0143	23,562	20,064	0.0204	890,661	748	2.39	12,969	9,657
	Mean	*29,439*	*0.09*	*11,775*	*0.0128*	*22,880*	*20,075*	*0.0210*	*943,149*	*760*	*2.33*	*12,065*	*9,377*
	COV	*0.11*	*0.25*	*0.11*	*0.1728*	*0.03*	*0.01*	*0.07*	*0.09*	*0.03*	*0.06*	*0.11*	*0.03*
2:1	SC-CW1	5,300	0.0717	2,132	0.0101	3,921	3,790	0.0175	217,817	152	2.79	4,344	3,214
	SC-CW2	6,928	0.1092	2,771	0.0180	4,352	4,218	0.0273	153,583	147	1.79	5,679	3,567
	SC-CW3	7,092	0.1039	2,837	0.0132	5,277	4,593	0.0216	210,362	174	2.25	5,813	4,325
	Mean	*6,440*	*0.09*	*2,580*	*0.0137*	*4,517*	*4,200*	*0.0222*	*193,921*	*158*	*2.28*	*5,279*	*3,702*
	COV	*0.15*	*0.21*	*0.15*	*0.2901*	*0.15*	*0.10*	*0.22*	*0.18*	*0.09*	*0.22*	*0.15*	*0.15*
4:1	SC-CW1	2,680	0.1077	1,072	0.0225	1,775	1,610	0.0339	47,524	51	1.44	4,467	2,958
	SC-CW2	2,281	0.1087	916	0.0251	1,531	1,365	0.0374	36,532	41	1.31	3,802	2,552
	SC-CW3	2,215	0.1087	886	0.0230	1,498	1,348	0.0347	39,236	43	1.41	3,692	2,497
	Mean	*2,392*	*0.11*	*958*	*0.0235*	*1,601*	*1,441*	*0.0353*	*41,097*	*45*	*1.38*	*3,987*	*2,669*
	COV	*0.11*	*0.01*	*0.10*	*0.0586*	*0.09*	*0.10*	*0.05*	*0.14*	*0.12*	*0.05*	*0.11*	*0.09*

Table 11B Moisture content (MC) & Specific gravity (SG) values for 1:1 aspect ratio.

Test	Log sample	MC	SG
SC-MW1	sill	10%	0.43
	1	16%	0.37
	2	19%	0.36
	3	16%	0.38
	4	19%	0.38
	5	17%	0.35
	6	14%	0.42
	7	12%	0.39
	8	14%	0.40
	9	13%	0.38
	10	14%	0.39
SC-CW1	sill	9%	0.50
	1	13%	0.44
	2	16%	0.42
	3	17%	0.40
	4	18%	0.43
	5	18%	0.33
	6	14%	0.56
	7	19%	0.42
	8	*61%	0.52
	9	*27%	0.38
	10	*24%	0.50
SC-CW2	sill	11%	0.40
	1	13%	0.43
	2	13%	0.43
	3	14%	0.45
	4	14%	0.39
	5	*21%	0.37
	6	13%	0.41
	7	13%	0.44
	8	13%	0.42
	9	13%	0.41
	10	12%	0.32
SC-CW3	sill	10%	0.40
	1	17%	0.44
	2	15%	0.41
	3	16%	0.31
	4	17%	0.59
	5	17%	0.41
	6	*52%	0.57
	7	19%	0.47
	8	19%	0.41
	9	17%	0.41
	10	19%	0.46
	MEAN=	18%	0.42
	COV=	0.54	0.14

*High MC value was caused by a small saturated pith area and is not representative of MC for whole log.

Table 12B Moisture content (MC) & Specific gravity (SG) values for 2:1 aspect ratio.

Test	Log sample	MC	SG
SC-MW1	sill	11%	0.39
	1	16%	0.51
	2	13%	0.41
	3	13%	0.38
	4	15%	0.41
	5	15%	0.43
	6	15%	0.39
	7	16%	0.43
	8	12%	0.43
	9	14%	0.49
	10	11%	0.40
SC-CW1	sill	10%	0.40
	1	13%	0.45
	2	15%	0.42
	3	11%	0.39
	4	12%	0.38
	5	13%	0.37
	6	16%	0.40
	7	16%	0.43
	8	14%	0.37
	9	13%	0.39
	10	13%	0.41
SC-CW2	sill	10%	0.41
	1	13%	0.38
	2	*36%	0.46
	3	*41%	0.50
	4	*24%	0.47
	5	12%	0.38
	6	14%	0.42
	7	14%	0.43
	8	12%	0.38
	9	*26%	0.43
	10	13%	0.40
SC-CW3	sill	10%	0.46
	1	17%	0.44
	2	17%	0.42
	3	16%	0.34
	4	*29%	0.46
	5	15%	0.34
	6	14%	0.38
	7	*53%	0.55
	8	14%	0.39
	9	13%	0.42
	10	12%	0.42
	MEAN=	16%	0.42
	COV=	0.52	0.10

*High MC value was caused by a small saturated pith area and is not representative of MC for whole log.

Table 13B Moisture content (MC) & Specific gravity (SG) values for 4:1 aspect ratio.

Test	Log sample	MC	SG
SC-MW1	sill	9%	0.40
	1	12%	0.41
	2	12%	0.42
	3	12%	0.42
	4	13%	0.41
	5	*40%	0.54
	6	*39%	0.53
	7	*44%	0.54
	8	*34%	0.52
	9	14%	0.55
	10	14%	0.44
SC-CW1	sill	9%	0.45
	1	14%	0.47
	2	13%	0.48
	3	14%	0.46
	4	14%	0.48
	5	14%	0.45
	6	15%	0.45
	7	14%	0.43
	8	12%	0.39
	9	12%	0.38
	10	13%	0.39
SC-CW2	sill	9%	0.44
	1	12%	0.37
	2	12%	0.39
	3	13%	0.41
	4	11%	0.42
	5	11%	0.41
	6	12%	0.41
	7	12%	0.42
	8	12%	0.40
	9	12%	0.41
	10	13%	0.42
SC-CW3	sill	10%	0.47
	1	14%	0.41
	2	17%	0.51
	3	15%	0.40
	4	17%	0.51
	5	16%	0.37
	6	18%	0.50
	7	16%	0.38
	8	17%	0.52
	9	17%	0.40
	10	16%	0.40
	MEAN=	16%	0.44
	COV=	0.51	0.12

*High MC value was caused by a small saturated pith area and is not representative of MC for whole log.

Table 14B Lag screw bending yield strength test results.

Test	M_y (N-mm)	F_{yb} (MPa)
1	88392	618
2	82057	542
3	84046	567
4	85519	589
5	89976	621
6	83788	573
7	84451	551
8	84856	570
9	82978	565
10	86808	578
11	81652	563
12	88245	596
13	89865	616
14	87361	599
15	88908	614
16	88282	606
17	86403	594
18	90381	617
19	85519	590
20	90123	584
Mean	*86481*	*588*
COV	*0.03*	*0.04*